Characterization of metabolic safeguarding factors in the context of direct cellular reprogramming

Dissertation

zur Erlangung des akademischen Grades

doctor rerum naturalium

(Dr. rer. Nat.)

eingereicht an der

Fakultät für Mathematik, Informatik und Naturwissenschaften der

Universität Hamburg

von

Amin Shadfar, Master of Science (Molecular Medicine)

2025

Vorsitzender:

Prof. Dr. Susanne Dobler

Gutachterinnen/Gutachter:

Prof. Dr. Baris Tursun

Prof. Dr. Tobias Lenz

Weitere/s Mitglied/er:

Prof. Dr. Zoya Ignatova

Date of defence:

03.06.2025

Conducted in University of Hamburg

Institute of Cell and Systems Biology of Animals Biology Department

Research Group: Gene regulation and Cell Fate Decision in *C. elegans*

August 2021 – February 2025

Submitted from Amin Shadfar

Matrikel-Nr. 7574421

Eidesstattliche Versicherung:

Hiermit versichere ich an Eides statt, die vorliegende Dissertationsschrift selbst verfasst und keine anderen als die angegebenen Hilfsmittel und Quellen benutzt zu haben. Sofern im Zuge der Erstellung der vorliegenden Dissertationsschrift generative Künstliche Intelligenz (gKI) basierte elektronische Hilfsmittel verwendet wurden, versichere ich, dass meine eigene Leistung im Vordergrund stand und dass eine vollständige Dokumentation aller verwendeten Hilfsmittel gemäß der Guten wissenschaftlichen Praxis vorliegt. Ich trage die Verantwortung für eventuell durch die gKI generierte fehlerhafte oder verzerrte Inhalte, fehlerhafte Referenzen, Verstöße gegen das Datenschutz- und Urheberrecht oder Plagiate.

Affidavit:

I hereby declare and affirm that this doctoral dissertation is my own work and that I have not used any aids and sources other than those indicated. If electronic resources based on generative artificial intelligence (gAI) were used in the course of writing this dissertation, I confirm that my own work was the main and value-adding contribution, and that complete documentation of all resources used is available in accordance with good scientific practice. I am responsible for any erroneous or distorted content, incorrect references, violations of data protection and copyright law or plagiarism that may have been generated by the gAI.

Hamburg, den 18.02.2025

Unterschrift 

Abstract

Cellular identities are established through the expression of fate-determining transcription factors (TFs). The terminally differentiated cell fates can be maintained by inhibitory mechanisms that suppress alternative TFs. Mis-expression of these fate-determining TFs can enable the reprogramming of the original cell fate into target cell fate. In *C. elegans*, the zinc-finger TF CHE-1 is essential for specifying the glutamatergic ASE neuronal fate. While ASE fate is normally repressed in non-neuronal tissues, it can be induced through ectopic expression of CHE-1 and knockdown of reprogramming barrier genes that safeguard cell identity. Using RNAi to remove these barriers, ASE neuron fate has been successfully expressed in diverse cell types.

We investigated the mechanisms of action of NAD^+-dependent mitochondrial isocitrate dehydrogenase 3 (IDH-3), a candidate reprogramming barrier gene. Our findings revealed reliable ASE neuron fate reporter expression in the germline upon ectopic expression of CHE-1 upon RNAi knockdown of alpha subunit (IDHA-1) of IDH3 complex. Furthermore, we identified FDGT-2, a putative membrane glucose transporter, that enhances germline reprogramming when co-depleted with IDHA-1. FDGT-2 was shown to be mainly expressed in regions covering the gut tissue and the germline. We also explored the role of TCA cycle metabolites, identifying **α**-ketoglutarate (**α**-KG) and fumarate as consistent enhancers of reprogramming efficiency. Additionally, we investigated the role of glutamine anaplerosis pathway in replenishment of **α**-KG levels depleted in the *idha-1*^{RNAi} phenotype. The TCA cycle emerges as a central hub, linking energy metabolism to the proliferative and developmental processes essential for life.

Examining male- and female-specific germline components, we observed that reprogramming overlaps with sperm and spermatheca-associated regions in closer proximity to vulva. Depletion of male-specific genes *spe-8* and *spe-27* reduced *idha-1*-mediated reprogramming rate, and genes required for gametogenesis and germline development were also necessary for reprogramming. Our study aimed to uncover the molecular mechanisms by which mitochondrial signals feedback to the nucleus, driving germ cell conversion into ASE neurons. These findings highlight the critical role played by metabolism in cell fate determination and reprogramming.

Zusammenfassung

Zellidentitäten werden durch die Expression von spezifischen Transkriptionsfaktoren (TFs) etabliert, die durch hemmende Mechanismen aufrechterhalten werden, die alternative TFs unterdrücken. Diese TFs ermöglichen das Umprogrammieren von vollständig differenzierten Zelltype in andere Zelltypen. In *C. elegans* ist der Zinkfinger-TF CHE-1 essenziell für die Festlegung des glutamatergischen ASE-Neurons. Während das ASE-Neuron normalerweise in nicht-neuronalen Geweben unterdrückt wird, kann es durch die ektopische Expression von CHE-1 und das Herunterregulieren von Umprogrammierungsbarrieren, die die Zellidentität schützen, induziert werden. Mit Hilfe von RNAi ist es möglich, diese Barrieren herunterzuregulieren, so dass das ASE-Neuron erfolgreich in verschiedenen Zelltypen exprimiert werden kann.

Wir untersuchten die Wirkmechanismen der NAD^+-abhängigen mitochondrialen Isocitratdehydrogenase 3 (IDH-3), eines Kandidaten für ein Umprogrammierungsbarrieren. Unsere Ergebnisse zeigten eine zuverlässige Expression eines ASE-Neuronreporters in der Keimbahn bei ektopischer Expression von CHE-1 nach RNAi der Alpha-Untereinheit (IDHA-1) des IDH3-Komplexes. Darüber hinaus identifizierten wir FDGT-2, einen Membran-Glukosetransporter, der die Keimbahn-Umprogrammierung bei gleichzeitiger Verringerung von IDHA-1 verstärkt. FDGT-2 wurde hauptsächlich in den Bereichen des Darmgewebes und der Keimbahn exprimiert. Wir untersuchten auch die Rolle von TCA-Zyklusmetaboliten und identifizierten **α**-Ketoglutarat (**α**-KG) und Fumarat als konstante Verstärker der Umprogrammierungseffizienz. Zusätzlich untersuchten wir die Rolle des Glutamin-Anaplerose-Weges bei der Auffüllung von **α**-KG-Spiegeln, die im *idha-1* RNAi-Phänotyp verringert waren. Der TCA-Zyklus ist ein zentraler Knotenpunkt, der den

Energiestoffwechsel mit den proliferativen und entwicklungsbiologischen Prozessen verknüpft, die für das Leben wesentlich sind.

Bei der Untersuchung männlicher und weiblicher spezifischer Keimbahnkomponenten stellten wir fest, dass die Umprogrammierung mit spermien- und spermathekarelevanten Bereichen in näherer Umgebung der Vulva überlappt. Die Verminderung männlicher spezifischer Gene wie *spe-8* und *spe-27* verringerte die *idha-1*-vermittelte Umprogrammierungsrate, und Gene, die für die Gametogenese und die Keimbahnentwicklung erforderlich sind, waren ebenfalls notwendig für die Umprogrammierung. Unsere Studie hatte das Ziel, die molekularen Mechanismen zu entschlüsseln, durch die mitochondriale Signale an den Zellkern weitergeleitet werden, um die Umwandlung von Keimzellen in ASE-Neuronen zu fördern. Diese Ergebnisse heben die entscheidende Rolle der Mitochondrien und des Stoffwechsels bei der Entwicklung und Umprogrammierung von Zellen hervor.

TABLE OF CONTENTS

1. INTRODUCTION

1.1 Cell fate determination and its bypassing, through direct cellular reprogramming

Whether unicellular or multicellular, all organisms are made of cells. In higher and more complex organisms there are more than one cell type contributing to a healthy, living, and reproductive organism. Different cell types have specialized functions to perform specific tasks. Neurons have extended cell bodies to transfer electrical currents and information. Epithelial cells have distinct basal and apical structural differences and the alveoli in the lungs are specialized to interact with the air for the most rapid and efficient oxygen and carbon dioxide exchange possible (Alberts et al., 2002; Whitsett & Alenghat, 2015). In humans, all cell types originate from a single progenitor cell: the zygote, formed by the fertilization of an egg and a sperm. This newly formed diploid cell is pluripotent, meaning it is capable of giving rise to all the necessary structures, tissues and cells needed to form a complete organism through successive cell divisions (Alberts et al., 2002). The three germ layers that give rise to an organism are endoderm, mesoderm and ectoderm, which form the foundation for all specialized cell types in the body (Feng et al., 2013; Solnica-Krezel & Sepich, 2012). The more specialized the cells become as they differentiate to take on different functions, the more they lose their pluripotency and plasticity, becoming more specialized and restricted in their developmental potential.

The genetic information needed for coding the sum of all the proteins in one organism, known as the proteome, is present in all the cells which make up that organism. The differential expression of these proteins and the degree to which they are expressed manifests the identity of that cell (Waddington, 1957). However, this differentiation comes at a cost; the differentiated cells lose their plasticity and under natural conditions cannot revert back to a pluripotent state. This is an important

aspect for healthy growth and compartmentalization of various parts of complex organisms. These processes in the cell are tightly regulated by transcription factors (TF), which can be decisive on cell types (Jaenisch & Bird, 2003; Spitz & Furlong, 2012).

Previously, it was widely believed that differentiated cells permanently inactivated or lose the genes redundant to their functions. The notion of fixed committed state of the differentiated cells was first challenged by Gurdon et al. in 1958. The challenge required transferring the nucleus of fully differentiated xenopus somatic cells into unfertilized oocytes and successfully generating tadpoles and adult frogs. The experiment revealed the existence of a considerable influence, which cellular environment exerted on cellular plasticity. Similarly, the same concept of somatic cell nuclear transfer was also experimented on mammalian cells, which resulted in the famous cloned sheep Dolly (Campbell et al., 1996). Between the years 1996 and 2018 more than 20 species of animals were cloned for scientific research purposes and the conservation of endangered species (Matoba & Zhang, 2018; Wani et al., 2017).

Nearly three decades after the first somatic cell nuclear transfer, a groundbreaking discovery revolutionized the field of cellular reprogramming. This was the demonstration of the potent use of transcription factors (TFs) in direct cell type conversion, specifically the reprogramming of fibroblasts into muscle cells using the TF MyoD (Davis et al., 1987) (Figure 1.2). This discovery established the concept of direct cellular reprogramming, which involves converting one differentiated cell type into another terminally differentiated cell type—a process we will explore in greater detail. This finding was transformative, as it challenged the previously held notion of unidirectional cell fate and demonstrated the power of TFs in altering cellular identity.

In fact, TFs are so decisive in determining cell fates that they have been used to revert fibroblasts, a type of terminally differentiated cell, back into pluripotent stem cells. This was achieved by Takahashi and Yamanaka (2006), who identified a set of TFs—Oct3/4, Sox2, Klf4, and c-Myc (now known as the Yamanaka factors)—capable of inducing pluripotency. His work earned him the Nobel Prize in Physiology or Medicine and led to the creation of induced pluripotent stem cells (iPSCs). Long before these experiments, it was widely believed that differentiated cells permanently inactivated or lost genes unnecessary for their specific functions.

Although without the somatic cell nuclear transfer the field of reprogramming and iPSC would not have developed as it has today, the process of cloning itself is a rather inefficient process as most clones die during the implantation or are born with serious birth defect (Jaenisch & Young, 2008). The cloned animals have a shorter life span and die of pneumonia or other microbial infections caused by immunological complications (Ogonuki et al., 2002; Smith et al., 2000). Other nuclear reprogramming approaches to form cells with single cellular identity had utilized fusing more than one cell type, which resulted in hybrids or heterokaryons (Figure 1.1) (Yamanaka & Blau, 2010). Heterokaryons harboring more than one nucleus do not proliferate, but the hybrids with fused nuclei have the ability to proliferate (Vierbuchen & Wernig, 2012). Hybrids can form from fusions between somatic cells or between somatic and embryonic stem (ES) cells. It has been observed that somatic cells fused with ES cells, share properties with their parental embryonic cells, indicating the dominance of pluripotency features over differentiated state and consequently activating previously silenced genes (Foshay et al., 2012; Yamanaka & Blau, 2010). However, due to inefficiency of this procedure and the tetraploid nature of these newly formed cells, this cannot be applied for therapy in the clinic (Alvarez-Dolado, 2007; Jaenisch & Young, 2008).

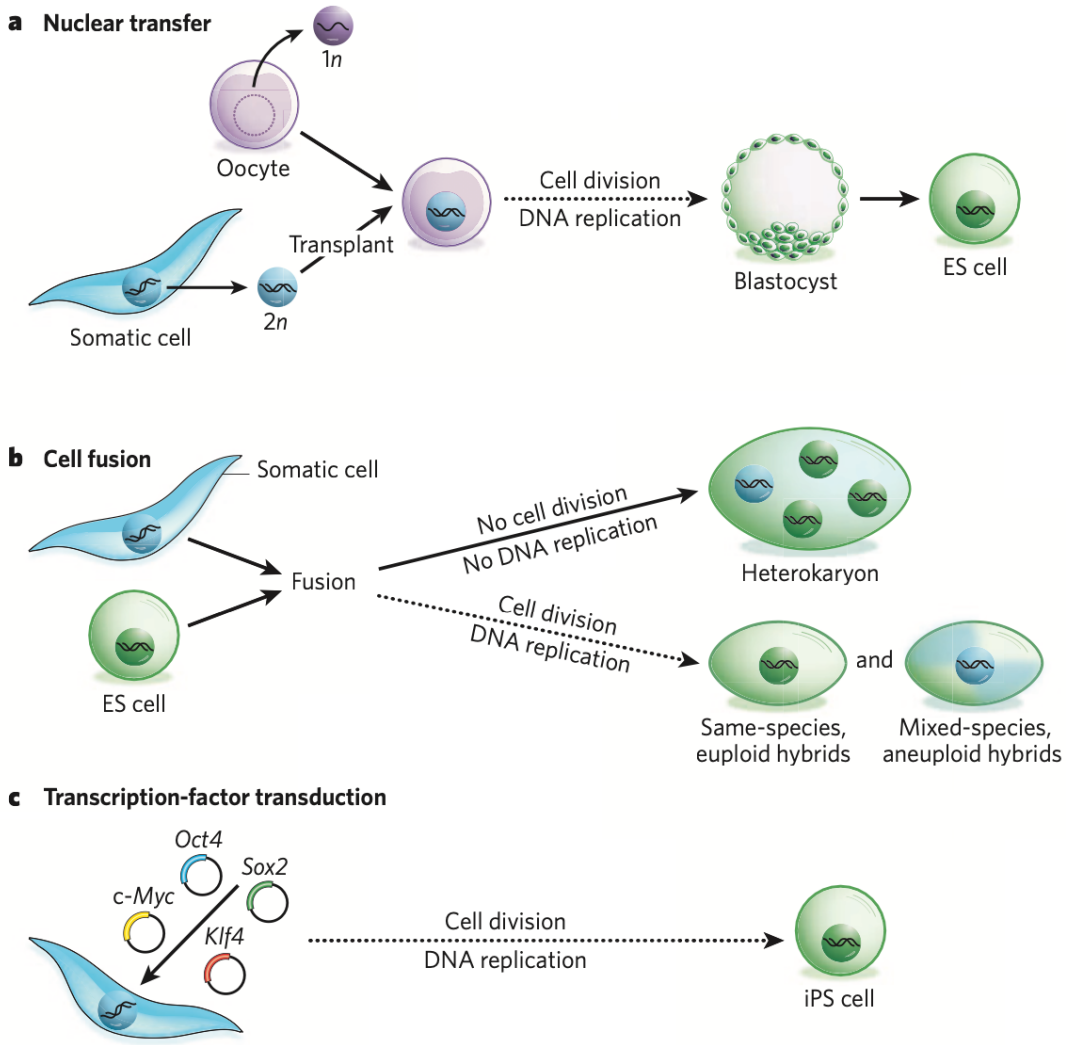

Figure 1.1 Approaches to achieve nuclear reprogramming for pluripotency. A) In nuclear transfer method, the nucleus of a somatic cell (diploid, 2n) is transplanted into the enucleated oocyte. The oocyte environment supports reprogramming of the somatic cell nucleus into pluripotency. The resulting blastocyst is used to generate embryonic stem (ES) cell lines in tissue culture. **B)** Cell fusion method combines two distinct cell types to form a single entity. The result is heterokaryons or hybrids used to study interaction between different genetic programs of the distinct nuclei. **C)** Transcription-factor transduction approach generates induced pluripotent stem cells (iPSCs) by reprogramming somatic cells through induction of four genes *Oct4*, *Sox2*, *Klf4*, *c-Myc*. The resulting cells have similar properties to ES cells (Reprinted from Yamanaka and Blau, 2010).

Direct cellular reprogramming has been extensively studied in various experimental setups, contributing to our understanding of cell identity and the mechanisms governing cell fate determination. For instance, researchers successfully converted fibroblasts into functional neurons using a combination of TFs: Ascl1, Brn2, Myt1l, and NeuroD1. This experiment highlighted the important role of these TFs in neuronal development and function (Vierbuchen et al., 2010). Fibroblasts have proven to be useful in reprogramming studies. Scientists reprogrammed fibroblasts into cardiomyocytes by introducing a cocktail of TFs, Gata4, Mef2c, and Tbx5, directly into living organisms (*in vivo*). This approach resulted in the generation of beating cardiomyocytes, demonstrating the potential of TFs to induce functional tissue regeneration (Leda et al., 2010). Moreover, reprogrammed cells have also been shown to generate functional beta cells. In a study involving hyperglycemic mice, researchers injected a combination of TFs, Ngn3, Pdx1, and Mafa into the exocrine vasculature. This intervention led to the production of reprogrammed beta cells that closely resembled endogenous beta cells and were capable of secreting insulin. This finding underscores the potential of TFs to drive *in vivo* functional changes and restore physiological processes (Zhou et al., 2008).

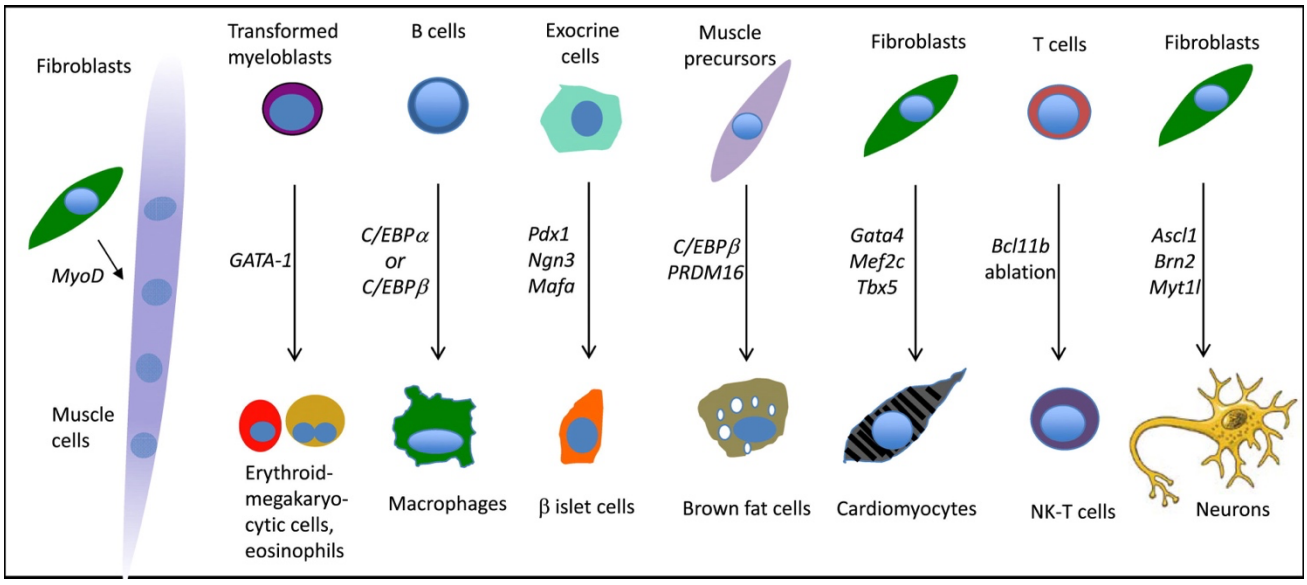

Figure 1.2 Transcription factor-induced trans-differentiation examples in the scientific literature. Conversion of fibroblasts into muscle cells. (Davis et al., 1987). Avian myelomonocytic cells conversion into eosinophils, thromboblasts, and erythroblasts (Kulessa et al., 1995). B cell reprogramming into macrophages (Xie et al., 2004). Reprogramming adult pancreatic exocrine cells into **β**-cells (Zhou et al., 2008). Myoblast to brown fat trans-differentiation (Kajimura et al., 2009). Direct reprogramming of fibroblast into cardiomyocytes (Leda et al., 2010). Reprogramming of T cells into natural killer (NK) cells (Li et al., 2010b). Direct conversion of fibroblasts into functional neurons. (Vierbuchen et al., 2010). (Reprinted from Graf, 2011)

Waddington´s epigenetic landscape model has been used to describe the journey of the cells from the very beginning at the stage of pluripotency to terminally differentiated cell forms as mentioned earlier (Figure 1.3). According to Waddington's epigenetic landscape if pluripotency is assumed to be a state at the peak of a slope, then the slope itself with its multiple groves and forks could represent all the potential forms, which a cell can develop into. This is called the cell lineage. Cells can be primed towards specific fates or progenitor cells for giving rise to various similar tissues and structures or continue differentiation to terminally differentiated cells as committed to only one form.

Moving in opposite direction of this slope can be called reprogramming, which is restoration of cellular plasticity through loss of previously differentiated features. In the example of iPSCs, fully differentiated cells are reprogrammed or in other words dedifferentiated by using overexpression of the TFs OCT4, SOX2, KLF4, c-MYC (OSKM factors) (Takahashi and Yamanaka, 2006). The direct conversion of a fully differentiated cell type to another fully differentiated cell type, as observed in Figure 1.1, is direct reprogramming of cell fates. Direct cellular reprogramming by the use of TFs eliminates the need for ascension through the landscape (Reid &Tursun, 2018).

The efficiency of direct reprogramming of a cell to a certain fate is also affected by the initial cell fate. In theory, there are assumed to be cell-fate safeguards, certain mechanisms that help to fixate a cell's identity and maintain its fate (Kolundzic et al., 2018; Guo & Morris, 2017). These mechanisms in the cell are needed in order to prevent cells from converting into one another (Tursun et al., 2011). It is argued that the closer the shared lineage of two different cells are, the more likely it is that the cell fate safeguards persist in maintaining the fate mechanisms and halt the possibility of trans-differentiation between the fates. When such mechanisms are disrupted abnormalities in cellular functions are expected as some cells acquire a more stem-like state and may progress to some forms of cancer (Jaenisch & Young, 2008).

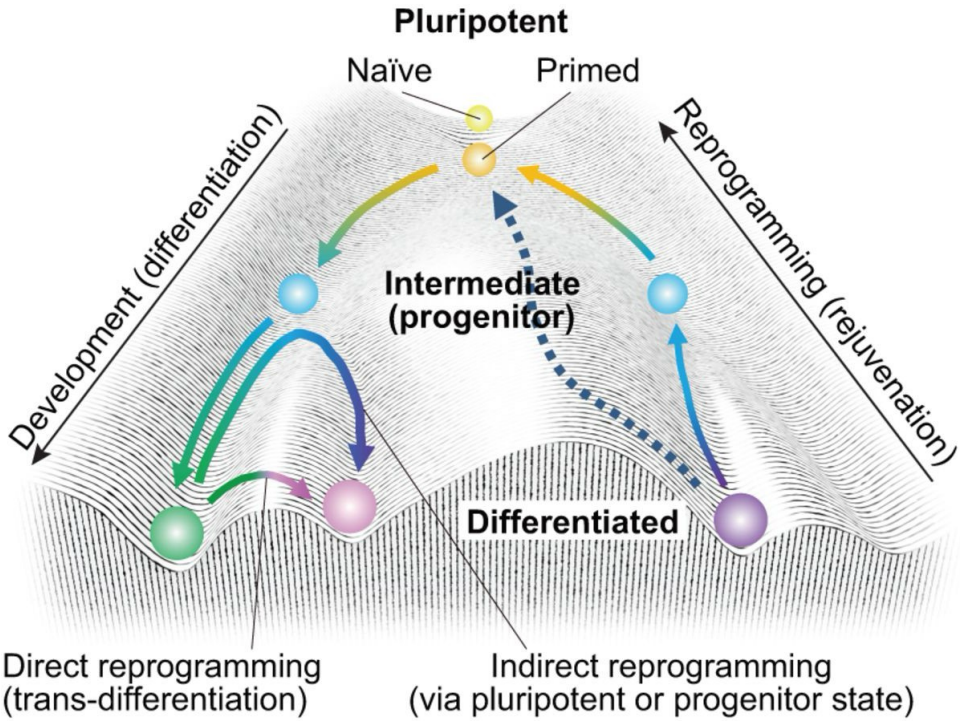

Figure 1.3 Cell fate conversions on the epigenetic landscape. Moving down the hierarchy of the landscape, beginning from the very top pluripotent naïve and primed stem cells (yellow and orange spheres) have the capacity of differentiating into any somatic lineage (green, pink) via the intermediate progenitor cells (blue) in a process called development. Direct reprogramming makes use of tissue-specific TFs to convert lineage committed cell (green) to another differentiated cell type (purple) without the need for pluripotent and intermediate

states. Indirect reprograming achieves the same goal via a combination of OSKM factors and optimal conditions to create a transient pluripotent state before lineage commitment. Reprogramming of mature somatic cells (purple) to pluripotent stem cells (yellow and orange) is achieved with or without the need for intermediate progenitor cell state (blue) by using OSKM factors (Takahashi, 2015). (Reprinted from Waddington, 1957).

1.2 Cell fate safeguard mechanisms

Cell fate safeguards play a critical role in maintaining a cell's identity and ensuring that gene expression is actively regulated rather than passively maintained. This active regulation is necessary because a cell's identity is not established through a single, definitive event and then permanently fixed. Instead, it is a dynamic process, as living organisms are constantly exposed to various exogenous and endogenous forces that can influence cell fate. These forces may include environmental cues, signaling pathways, or internal metabolic changes, all of which can potentially alter a cell's state. Thus, cell identity is not static but is actively maintained through mechanisms that counteract these potential disruptions. Cellular safeguards, which also act as barriers to reprogramming, help to maintain the ratio of positive and negative regulators of the cell state through modulating the synthesis and the degradation rate of the gene products and subsequently modulate their network and interactions with other proteins (Blau & Baltimore, 1991). During the trans-differentiation process, the ability of a TF to impose power over the aforementioned regulations and to overcome these safeguarding mechanisms in a given cell type, highlights the context dependency of cellular reprogramming and discloses the low efficiency of this process (Polo et al., 2010; Kolundzic et al. 2018; Wang et al., 2021).

The current scientific knowledge on cell fate decision regulation suggests, that it is significantly more diverse than previously understood. The concept has transformed from being a matter of chromatin accessibility to chromatin modifications, epigenetic

mechanisms, non-coding RNAs and RNA polymerase activity modulators, which are to both establish and maintain cellular identity (Parthun et al., 1996; Mattick and Rinn, 2015; Brumbaugh et al., 2019). Chromatin modifiers can repress and activate transcription of genes where they are needed, thus they can act as barriers to reprogramming. Some such chromatin modifiers that have been studied are members of the Polycomb group of proteins (PcG) and Trithorax group of proteins (trxG), both of which have been shown to play role during development and cell cycle regulation (Kuzmichev et al., 2002; Milne et al., 2002; Nakamura et al., 2002; Muller et al., 2002). Transcription factors (TFs) play diverse roles across various stages of the cell cycle and cell fate determination, from embryonic development to adulthood, adding a temporal dimension to their functions (Simon et al., 2013; Orlando et al., 2003). Recent research has further revealed that mitochondrial metabolites also serve as co-factors and signaling molecules for chromatin modifiers. Metabolites such as alpha-ketoglutarate (**α**-KG), acetyl coenzyme A (acetyl-CoA), citrate, and NADH/NAD+, along with other intermediates of the citric acid cycle, play critical roles in epigenetic modifications. These metabolites influence global gene expression and significantly impact cell fate decisions (Tsukada et al., 2006; Fomes & Terzic, 2014; Harvey et al., 2016). Among the chromatin-modifying enzymes affected by metabolic intermediates are histone methyltransferases (HMTs), histone acetyltransferases (HATs), NAD+-dependent histone deacetylases (HDACs), the sirtuin family of histone deacetylases, and Ten-Eleven Translocation (TET) dioxygenases (Shyh-Chang et al., 2013a; Xiao et al., 2012). These enzymes link cellular metabolism to epigenetic regulation, highlighting the intricate interplay between metabolic states and gene expression.

One of the very eminent reprogramming barriers to have been identified is the chromatin remodeling protein LIN-53 (*C. elegans* ortholog of mammalian CAF-1p48). LIN-53 is one of the components of the polycomb repressive complex. LIN-53 along

with Bmi1 had been shown to be barriers to reprogramming in *C. elegans* and mice respectively (Tursun et al., 2011; Cheloufi et al., 2015; Zhou et al., 2016). Moreover, another chromatin regulator complex called FACT (Facilitates Chromatin Transcription) was also found to be a barrier in reprogramming to neuronal fate in *C. elegans* (Kolundzic et al. 2018). Similarly, reprogramming efficiency had been documented to increase as the histone methyltransferases DOT1L was knocked down and this change had come forth through alteration of histone methylation patterns eventually impacting chromatin accessibility (Onder et al., 2012). Furthermore, the chromodomain containing chromatin regulator MRG-1 (Mortality factor-Related Gene) and SET1/MLL complex member RBBP-5, were identified as reprogramming barriers, that prevented germ cell conversion to neurons, confirming the existence and significance of epigenetic regulators as cell fate safeguards (Hajduskova et al., 2019; Kazmierzcak et al., 2020). Post-translational modification of genes involves modification to the gene products as seen in ubiquitylation of proteins. Another such example of post-translational modification is SUMOylation, which is addition of SUMO (small ubiquitin-like modifiers) to lysine residues. It had been shown that SUMO2 acted as a barrier in reprogramming during generation of iPSCs of mouse embryonic fibroblasts, as SUMO2 depletion enhanced reprogramming, signifying importance of such protein level modifications on cell fate changes (Borkent et al., 2016).

Some other epigenetic mechanisms to be implicated in chromatin structure and accessibility utilize histones (Bannister & Kouzadires, 2011; Allis & Jenuwein, 2016). Histones are found throughout the genome; they are used in folding DNA around to form the more compact form of chromatin called the heterochromatin. The study of histone modifications can raise a general idea of the regulatory landscape of the genome under certain treatments or conditions. For example, it has been shown that

trimethylation of histone 3 lysine 9 (H3K9me3) is correlated with reduced gene activity, it represses numerous genes required for pluripotency, thus reducing reprogramming efficiency by hindering the binding of TFs (Barski et al., 2007). Methyl groups can be added to both histones and the DNA. However, methylation of DNA is mostly associated with transcriptional repression unlike the methylation of histones, which can result in both decreased and increased levels of transcription (Zhang & Reinberg, 2001; Bird, 2002; Kouzarides, 2002).

It is not a surprise that some signal transduction pathways such as SMAD signaling in Transforming Growth Factor beta (TGF-β) family of receptors can also play role in cell fate, given their importance in cell development (Wrana & Attisano, 2000). In a study by Ladewing and colleagues, cellular signaling pathways of glycogen synthase kinase-3β (GSK-3β) and SMAD signaling were implicated in reprogramming of neonatal human fibroblasts into functional neuron-like cells (Ladewig et al., 2012).

Some of the more recent studies have also built some evidence on involvement of metabolism in cell fate and identity. It has been noted that during the human pluripotent stem cell transition to endoderm and mesoderm metabolic switching happens from glycolysis to oxidative phosphorylation, showing that metabolic switching is germ layer specific (Cliff et al., 2017). In a study by Tatapudy et al., involvement of metabolism in cell fate was described as being one of the drivers of differentiation instead of shifts in metabolism being byproducts of changes in cellular state (Tatapudy et al., 2017). This phenomenon has also been observed in the reprogramming of induced pluripotent stem cells (iPSCs), where metabolic shifts, such as the transition from oxidative phosphorylation (OXPHOS) to glycolysis, occur prior to changes in gene expression (Hansson et al., 2012). Building on this

observation, it is reasonable to hypothesize that cell fate safeguards may be embedded within metabolic and mitochondrial mechanisms.

It is increasingly evident that cell fate safeguards are numerous and have evolved over time to ensure the healthy development of organisms through multiple, interconnected cellular pathways. These safeguards are deeply integrated into various aspects of cellular machinery, reflecting their critical role in maintaining cellular identity and function. The interplay between mitochondria and cellular reprogramming has given rise to a new field of study known as metabolic reprogramming (Ryall et al., 2015). However, due to the relatively recent emergence of this field, the regulatory mechanisms driven by metabolic events, their conservation across species, and their roles in developmental processes remain poorly understood. Further research is urgently needed to unravel these complex relationships and their implications for cellular behavior and organismal development.

1.3 Metabolic reprogramming, the mitochondria derived changes in cell identity

Energy supply is necessary for living beings. In eukaryotes an organelle known as the powerhouse of the cell, called the mitochondria, is highly specialized and dedicated to efficient production of adenosine triphosphate, ATP (Kuhlbrandt, 2015). The chemical energy is derived from breaking bonds in carbon-based molecules. Aerobic organisms use oxygen to release the chemical energy stored in glucose to produce ATP in an electron transport linked process called oxidative phosphorylation (OXPHOS), which is the most ATP generating step in the cell (Rajendran et al., 2017). Citric acid cycle also named tricarboxylic acid cycle (TCA) is where acetyl coenzyme A (CoA) is modified in the mitochondria to produce other metabolic precursors for OXPHOS (Berg JM et al., 2002; Melendez-Hevia et al., 1995). Nearly all organisms

carry out glycolysis as part of their metabolism, which similarly provides energy in form of ATP. However, it has a lower ATP output and takes place in the cytoplasm. In eukaryotes this step provides the pyruvate needed for OXPHOS. In certain cells aerobic glycolysis, also termed "the Warburg effect", is observed to function as a less efficient but major energy provider in rapidly proliferating cells such as cancer cells, progenitor cells and stem cells (Vander Heiden et al., 2009; Shyh Chung et al., 2013). The Warburg effect helps cancer cells to proliferate at a higher rate by retaining a rather undifferentiated state which is also characterized by poorly developed and isolated mitochondrial structures (Guerra et al., 2017). A similar pattern can be observed during the embryonic development of mice; as the naïve or primed stem cells start to differentiate into rather specialized cells, the mitochondrial size increases shifting to OXPHOS for respiration (Folmes et al., 2011). Apart from the energy production duties, mitochondrial dynamics has other considerable implications in the cell. Respiration and metabolic reactions produce a wide variety of chemical reactions resulting in metabolites involved in mitochondria, ranging from amino acids to phospholipids; nucleotides contributing to cell division, reactive oxygen species (ROS) signaling and Ca^{+} storage. (Ly et al., 2020; Lunt and Vander Heiden, 2011; Flippo & Strack, 2017). Depending on the function and size of the cell, the demand for energy production changes in that particular cell type (Harvey, 2019). Naturally, the energy demand of cells also changes during different phases of the development, for example during the earlier stages of the embryonic development the mitochondria is observed to have a rather poorly developed membrane of cristae which generate ATP via electron transport chain (Blerkom et al., 2019). However, the more developed somatic cells show more complex, tubular, dense matrix and higher levels of mitochondrial DNA due to progressive differentiation (John et al., 2005; Suhr et al., 2010; Folmes and Nelson, 2011). It is also important to note that mitochondria possess their own DNA, known as mitochondrial DNA (mtDNA). Certain proteins

essential for mitochondrial function are encoded exclusively by mtDNA, and the replication of mtDNA occurs within the mitochondria itself. The structure, number, and dynamics of mitochondria, such as fusion and fission, vary depending on the cell type and its developmental or functional stage (Wai & Langer, 2016).

As differentiation progresses in multicellular organisms, cells undergo lineage commitment and become increasingly specialized. To meet the heightened energy demands of these specialized cells, the three-dimensional mass of mitochondria expands (Chung et al., 2007; Picard & Shirihai, 2022). As cells become more specialized, their reliance on efficient mitochondrial ATP production grows. This pattern is evident in cells like cardiomyocytes, where increased mitochondrial matrix complexity supports their biological functions (Hom et al., 2011). Additionally, mitochondrial development is not only linked to energy production but also to cellular signaling. For instance, increased reactive oxygen species (ROS) output from developed mitochondria has been shown to drive differentiation in adipocytes (Tormos et al., 2011; Lee et al., 2009). This weaves mitochondria into the web of cell fate decision making process rather than a spectator to the unfolding biological events.

With such important function in the cell, it can be expected that the mitochondria play role in cellular differentiation. It has been documented that the process of differentiation is a multifaceted concept and has many layers extending from epigenomic, transcriptomic, proteomic to metabolic levels. Thus, the study of cellular identity and differentiation can be furthered through multiple means. Metabolism and its functional intermediates extend from the mitochondria to the nucleus to orchestrate a series of mechanisms, which shape the path cells take on throughout an organism's life. This highly encourages science to take a new approach in studying

the subject of cell fate and reprogramming through metabolism and the dissection of its mechanisms which lead to various cellular identities. A large array of metabolites which were previously thought to be only byproducts of metabolism have recently been studied for their properties as signaling molecules, co-factors for enzymes and as modifiers for epigenetic regulators. Recent studies have shown that increased ROS levels have been associated with better reprogramming and that ROS activate developmental gene expression via NFR2 pathway dependent manner (Zhou et al., 2016; Khacho et al., 2016). Alpha ketoglutarate (a-KG) a metabolite in the TCA cycle has been reported to induce histone demethylation via the activity of various demethylases and translocation enzymes, a-KG has also been shown to extend lifespan through inhibiting ATP synthase and interacting with target of rapamycin (TOR) pathway (Kaelin & McKnight, 2013; Chin et al., 2014). Moreover, some studies have demonstrated that dominant defects in TCA cycle related enzymes isocitrate dehydrogenase (IDH), succinate dehydrogenase (SDH), and fumarase have resulted in tumorigenesis (Raimundo et al., 2011; Martinez-Reyes & Chandel, 2020). Moreover, other metabolites such as acetyl CoA, citrate and NADH/NAD^+ have proven to be of great importance for epigenetic changes in stem cell maintenance and self-renewal (Figure 1.4). The crucial activity of histone modifiers, such as methyl transferases and demethylases, depend on intracellular levels of metabolites; S-Adenosyl methionine (SAM), serine, glycine, a-KG, succinate and fumarate (Shi et al., 2004; Tsukada et al., 2006).

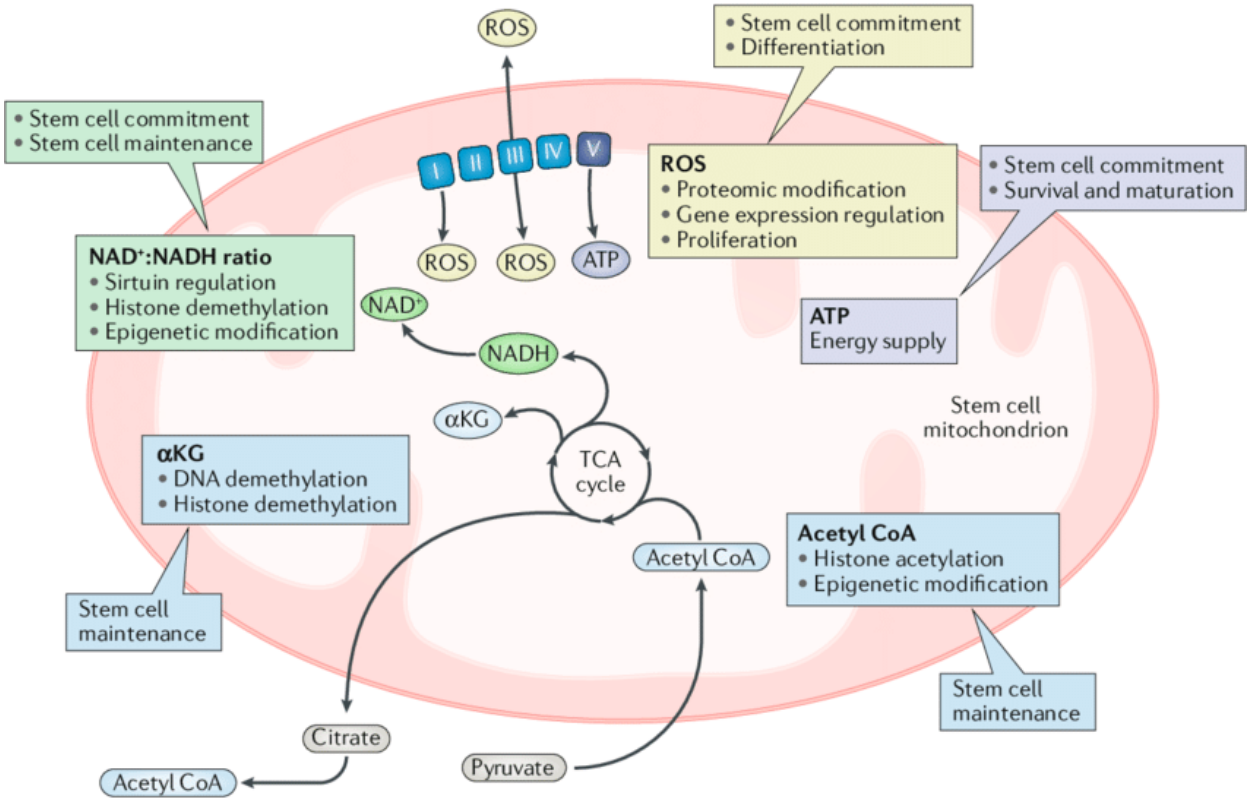

Figure 1.4 Regulation of stem cell functions by mitochondrial metabolism. Metabolites generated in tricarboxylic acid (TCA) cycle namely, nicotinamide adenosyl diphosphate NAD+/NADH, reactive oxygen species (ROS), adenosine triphosphate (ATP), Acetyl CoA, a-ketoglutarate (a-KG) affect multiple aspects of stem cell maintenance and function. The color-coded boxes green, yellow, purple, and blue, each feature one of the prospects of stem cell development and maintenance (Reprinted from Khacho et al., 2019).

1.4 NAD⁺ dependent mitochondrial isocitrate dehydrogenase

The mitochondrial enzyme isocitrate dehydrogenase 3 (IDH3) of *C. elegans* has 3 subunits, α, β, γ each coded by genes *idha-1*, *idhb-1* and *idhg-1*, respectively. Among these IDHA-1 and IDHG-1 subunits are the catalytically active subunits, and form homodimers, while IDHB-1 subunit mostly provides structural support to the isocitrate dehydrogenase enzyme complex. *idha-1* codes for the most catalytically active subunit (Huh et al., 1996; Dang et al., 2016). Isocitrate dehydrogenase is responsible

for production of a-KG in TCA cycle (Lunt & Vander Heiden, 2011). The human ortholog of the gene (IDH3A) shares a 96% amino acid homology with IDH3 (WormBase). In a study conducted by Kolundzic et al., *idha-1* and *idhg-1* were found to be barriers to reprogramming of *C. elegans* germ cells into ASE neurons (Kolundzic et al., 2018; Ul Fatima, Unpublished). Lifespan extension has been reported in animals overexpressing *idha-1* through elevating tolerance to oxidative stress and possible involvement of *idha-1* mediated lifespan in TOR signaling pathway (ZH Lin et al., 2022). This extension in lifespan of animals overexpressing *idha-1,* may be attributed to increased levels of a-KG as the reduction of a-KG levels has been shown to have the very opposite effect. In one study, relative decrease in a-KG level compared to its antagonists, succinate and fumarate were reported to promote a switch to glycolysis in cancer associated fibroblasts (Zhang et al., 2015).

IDH has three isoforms, IDH1, IDH2 and IDH3. While IDH1 and IDH2 are $NADP^+$ dependent, IDH3 depends on NAD^+ (ZH Lin et al., 2022). The molecule nicotinamide adenine dinucleotide (NAD^+) is one of the most common cellular co-enzymes in living cells involved in metabolic reactions cell signaling and regulatory processes (Canto et al., 2015; Conlon, 2021). The decrease of NAD^+ levels has been documented in aging due to its reduced synthesis, while its replenishment is associated with an increase in lifespan and better health markers (Reiten et al., 2021). The ratio of NAD^+ to NADH has been reported to be of significant importance for maintenance of stem cell fate as it is a classical co-enzyme mediating many redox reactions and is depleted by sirtuin family of deacetylases (Imai & Guarente, 2014). NAD^+ and NADH are both produced and used in multiple cellular reactions including TCA cycle, OXPHOS and glycolysis, but the stability in ratio of NADH:NAD^+ is of critical importance in longevity, energy state, cell signaling, apoptosis and gene regulation (Canto et al., 2012; Ying, 2008; Imai et al., 2000) (Figure 1.5).

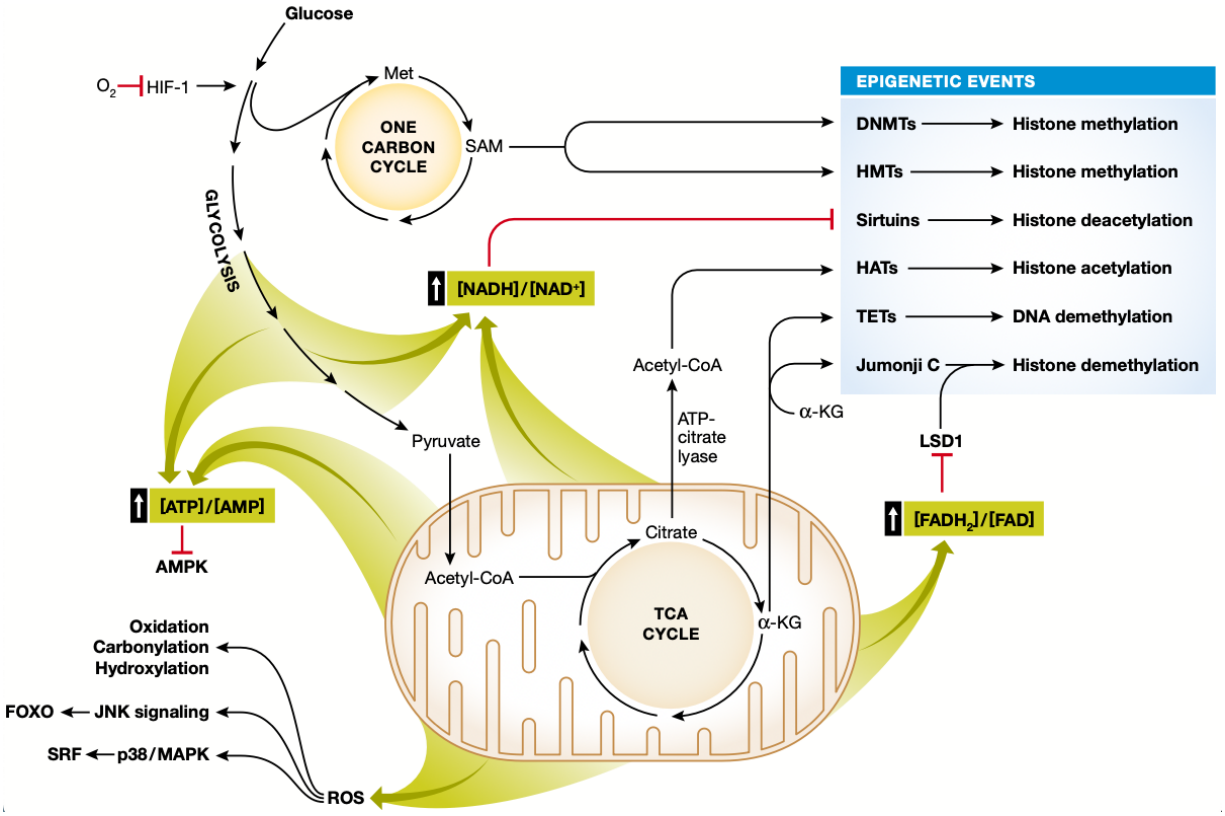

Figure 1.5 The connection between cell fate decision and metabolism. Metabolic inputs can influence the epigenetic landscape and cell signaling pathways, which regulate and maintain the cell fate. In the cytoplasm metabolites produced during glycolysis feed into folate and one carbon metabolism cycle to produce S-adenosylmethionine (SAM), which is a cofactor for DNA methyltransferases (DNMTs) and histone methyltransferases (HMTs). The availability of NAD^+, a cofactor for sirtuin, decreases during energy production as during glycolysis NAD^+ is converted to NADH. Moreover, AMP an activator to AMP-activated protein kinase (AMPK) is converted to ATP, similarly activated by energy production. Acetyl-CoA, derived from pyruvate, can enter the tricarboxylic acid (TCA) cycle after being converted into citrate. Conversely, citrate can be converted back into acetyl-CoA through the activity of ATP-citrate lyase. The resulting acetyl-CoA can then contribute to the nuclear acetyl-CoA pool, where it serves as a substrate for histone acetylation reactions catalyzed by histone acetyltransferases (HATs). Another key metabolite of the TCA cycle, alpha-ketoglutarate (**a**-KG), acts as a cofactor for enzymes such as TET and Jumanji C (JmjC), which are involved in the demethylation of DNA and histones, respectively. Additionally, increased oxidative phosphorylation (OXPHOS) generates reactive oxygen species (ROS), which promote oxidative modifications such as carbonylation and hydroxylation. ROS also enhance the activity of

the JNK/p38 MAPK signaling pathway. Under low oxygen conditions, glycolysis is upregulated by the hypoxia-inducible factor-1 (HIF-1), which promotes metabolic adaptation to hypoxia (Adapted from Tatapudy et al., 2017).

1.5 *C. elegans* as a model organism

C. elegans is a soil dwelling nematode that is found throughout the world. It was first used and made popular in a laboratory setting by Sydney Brenner (1974). Introduction of *C. elegans* was paced relatively fast as scientists found ease with handling this small animal and soon it became a well-established model organism. The fame of this nematode was due to multiple factors. One of the key advantages of *C. elegans* is its ease of maintenance, attributed to its small size, simple feeding requirements, and ability to thrive on petri dishes, as well as its short life cycle (Corsi et al., 2005). Beyond these practical benefits, *C. elegans* possesses several molecular qualities that make it particularly attractive to geneticists. These include the ease of genetic manipulation, the ability to cross individual strains with different genetic backgrounds, and the capacity to produce offspring with traceable lineages. Since 1998, the *C. elegans* genome has been fully mapped and it was the first multicellular organism to have its genome sequenced (*C. elegans Sequencing Consortium*, 1998). Approximately 60% of the *C. elegans* genes have homologs in the human genome and about 83% of the *C. elegans* proteome has homologs with the human proteome (Sonnhammer & Durbin,1997; Hung Lai, 2010). This high level of homology also harbours with it important pathways such as Notch, Ras, Wnt and insulin signaling, which are highly implicated in human diseases (Baumeister et al., 2002). The transparent animal can be easily visualized under a dissection bright-field microscope and differential interference contrast (DIC) imaging microscope. Moreover, by fluorescent labelling of various proteins of cellular compartments, different tissues such as the muscles, germline, neurons, digestive track, and the epidermis can also be visualized (Figure

1.6). The resulting genetically engineered animals can be used to study cell development, protein-protein interactions and tracing of different cell lineages. (Corsi et al., 2015; Boulin et al., 2006). Both wild type and the transgenic strains of *C. elegans* can be frozen and retrieved from -80°C long term storage, providing ease in handling multiple strains simultaneously and permit creation of great collections of various strains (Brenner, 1974; Corsi et al., 2015).

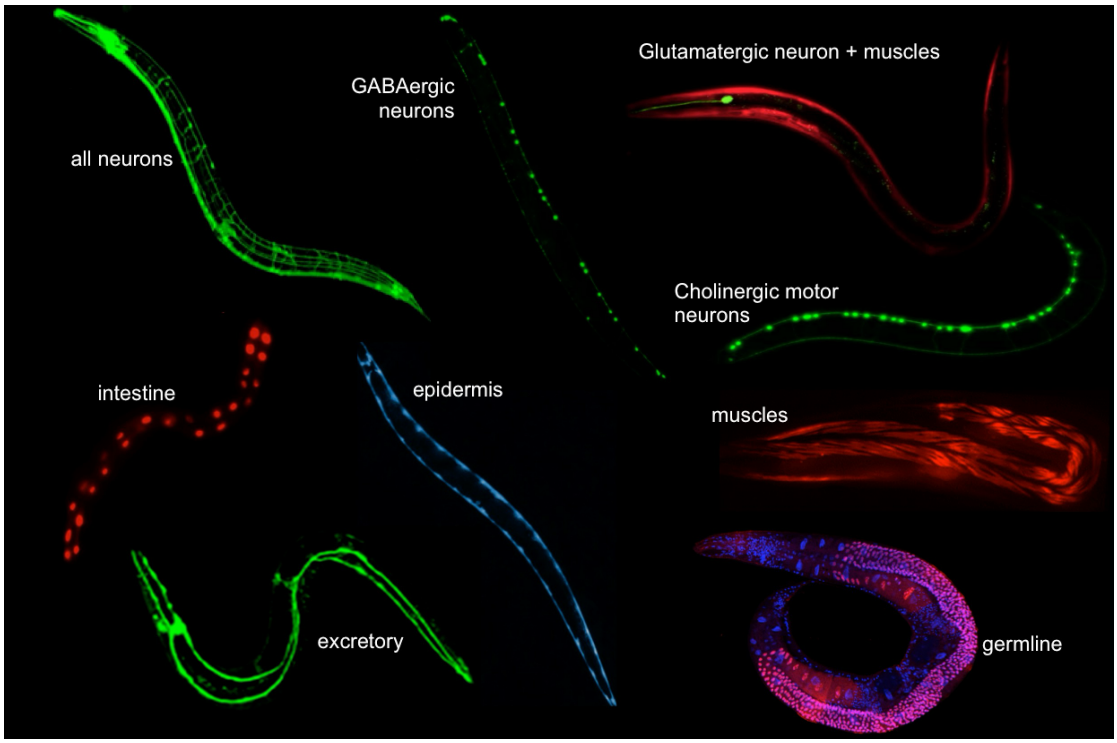

Figure 1.6 Fluorescent labelling of *C. elegans* tissues. Translucent body of *C. elegans* can be fluorescently labelled and visualized. By utilizing tissue specific promoters, a certain subset of cells can express reporter genes fused with fluorescent protein sequence insertions. Fluorescently labelled tissues and cells can be localized in vivo - neuronal cells, muscle tissues, the germline, epidermal tissue and intestinal lining (Tursun et al.).

C. elegans has also established itself as a well-studied model organism in the field of reprogramming. In 1994, Jin et al. demonstrated the TF UNC-30 to be a terminal selector for GABAergic neurons controlling locomotion in the animal. Ectopic

expression of the TF caused emergence of GABAergic neuronal characteristics in other somatic cells. Since then, a number of other transcription factors have also been studied in reprogramming *C. elegans* cells. The *C. elegans* homolog to human MyoD, HLH-1, was shown to induce muscle fate when ectopically expressed in the embryos (Fukushige & Krause, 2005). Moreover, it has been reported that endoderm specifying GATA factor END-1, when ubiquitously expressed in embryos, caused expression of endoderm in ectodermal and mesodermal lineages (Zhu et al., 1998). Similarly, ectopic expression of the gut-specifying *elt-2* gene in the early embryos was shown to cause induction of gut fate markers in almost all the cells during reprogramming (Fukushige et al., 1998). Tursun et al. carried out another study and identified the zinc-finger TF CHE-1 to be a terminal selector in gustatory ASE neuronal fate (Tursun et al., 2011). They used a transgenic model of *C. elegans* with a heat shock inducible promoter that drove *che-1* overexpression (CHE-1^{oe}), and also expressed a GFP protein fused to *gcy-5* (*gcy-5^{prom}::GFP*) normally expressed in the right ASE neuron as a fate reporter (Figure 1.7) (Yu et al.,1997; Tursun et al., 2011; Patel et al., 2012).

Ubiquitous overexpression of CHE-1 in early gastrulation stage embryos causes broad activation of ASE neuron fate and results in deformations and developmental arrest in embryos. However, the broad induction of the heat shock CHE-1^{oe} becomes increasingly more restricted during the later developmental stages, at L4 and adult stages only a handful of anterior neurons express the *gcy-5^{prom}::GFP* reporter, indicating that, these cells provide the molecular context susceptible to *che-1* activity (Patel and Hobert, 2017; Tursun et al., 2011). Similarly, the efficiency of reprogramming by the MyoD homolog HLH-1 had also been reported to decrease in the embryos of later stages (Fukushige & Krause, 2005). Moreover, the TF PHA-4, inducing the pharynx fate, was also shown to be restricted to earlier stages of the development (Horner et al., 1998; Mango et al., 1994). These experiments point out

to the eventual loss of the cellular plasticity as differentiation changes the cell state. This in return conceals the ability of fate-determining TFs from functioning broadly in the soma. The loss of plasticity in differentiated cells has been linked to the activity of Polycomb group complex 2 (PRC2) protein MES-2/E(Z) (Yuzyuk et al., 2009). During the progression of the development PRC2 recognizes the chromatin structure and reorganizes it to restrict the plasticity of blastomeres in developing embryos (Yuzyuk et al., 2009).

Using the heat shock inducible promoter driven CHE-1^{oe} transgenic model, Tursun and colleagues identified the conserved histone chaperone LIN-53 (mammalian CAF-1p48/RBBP4/7) to be a barrier in reprogramming of germ cells into neuron- or muscle-like cells (Tursun et al., 2011). Moreover, other members of the PRC2, such as *mes-2*, *mes-3*, *mes-6* were also found to be reprogramming barriers and that GLP-1/Notch signaling pathway antagonized PRC2, in addition to the fact that GLP-1/Notch signaling was observed to play a critical role in maintenance of undifferentiated germline stem cells/progenitors (Patel et al., 2012; Seelk et al., 2016). More recently, using the same CHE-1^{oe} system, the chromatin regulator FACT was also found to act as a reprogramming barrier in conversion of intestinal cells and germ cells into ASE neuron-like cells in *C. elegans* and in reprogramming of human fibroblasts into iPSCs (Kolundzic et al., 2018).

Studying reprogramming in an *in vivo* model offers the great advantage of studying a more complete system and provides full understanding of how reprogramming might work in complex organisms as opposed to *in vitro* studies. Reprogramming in *C. elegans* relies on already differentiated cells and has no use of embryonic stem cells, which eliminates some of ethical limitations and moral issues to be considered in this field of research. The recent findings not only shed light on the role played by

chromatin regulators and histone modifiers in cell fate conversion, but also demonstrate the conserved mechanisms shared between *C. elegans* and mammals revealing a great potential for the field of cell fate reprogramming.

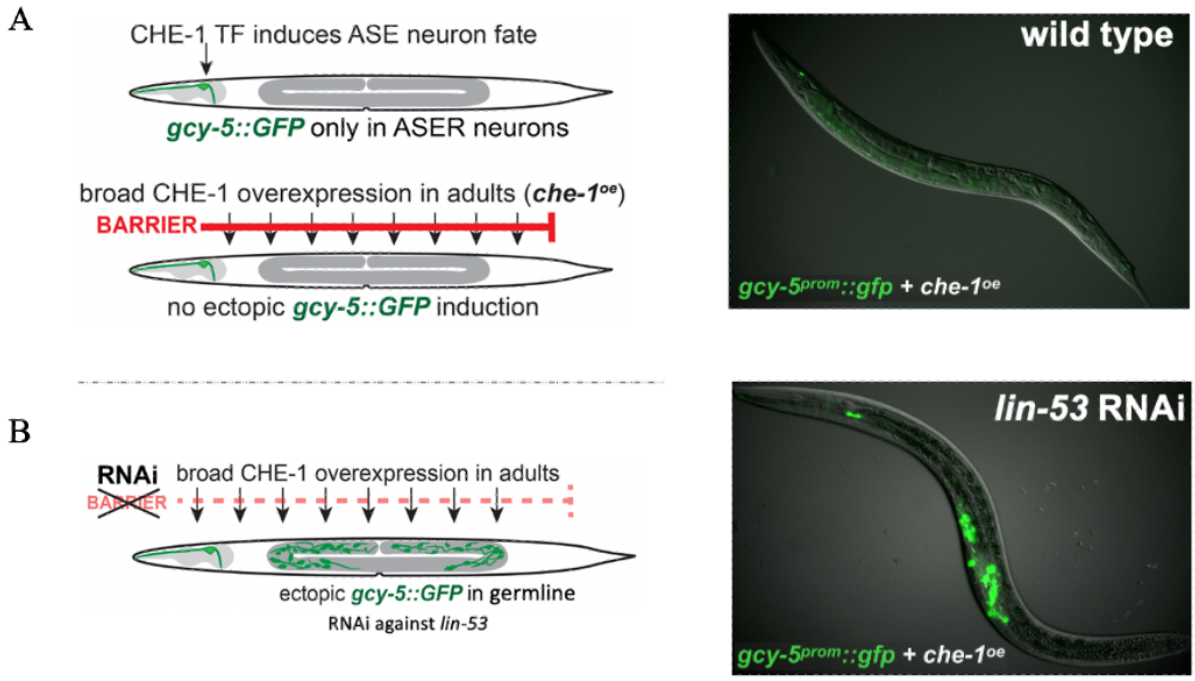

Figure 1.7 The germline conversion phenotype upon overcoming reprograming barriers. A) the glutamatergic taste neuronal fate marked by *gcy-5* ^{prom}*::GFP* reporter is expressed in the right ASE neuron induced by CHE-1 TF overexpression. However, expression of *gcy-5* ^{prom}*::GFP* reporter in other tissues is blocked due to reprogramming barriers. B) The simultaneous broad expression of CHE-1 TF and depletion of the reprogramming barrier (red line) via RNAi induces ectopic expression of the ASE neuronal fate in the germline of the animals (Ul Fatima, Unpublished).

1.6 *C. elegans* life cycle

C. elegans by its nature is a hermaphroditic (they/them) animal. Most animals harbor features of the male and female anatomy both spermatocytes and oocytes. On a very low frequency of about 0.2% of the animals are male. In nature this often occurs after stressful environmental conditions such as severe heat or drought which drives the prevalence of males. In theory, this enables transfer of genes across individuals and helps maintain genetic diversity within a population in contrast to self-fertilization which normally leads to every generation to be clones of the previous generation.

C. elegans has a relatively short life cycle. It is approximately 3 days at favorable conditions, which is temperatures between 10°C and 22°C. The life cycle consists of the egg development, growing of the larvae from the larval stages L1 to L4, the adult stage and finally the egg laying hermaphrodite (Figure 1.8). An alternative path can be taken for *C. elegans* at L2 stage if energy needs of the animal are not met. This is called the Dauer stage. In this form, the animal can live for several months in search for food. In the presence of food, they can re-enter L4 and complete the larval stages into adulthood. A hermaphrodite can lay between 300 to 350 self-fertilized eggs and perhaps more in presence of a fertile male. Every egg is laid at the 24-cell stage. The hard-shelled egg completes its maturation outside the parent and the full embryogenesis takes approximately 16 hours. The remaining life span of *C. elegans* after having already reached the adult stage is 2 to 3 weeks in approximation (Wormatlas).

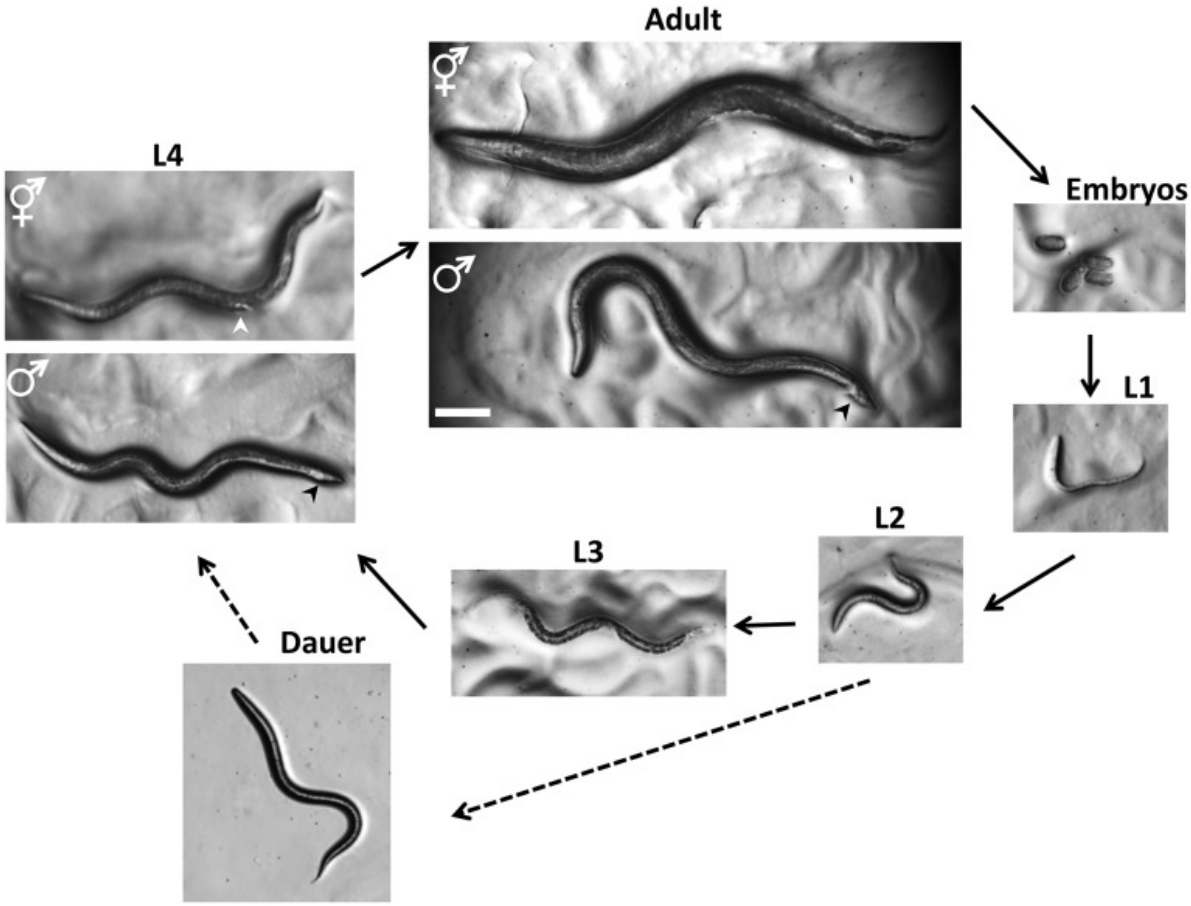

Figure 1.8 Life cycle of *C. elegans*. *C. elegans* life cycle consists of four larval stages and adulthood. Until the L4 stage the individual sexes are not easily distinguishable. At this stage, hermaphrodites form a tapered tail, and the vulva (white arrow) develops as a lightly colored crescent in the center of the ventral side. The L4 males have a wider tail. In adults, the hermaphrodites are distinguished by wider girth and tapered tail, while the males maintain a slimmer girth and a fan-shaped tail (black arrow). The Dauer larvae are the slimmest of all the other larval stage animals. Bar: 0.1 mm (Reprinted from Corsi et al., 2015)

1.7 *C. elegans* germline and the somatic gonad

The highly reproductive hermaphroditic animal, *C. elegans*, owes its evolutionary success to its efficient reproductive system where gametogenesis takes place. A large portion of the *C. elegans* anatomy is designated for reproduction. The germline starts forming at an early stage during the development, this corresponds to primordial germ cell (PGC) specification, which give rise to the oocyte and spermatozoa and the early separation of the tissues in itself ensures the maintenance of totipotency (the ability to give rise to all the tissues) (Marlow, 2015; Sybirna et al., 2019; Sepulveda-Rincon et al., 2024). At 16-24 cell stage of embryogenesis the germline and the soma start to become distinct tissues (Sulston et al., 1983). The germline and the soma are separated yet in contact through the somatic gonad, which affects organization of the tissues and the development of the *C. elegans* (McCarter et al., 1997; Hall et al., 1999). Before the L2/L3 larval molt the germline and the somatic gonad are in an intercalated network. During this stage the germline forms a large cytoplasmic mass called the syncytium, which is characterized by the germ cells connecting to one another through poorly defined borders and a central canal called the rachis (Hirsch et al., 1976).

The germline consists of two gonadal arms. The components of each arm are the distal tip cells (DTCs), mitotic zone, Pachytene and spermatheca. Both arms connect at the uterus and embryos exit through the vulva (Figure 1. 9). The DTC, at the most distal end of the gonadal arm forms a basis to generate mitotic signals which causes mitosis in the adjacent germline stem cells (GSC) (Byrd et al., 2014). Then as the germ cells go through the stages of meiosis they move away from DTC and pass through the transition zone (Hirsch et al., 1976). Moving through the pachytene the cells grow to form the oocytes and reach the proximal arm. Major sperm cytoskeletal protein (MSP) causes oocyte maturation and gonadal sheath contraction which directs the

oocytes into spermatheca for fertilization (Miller et al., 2001). The fertilized egg develops into an embryo.

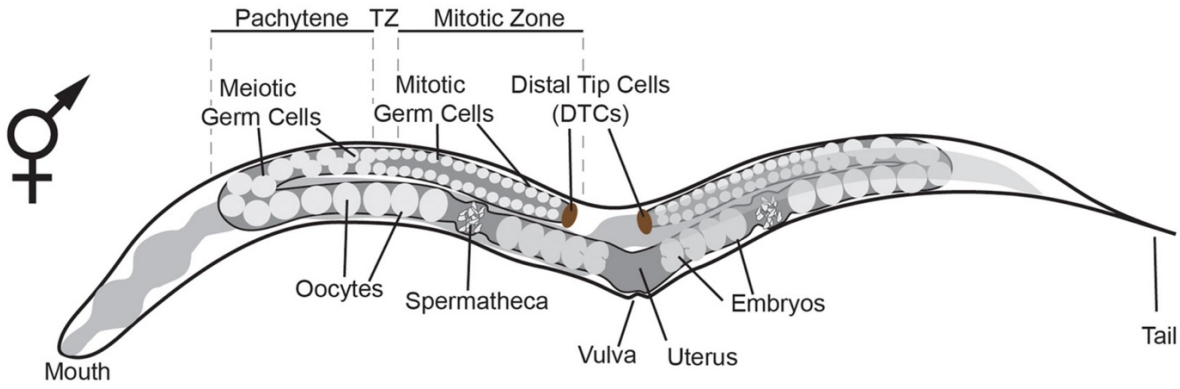

Figure 1.9 Schematic depiction of *C. elegans* germline. The germline consists of two gonadal arms. At the very tip of every gonadal arm, mitotic division signals are generated by distal tip cells (DTC). Subsequently germ cells go through mitosis, meiosis, form the oocytes and finally pass through spermatheca to be fertilized. The fertilized eggs form embryos passing through the uterus and finally exit the parental worm via vulva (Reprinted from Marchal & Tursun, 2021).

Spermatogenesis takes place during the L4 stage of the life cycle in both male and hermaphrodites. However, in hermaphrodites the germline ceases spermatogenesis and switches to oogenesis in adult stage during which the produced sperm are consequently used for fertilizing oocytes throughout the reproductive life of the *C. elegans* (L'Hernault, 2006).

Despite the major physiological differences between hermaphrodites and the males, spermatogenesis is similar in both (Figure 1.10). Spermatids accumulated in the proximal gonadal arms are pushed into spermatheca along with the ovulation which rapidly transforms spermatids into spermatozoa for fertilization (L'Hernault, 2006). There are about 40 genes involved in healthy spermatogenesis in both genders (L'Hernault & Singson, 2000). However, spermatogenesis in hermaphrodites and

males still differs in two known ways, the first difference being the larger size of the spermatozoa produced by true males and the second difference is the involvement of *spe-8* pathway in fertile hermaphrodite spermatogenesis (L'Hernault et al., 1998; Minniti et al., 1996; Nance at al., 1999 Nance at al., 2000; Shakes & Ward, 1989).

The somatic gonad of *C. elegans* is the nematode's non-reproductive part of the gonad. It comprises of the sheath cells and the DTC. The somatic gonad provides structural support through the gonadal sheath cells, it aids in the maintenance of germline stem cells by DTCs and also helps in development of the germline (Kimble & Hirsh, 1979; Hall et al., 1999; Greenstein, 2005). In the proximal gonad, the early oocytes and the gonadal sheath cells connect through gap junctions which cease to exist upon ovulation as the oocyte is pushed further down the gonadal arm by contractions of the gonadal sheath cells (Hall et al., 1999). Another plausible and important interaction between the germline and the somatic gonad is the interaction between LAG-2, that is a Delta/Serrate/LAG-2 ligand family protein and GLP-1, which is a LIN-12/Notch/GLP-1 family of transmembrane receptors. LAG-2 signals sourced from the DTC interact with germline receptors encoded by *glp-1* gene, which maintain the stem cell niche in the gonads (Lambie & Kimble, 1991; Tax et al., 1994; Henderson et al., 1994, Austin & Kimble, 1987; Yochem & Greenwald, 1989). Maintenance of the germline stem cells is of outmost importance for the *C. elegance* life cycle. The germline of *C. elegans* is one of the most frequently studied tissues in developmental and genetic studies due to its receptive nature (Kimble & Ward 1988; Shedl, 1997).

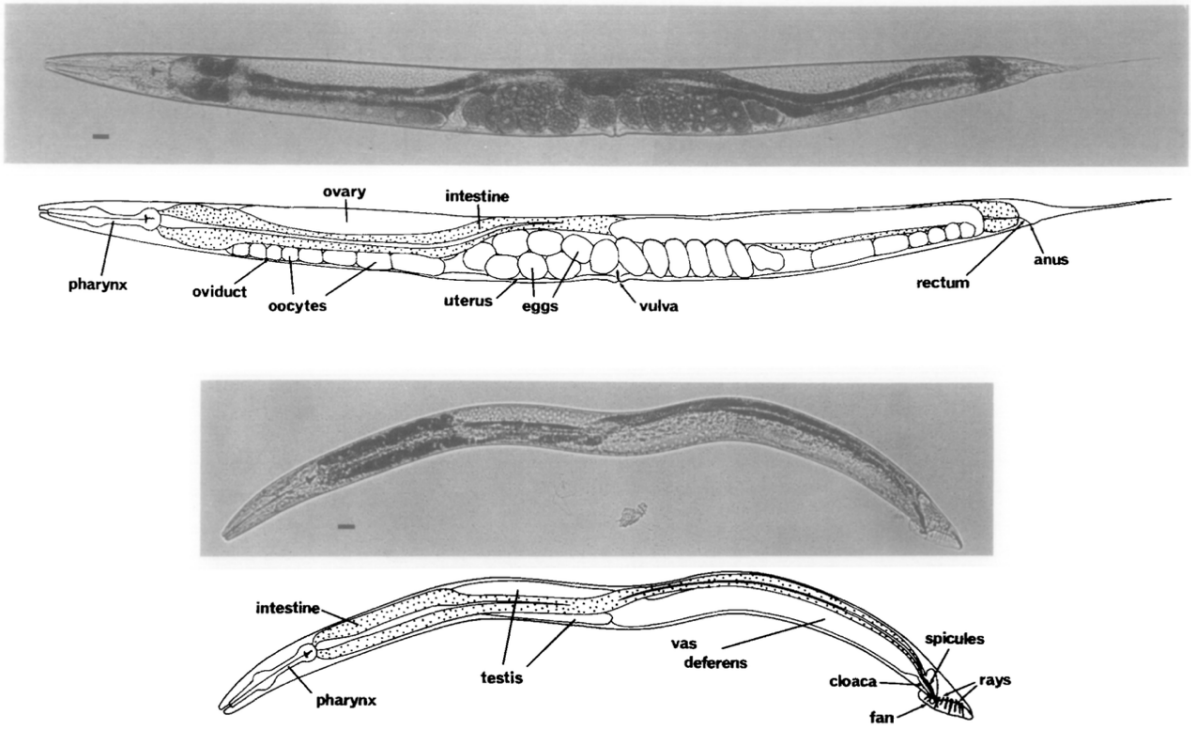

Figure 1.10 Hermaphrodite and male physiological differences in *C. elegans*. Above, adult hermaphrodite, below, male. Lateral view and bright field illumination 137x. Bar: 20 µm
(Reprinted Sulston & Horvitz, 1977)

1.8 Aim of the project

Based on our accumulated knowledge of cell fate regulation *in vivo*, we have identified various factors involved in cellular functions. Some of these factors are well-known regulators, such as chromatin modifiers, aging-related genes, and transcription factors, while others are more unexpected, including mitochondrial enzymes. The primary goal of this project was to identify mitochondrial safeguarding mechanisms that hinder CHE-1 transcription factor (TF)-induced cell fate conversion in *C. elegans*.

During this project, we studied various aspects of reprogramming the germline into ASE neuron-like cells. My work involved dissecting the reprogramming mechanisms

which lead from the mitochondria to the nucleus upon overexpression of the TF CHE-1 along with simultaneous knockdown of the cell fate safeguard, *idha-1*, the catalytically active component of conserved mitochondrial enzyme isocitrate dehydrogenase 3 (IDH3). We hypothesized IDH3 depletion-mediated reprogramming caused disturbances to numerous biochemical reactions in the TCA cycle, an integral component of the metabolism, which produces precursors to reducing agents, energy, amino acids, various metabolites and crucial co-factors to DNA and chromatin modifiers and maintains cellular homeostasis. Moreover, we hypothesized a crosstalk between germline and non-germline tissues to be involved in this fate change. My work also aimed to identify the type of cells reprogramming in the germline in respect to male and female reproductive physiology. Another subset of the experiments carried out in this project consisted of integrating the IDH3 depletion-mediated reprogramming along with components of other well studied cellular machinery and signaling pathways, which were known to lead to the nucleus.

Studying reprogramming of differentiated mature cells plays a pivotal role in development of personalized regenerative medicine. It becomes vital in treating patients with neurodegenerative and metabolic diseases, as it strengthens our current knowledge on patient derived cell therapies. We are determined that our research will shed light on the involvement of metabolism on neuron health and endorse advancements in therapeutic techniques designed for the increasing numbers of patients suffering from metabolic disorders and age-related neurological pathologies.

2 RESULTS

2.1 Depletion of mitochondrial isocitrate dehydrogenase promotes the expression of ASE neuron fate marker in the germline

With the rationale that barriers may block direct cellular reprograming, a genome-wide RNA interreference (RNAi) screen was conducted. From a library of approximately 20,000 genes, approximately 170 candidates were found to cause ectopic expression of the ASE neuronal reporter, suggesting successful cellular reprogramming. This reprogramming phenotype was first observed in the whole-genome RNAi screen conducted by Kolundzic and colleagues using the Ahringer *C. elegans* RNAi library. This library is a comprehensive collection of bacterial strains designed for RNAi, enabling systematic gene knockdown in *C. elegans*. The screen utilized a transgenic animal model expressing a heat-shock-inducible transcription factor, CHE-1, and a *gcy-5* ^{prom}*::GFP* fluorescent reporter specific to the right ASE neuron in the head (Tursun et al., 2011). Previous studies demonstrated that depletion of mitochondrial isocitrate dehydrogenase (IDH-3), which catalyzes the conversion of isocitrate to alpha-ketoglutarate (**α**-KG), induces reprogramming of germ cells into ASE neurons (Kolundzic et al., 2018; Ul Fatima, unpublished).

For the RNAi treatment, P0 animals were initially cultured on OP50 bacteria until the L4 stage and then transferred to RNAi bacterial plates to silence genes potentially safeguarding cell fate. The L4 stage F1 generation was heat-shocked for 30 minutes at 37°C and scored the following day for reprogramming-positive animals after an overnight incubation period at 25°C. The timing of RNAi treatment has been shown to be critical for reprogramming efficiency, as reported by Kamath and colleagues (2000). A similar timing pattern was observed with *lin-53* depletion-mediated direct cellular reprogramming, where RNAi treatment in the P0 generation primed the germline of the F1 progeny to become more permissive to reprogramming. This

finding established the basis for the current experimental protocol (Tursun et al., 2011; Patel et al., 2012; Seelk et al., 2016).

Given the growing interest in metabolism research the role of mitochondrial activity in cell proliferation, pluripotency and differentiation, *idha-1* depletion-mediated reprogramming became the focal point of our research (Lee, 2024; Xu et al., 2013). IDH-3 consists of two alpha subunits, one beta and one gamma subunit. The catalytically active subunits are coded by the *idha-1* (α subunit) and *idhg-1* (γ subunit) (Huh et al., 1996; Dang et al., 2016). Previous studies showed that knockdown of both *idha-1* and *idhg-1* resulted in *gcy-5*^{prom}*::GFP* expression in the germline, but *idha-1* depletion produced a more pronounced reprogramming (Figure S1 A) (Ul Fatima, Unpublished). This difference may be attributed to the formation of a homodimer protein structure by the *idha-1* coded subunit, compared to the single amino acid sequence of the γ subunit (Figure 2.1.2 C). Degradation of *idha-1* by AID system confirmed the induction of reprogramming in the CHE-1^{oe} background, as evidenced by ectopic expression of the *gcy-5*^{prom}*::GFP* reporter in the germline (Ul Fatima, Unpublished).

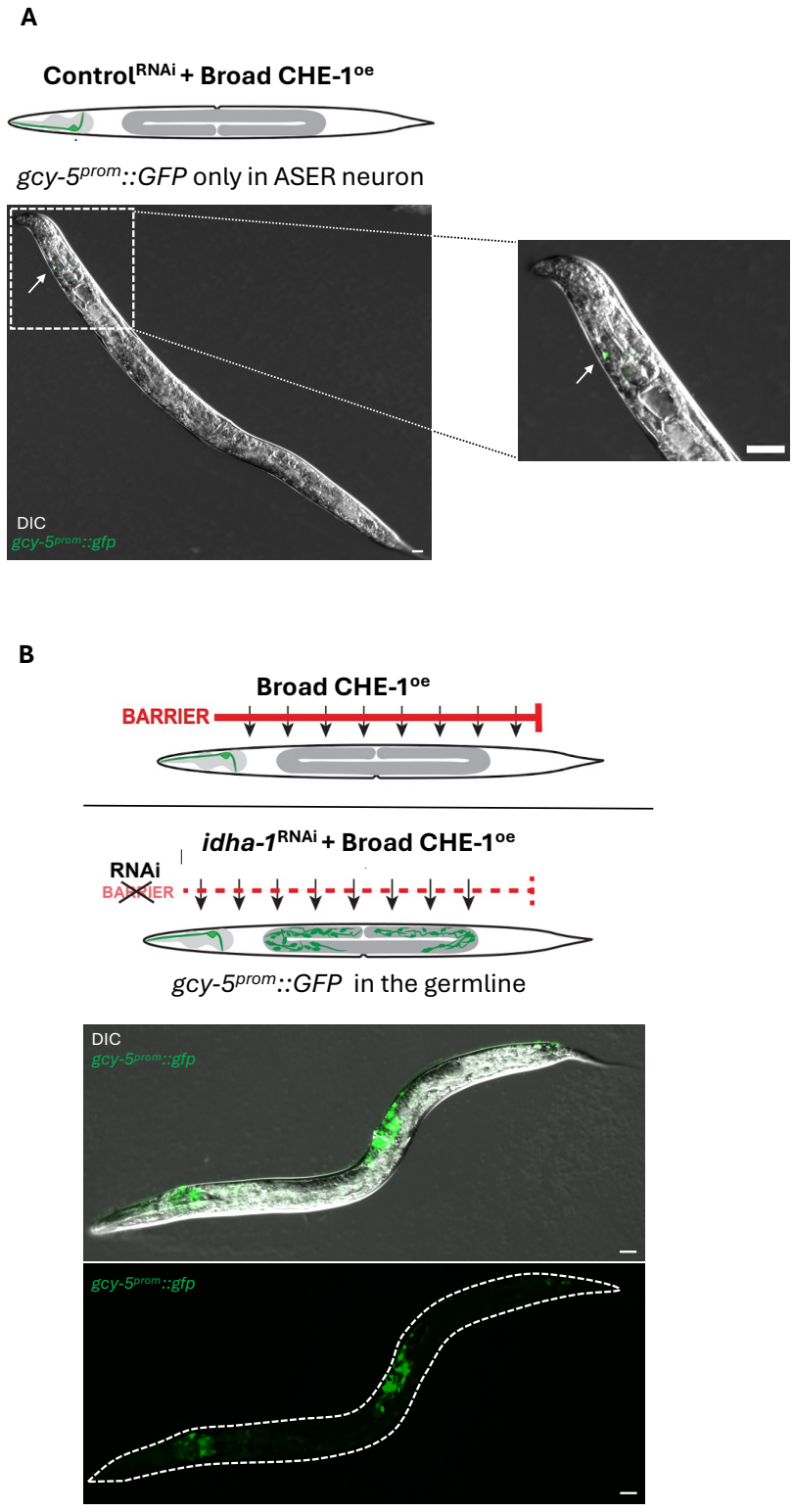

Figure 2.1.1 *idha-1* suppression promotes reprogramming of germ cells into neurons. A) In the wildtype conditions, barriers to reprogramming block conversion of cells into ASE neuronal fate despite overexpression of TF CHE-1. *Rluc* was used as a negative control for RNAi. Without the

depletion of reprogramming barriers, the *gcy-5^{prom}::GFP* ASE neuron reporter is expressed exclusively in the head region (indicated by a white arrow). **B)** Broad expression of TF CHE-1 (CHE-1^{oe}) combined with reprogramming barrier removal through *idha-1^{RNAi}* induces ASE neuronal fate reporter *gcy-5^{prom}::GFP* in germ cells. Scale bar: 50 µm

Upon *idha-1* depletion in the CHE-1 overexpression (CHE-1^{oe}) background and induction of the heat shock promoter, the *gcy-5^{prom}::GFP* fate reporter was expressed in the germline of the *C. elegans*, implying the conversion of the germ cells into neurons (Figure 2.1.1 B). The *idha-1* depletion-mediated reprogramming most commonly resulted in GFP positive neuron-like bodies concentrated around the vulval region. These RNAi results were further validated by using an auxin inducible degron (AID) protein degradation method which utilized TIR1 directed protein degradation upon Auxin supplementation (Zhang et al., 2015). Using CRISPR/cas9 gene editing, *idha-1* was tagged with a genetic sequence coding the AID protein and crossed with the CHE-1^{oe} *gcy-5^{prom}::GFP* reporter expressing *C. elegans* strain. This was combined with strains expressing TIR1 machinery under various tissue specific promoters, allowing spatiotemporal degradation of IDHA-1 protein (Ashley et al., 2021).

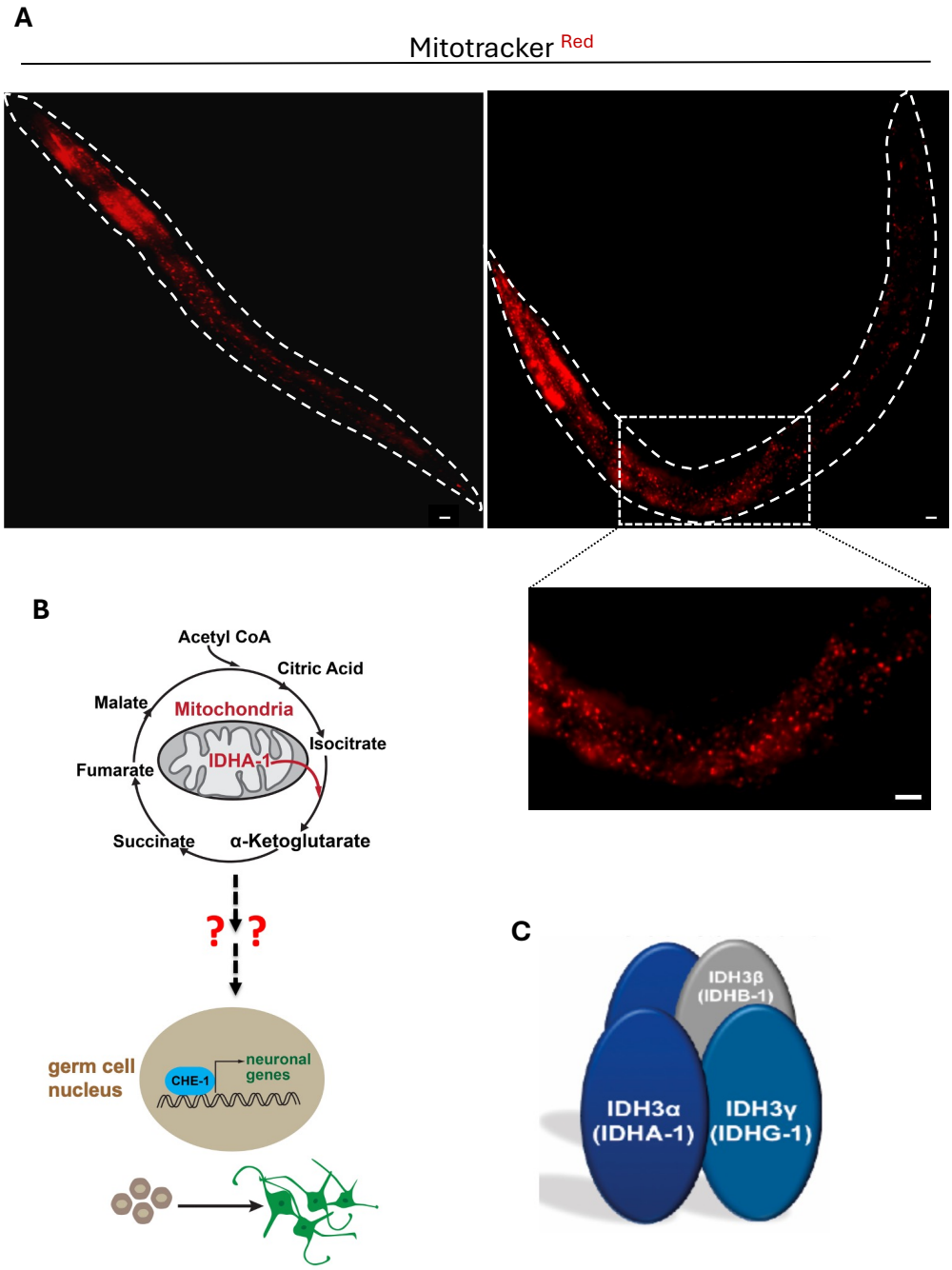

Figure 2.1.2 The role of mitochondria in germ cell reprogramming A) Mitotracker staining of *C. elegans* showing the distribution and abundance of mitochondrial structures withing the worm, as visualized under fluorescent microscope. The dashed box represents magnified area. Scale bar: 50 µm. **B)** Graphic model outlining the proposed, yet undetermined mechanisms by which depletion of IDHA-1 protein in the TCA cycle initiates a series of chromatin-modifying signals from the mitochondria to the nucleus. These events enable the conversion of germ cells into neurons in CHE-1^{oe} model. **C)** Schematic representation of IDH-3 subunits is shown. Two alpha, one beta and one gamma subunit.

2.2 IDHA-1 suppression-mediated reprogramming has limitations in male *C. elegans* germline

Given *C. elegans* is a hermaphroditic organism, its germline comprises of both female and male components (Figure 1.9). To further investigate which parts of the germline were likely to be expressing the reprogramming reporter *gcy-5^{prom}::GFP*, we observed the expression patterns of the reporter. The frequently reprogramming germline regions were mainly around the vulval region. We hypothesized the male-specific parts of the gonad such as the spermatheca and the sperm infused into the oocytes during the process of fertilization might be involved in the reprogramming. To test this, we used a high incidence of male (him phenotype), *him-8 (e1489)* mutant strain in which 20-40% of the population are expected to be males (Phillips et al., 2005; Hodgkin et al., 1979). The P0 progeny were treated with *idha-1*^{RNAi} as previously described, and the F1 progeny males were heat shocked to induce CHE-1^{oe}. These males were then examined under a fluorescent microscope for evidence of reprogramming (Figure 2.2.1 and Figure 2.2.2). The images revealed expression of *gcy-5^{prom}::GFP* in the head and the tail regions of the male worms. However, these regions correspond to pre-existing neurons, suggesting that the observed fluorescence might be an artifact resulting from CHE-1^{oe} in other chemosensory neurons, which are more permissive to reprogramming (Figure 2.2.1). Additionally, autofluorescence was observed in some of the male worms. In very rare occasions at a prevalence of approximately 1 out of every 100 male worms, expression of the *gcy-5^{prom}::GFP* ASE neuron fate reporter was observed (Figure 2.2.2). As an internal control, hermaphrodites of the *him-8* mutant strain, which constituted the remaining 60-80% of the population, were also examined (Figure 2.2.3). A comparison between the males and hermaphrodites revealed that *idha-1* depletion-mediated germline reprogramming occurred in the hermaphrodites, while males of the mutant *him-8* strain were not efficient in germline reprogramming.

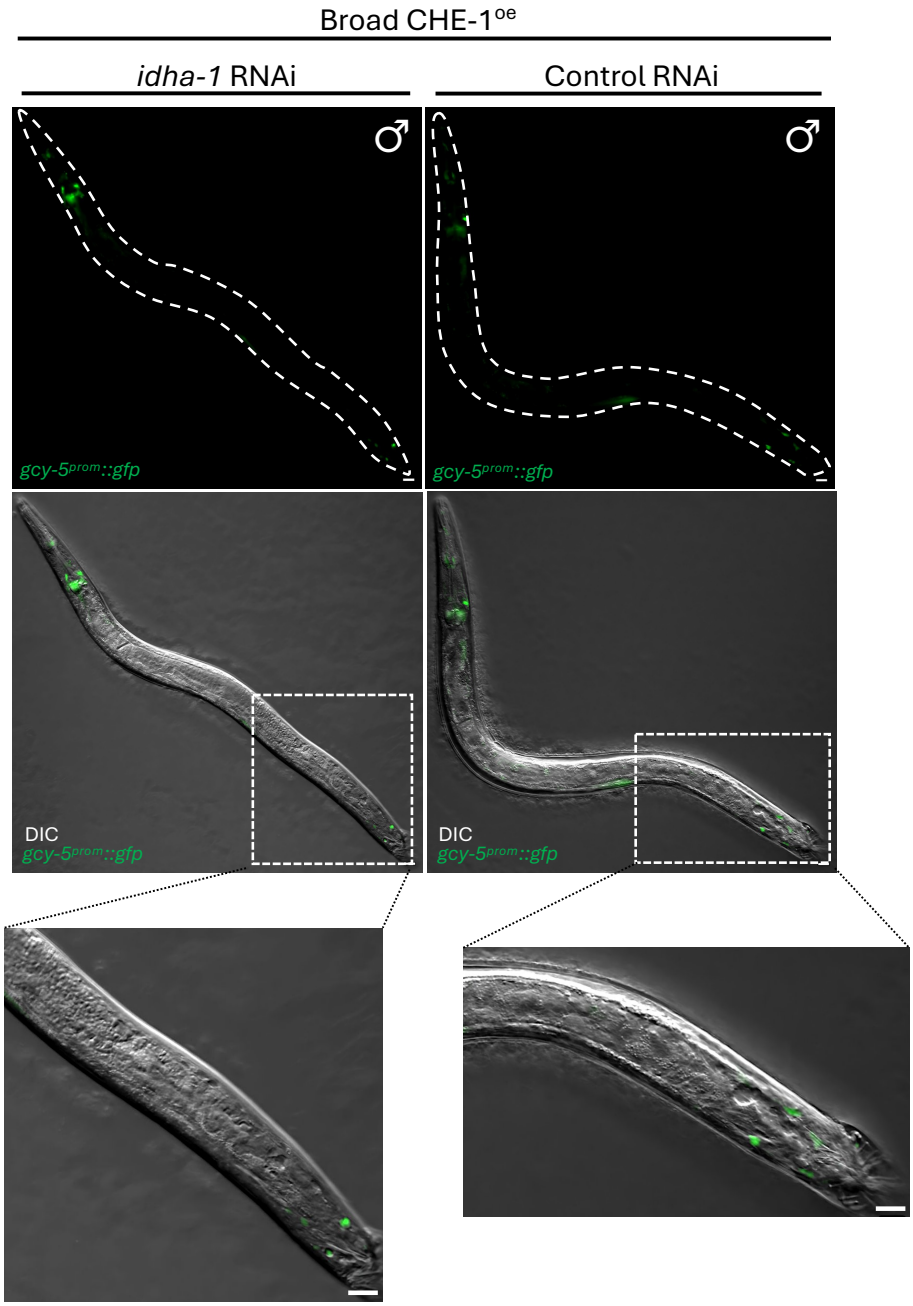

Figure 2.2.1 *idha-1* depletion in male *C. elegans* germline. In *him-8(e1489)* mutant male worms, TF CHE-1^{oe} combined with *idha-1*^{RNAi} did not induce *gcy-5*^{prom}*::GFP* expression in the germline. Instead, over-excitation of existing neurons and autofluorescence were observed. Dashed boxes represent magnified area. Scale bar: 50 µm.

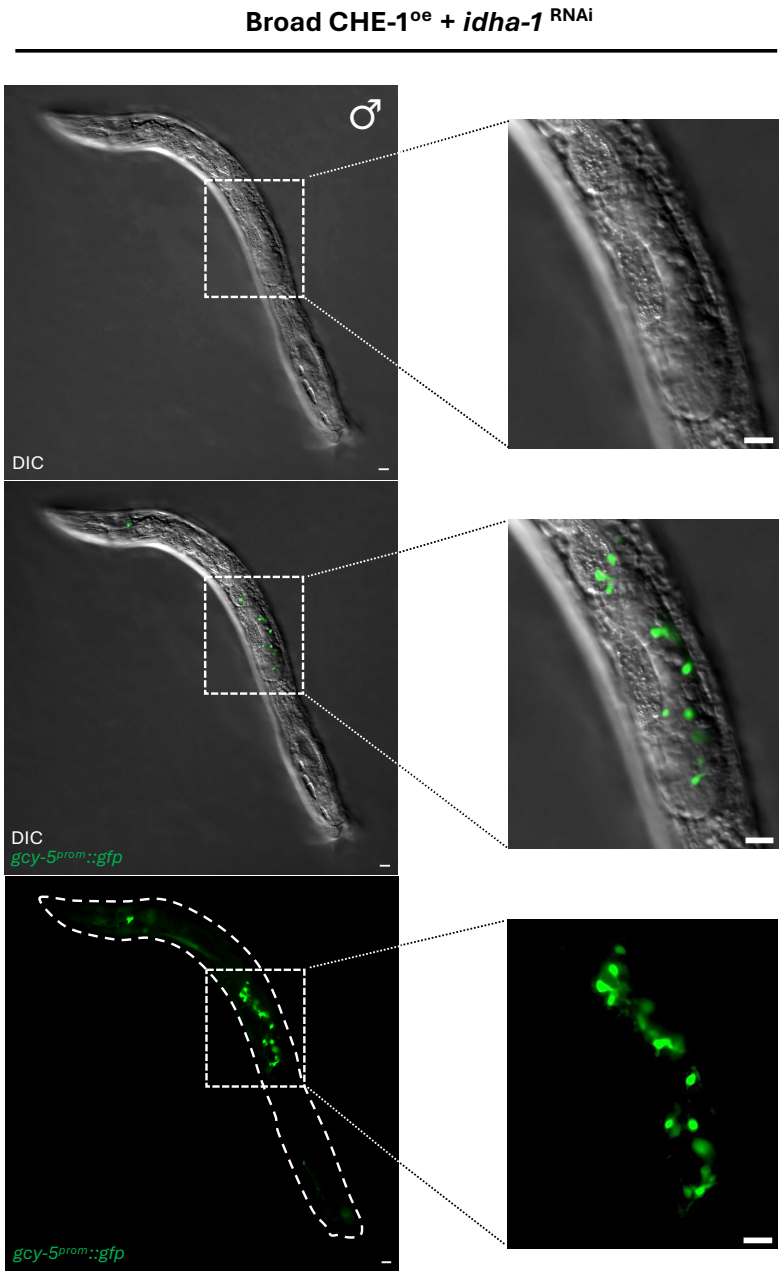

Figure 2.2.2 Male germline reprogramming. Representative images of ectopic overexpression of TF CHE-1 in *him-8 (e1489)* mutant male worm under *idha-1*^{RNAi} experimental condition. The ASE neuronal fate reporter *gcy-5*^{prom}*::GFP* induction is observed in the male germline and in the head. Dashed boxes represent magnified area. Scale bar: 50 µm.

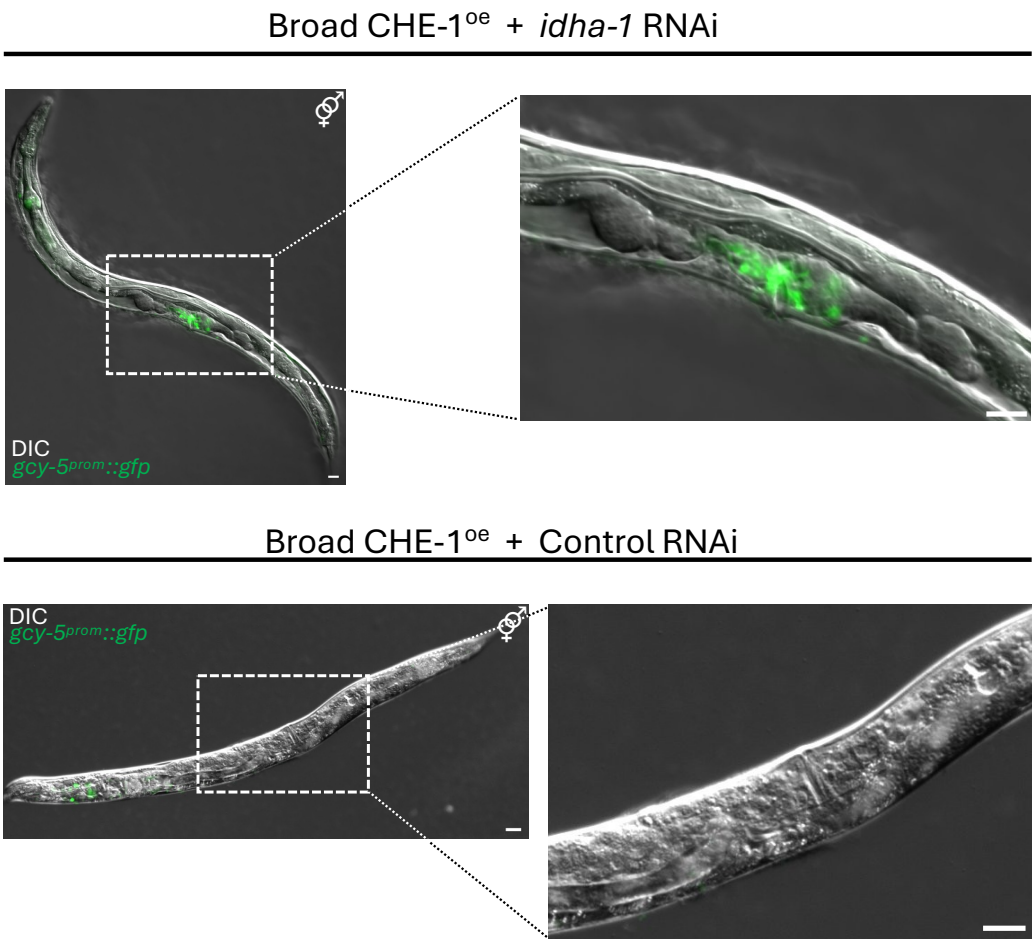

Figure 2.2.3 *idha-1* depletion in *him-8* mutant hermaphrodites. Representative images *him-8 (e1489)* mutant hermaphrodites upon TF CHE-1^{oe} under *idha-1*^{RNAi} and *Rluc* ^{RNAi} (Control). Reprogramming to cells with neuron-like projections was observed around the vulval region under the *idha-1*^{RNAi}. Induction of *gcy-5*^{prom}*::GFP* in control condition is not observed. Dashed boxes represent magnified area. Scale bar: 50 µm.

2.3 Feminized *C. elegans* mutants show decreased reprogramming capabilities

The *C. elegans* germline is composed of various types of cells, including germ cells (spermatogonia and oogonia) and somatic components. The somatic components contribute to the formation of eggshells, the spermatheca used for sperm storage in hermaphrodites, and the distal tip cells, which paly role in germline stem cell maintenance (Hirsch et al., 1976; Greenstein, 2005; Kimble and Crittenden, 2005;

Crittenden et al; 2006). To narrow down the type of the cells undergoing reprogramming to one of the male or female components of the germline, we conducted experiments using the *fem-2(b245)* mutant strain (Kimble et al., 1984). This mutant completely feminizes the worms when maintained at 25°C. Transfer of the hatched L1 stage worms to 25°C halts the expression of *fem-2* gene which plays role in male sex determination. The *fem-2* mutant worms used in this experiment also carried CHE-1^{oe} background and expressed *gcy-5^{prom}::GFP* ASE neuron reporter to assess reprogramming efficiency. For RNAi treatment, P0 animals were initially maintained at 15°C on OP50 bacteria until L4 stage and then transferred onto RNAi plates. The F1 generation were transferred to 25°C before completing the L2 stage to ensure *fem-2* silencing. In parallel, control condition plates were kept at 15°C for comparison. To score reprogramming rate, the experimental plates were heat-shocked at the L4 stage for 30 minutes at 37°C, and reprogramming positive animals were quantified the following day for.

Figure 2.3.1 shows that the WT and the *fem-2* knockdown animals exhibit similar rates of *idha-1^{RNAi}*-mediated reprogramming, approximately 40%, when maintained at 15°C condition prior to heat-shock, consistent with the standard RNAi experimental setup. However, there was a significant decrease in reprogramming efficiency for both strains when maintained at 25°C. As a positive control, *lin-53^{RNAi}* was used due to its well-documented phenotype penetrance. Reprogramming of germ cells to neurons was at a rate of approximately 40-50% in both WT and knockdown *fem-2(b245)* mutant animals with *lin-53^{RNAi}* at 15°C. However, this efficiency also declined for both strains at 25°C.

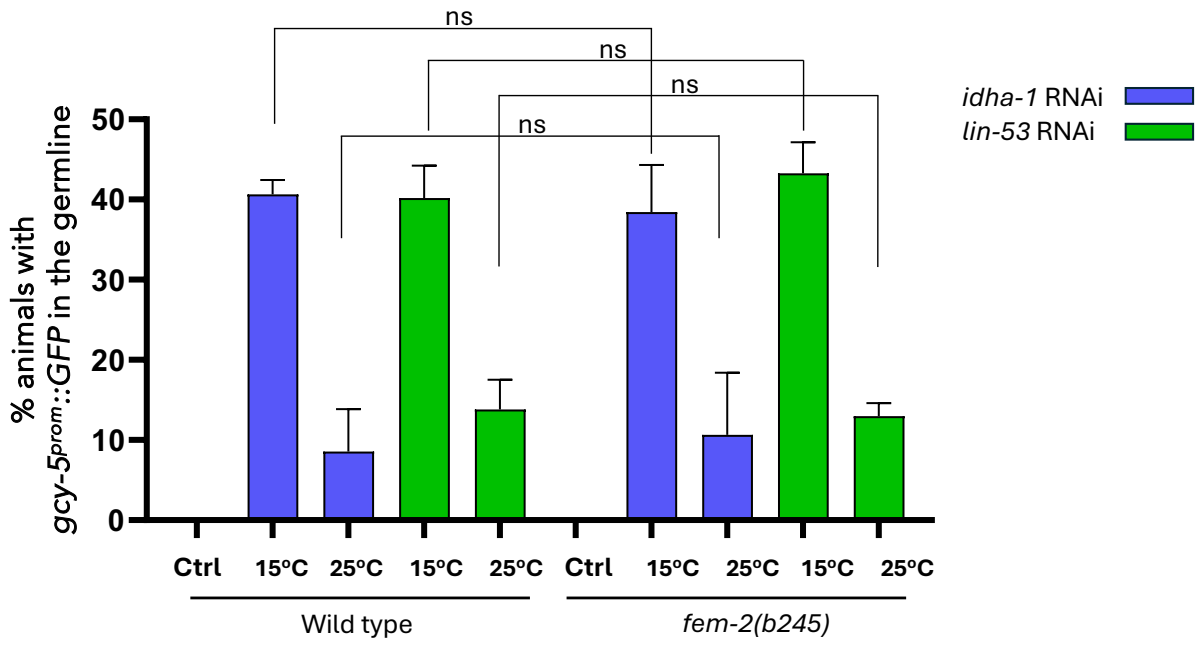

Figure 2.3.1 Reprogramming rate decreases in *idha-1*^{RNAi} and *lin-53*^{RNAi} when maintained at 25°C

Quantification of animals with positive *gcy-5*^{prom}*::GFP* induction in the germline upon CHE-1^{oe}. *fem-2(b245)* and WT strains were maintained on *idha-1*^{RNAi} and *lin-53*^{RNAi} at 15°C and 25°C for reprogramming efficiency comparison. *Rluc* was used as negative control RNAi (Ctrl). Three biological replicates each three technical repeats. n≥450 for each condition. Ordinary One-way ANOVA was used for statistical comparison, ns: not significant. Error bars represent SEM.

WT and *fem-2(b245)* mutant animals maintained on *idha-1*^{RNAi} were observed under fluorescent microscope to assess germline health and reprogramming (Figure 2.3.2). Animals maintained at 15°C prior to CHE-1^{oe} by heat-shock exhibited normal size, with clear *gcy-5*^{prom}*::GFP* induction in the germline. In contrast, animals maintained at 25°C displayed a stunted growth and a smaller frame suggesting a suboptimal environment for germline reprogramming. Animals that do not carry the transcription factor *CHE-1*^{oe} and are WT *fem-2*, when maintained at 25°C, retain all components of the germline (Figure 2.3.3). This shows the intact and functional germline anatomy under normal conditions.

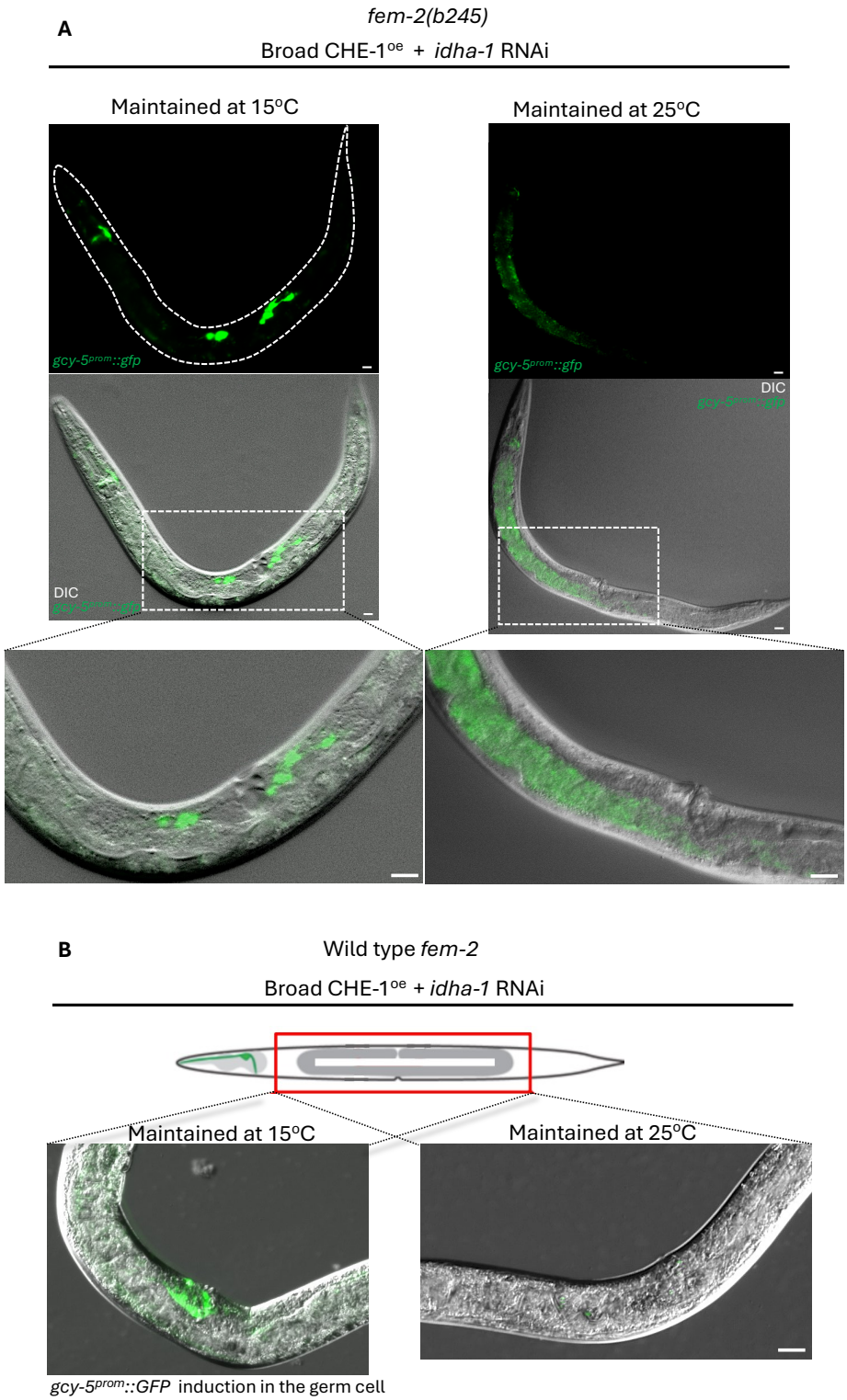

Figure 2.3.2 Fluorescent imaging of WT and *fem-2* mutant *C. elegans* at different temperatures

Representative images of *gcy-5^{prom}::GFP* induction in the germline of WT and feminized *fem-2(b245)* mutant hermaphrodites treated with *idha-1^{RNAi}* under CHE-1^{oe}. **A)** *fem-2(b245)* mutant hermaphrodites

maintained at 15°C show germline reprogramming, whereas *fem-2(b245)* mutant hermaphrodites feminized at 25°C show autofluorescence, but no signs of reprogramming. **B)** WT *fem-2* hermaphrodites maintained at 15°C show germline reprogramming, but WT *fem-2* hermaphrodites maintained at 25°C do not show any reprogramming in the germline. Dashed boxes represent magnified area. Scale bar: 50 µm.

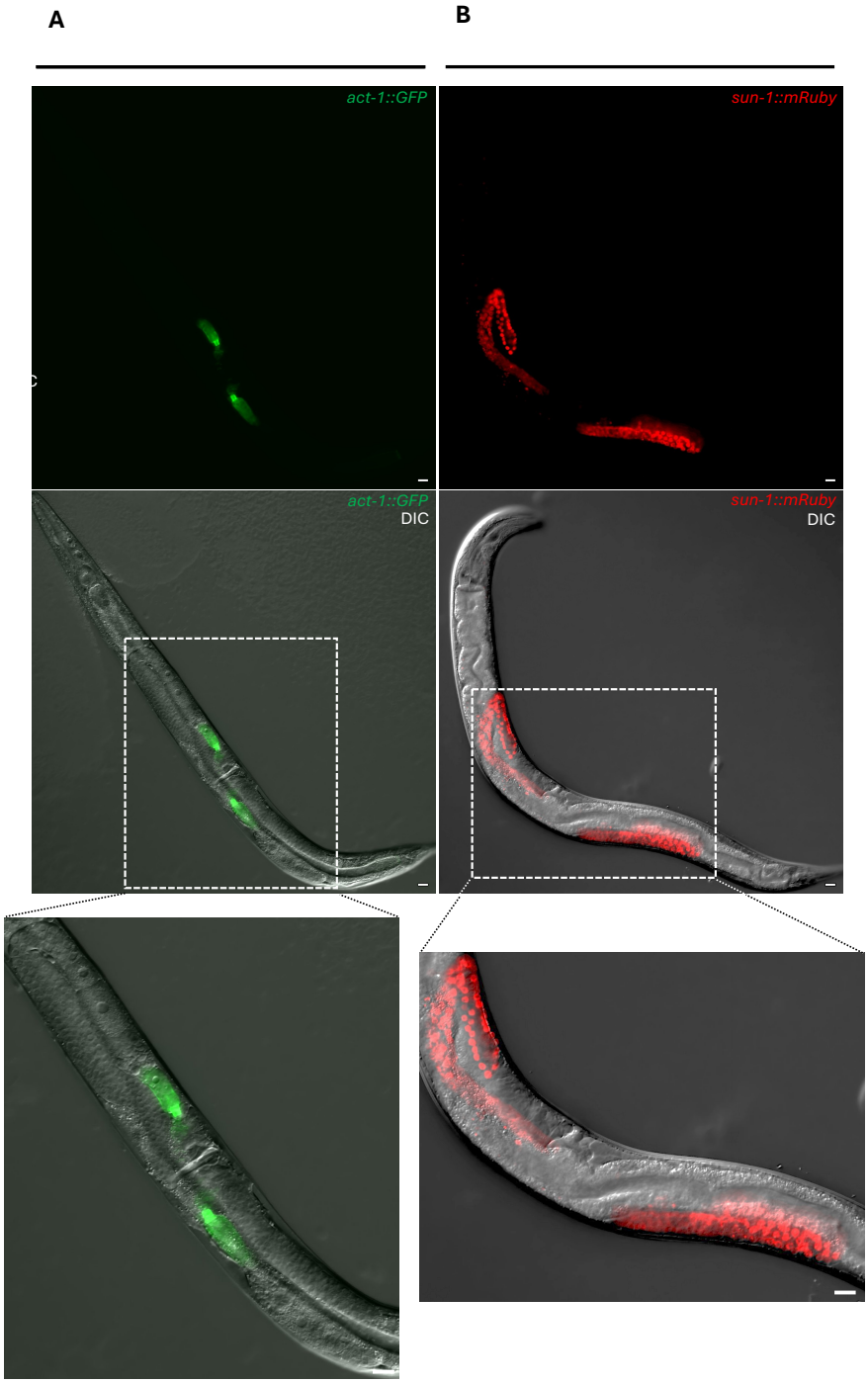

Figure 2.3.3 Localization of spermatheca and germline. WT *fem-2* hermaphrodites without CHE-1^{oe}

background maintained at 25°C prior to fluorescent imaging **A)** spermathecal cells expressing GFP labelled actin (ACT-1::GFP) **B)** SUN-1 protein labelled with red fluorescent protein mRuby, expressed in germline nuclei. Dashed boxes represent magnified area. Scale bar: 50 µm.

2.4 Absence of putative monosaccharide transmembrane transporter FDGT-2 enhances *idha-1* depletion-mediated reprogramming

A double RNAi screen revealed that simultaneous knockdown of *idha-1* and *fdgt-2* significantly enhanced reprogramming efficiency compared to *idha-1*^{RNAi} alone. The protein FDGT-2 is a putative monosaccharide transmembrane transporter which is localized to the cell membrane (Sequence: F14E5.1, WormBase). Using CRISPR/Cas9 gene editing technique we generated viable knockout mutants by deleting the *fdgt-2* gene locus. These *fdgt-2* knockout mutants (*fdgt-2*$^{-/-}$) were then crossed into the CHE-1^{oe} and *gcy-5*^{prom}*::GFP* ASE neuron reporter background, enabling enhancement/suppression screening without the need for double RNAi (Figure 2.4.1).

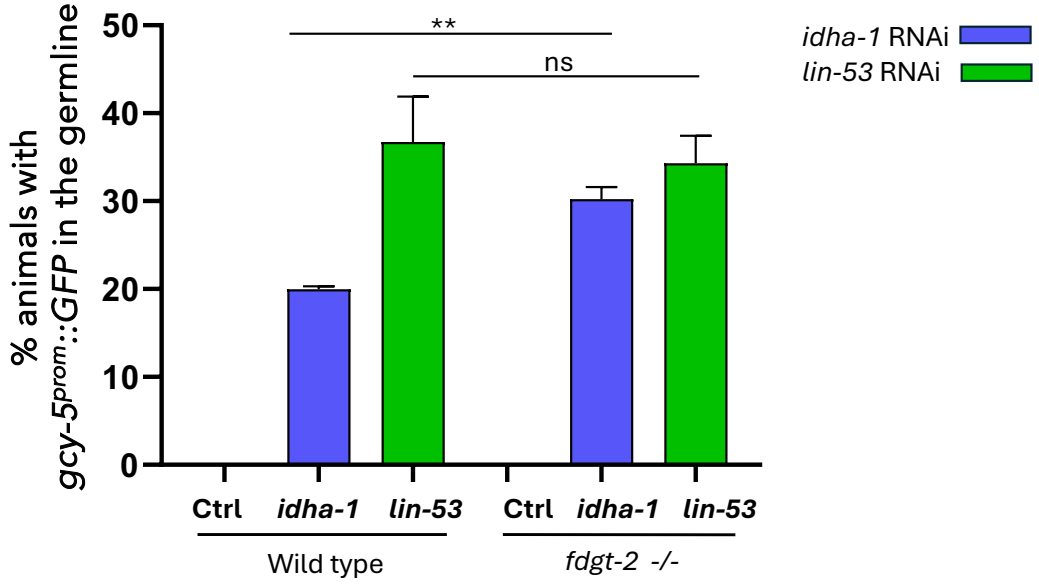

Figure 2.4.1 FDGT-2 depletion specifically enhances germline reprogramming in *idha-1*^{RNAi}. Quantification of animals showing ASE neuronal fate marker, *gcy-5*^{prom}*::GFP*, induction in the germline upon TF CHE-1^{oe} in conjunction with *idha-1*^{RNAi} and *lin-53*^{RNAi}. Comparison of reprogramming efficiency in *fdgt-2*$^{-/-}$ mutants and WT animals. Knockout of *fdgt-2* enhances *idha-1*^{RNAi} but not *lin-53*^{RNAi}. *Rluc* was

used as negative RNAi control. Three biological replicates each three technical repeats. n≥450 for each condition. Unpaired student's t-test was used for statistical comparison, ** $p< 0.01$, ns: not significant. Error bars represent SEM.

In addition, to confirming that *fdgt-2* deletion enhances *idha-1* depletion-mediated reprogramming, we sought to determine whether the reprogramming enhancing effect of *fdgt-2*^{RNAi} was specific to co-depletion with *idha-1*^{RNAi} or represented a general RNAi enhancing property, which the putative glucose transporter had possessed. The results from Figure 2.4.1 demonstrate that double knockdown of *fdgt-2* and *idha-1* let to a higher rate of *gcy-5*^{prom}*::GFP* induction in the germline compared to *idha-1*^{RNAi} alone upon TF CHE-1^{oe}. Furthermore, *idha-1*^{RNAi} and *lin-53*^{RNAi} of the *fdgt-2*^{wt} and *fdgt-2*$^{-/-}$ strains show that the reprogramming-enhancing effect of the putative glucose transporter is specific to *idha-1* depletion-mediated reprogramming.

Given the limited expression data available for FDGT-2, a less studied protein, we aimed to investigate its localization and expression pattern in *C. elegans*. To achieve this, we performed immunostaining on late L4 to young adult worms expressing FDGT-2 tagged with a Human Influenza Hemagglutinin (3xHA) epitope (FDGT-2::3xHA), generated using CRISPR/Cas9. This approach allowed us to determine the spatial distribution of FDGT-2 within the worm's anatomy. Following immunostaining, visualization of the stained worms revealed that FDGT-2 is predominantly localized along the central axis of the worm, extending from the anterior to the posterior end. The protein appears to surround the gut and germline, with particularly strong signals concentrated around the vulval region (Figure 2.4.2).

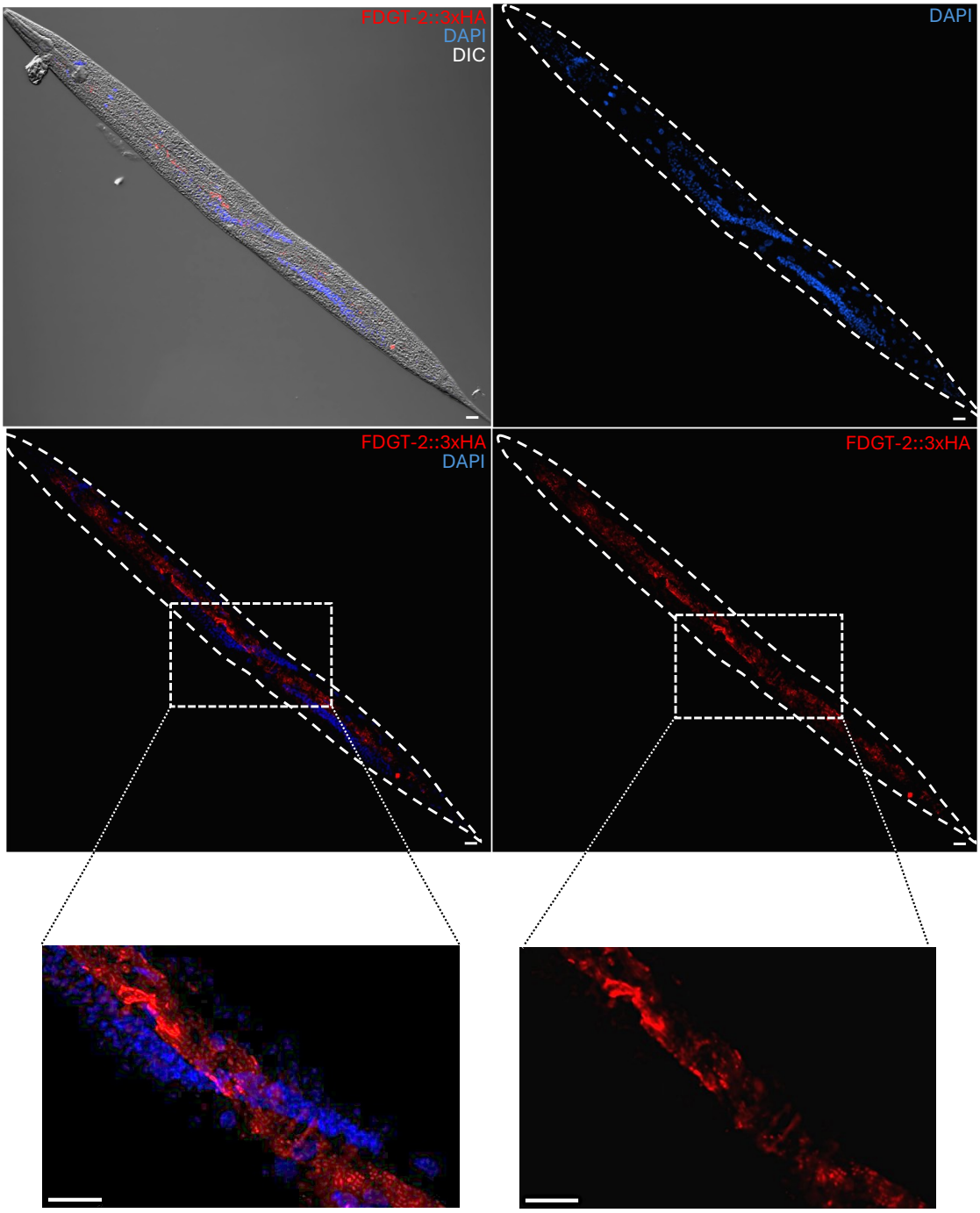

Figure 2.4.2 Expression pattern of FDGT-2. Immunofluorescent staining of 3xHA tagged FDGT-2 protein showing its expression pattern in early adult *C. elegans*. Dashed boxes represent magnified area. Scale bar: 50 µm.

2.5 Exogenous supplementation of TCA cycle metabolites enhance *idha-1* depletion mediated reprogramming

As IDH-3 is a key enzyme in the TCA cycle, it is located in the mitochondria. It is responsible for catalyzing conversion of isocitrate to alpha-ketoglutarate (a-KG), which is an important step in the progression of the cycle (Figure 2.5 B) (Martinez-Reyes et al., 2020; Arnold & Finley 2023). We hypothesized that the disruption of metabolic flow caused by *idha-1*^{RNAi} could lead to changes in TCA cycle dynamics and ultimately affect germline reprogramming. Given its role as a key metabolite, replenishment of a-KG through supplementation would revive its function in the cell. One of such roles for a-KG is binding to EGL-9 and enabling its proline hydroxylation activity, which results in degradation of HIF-1, a TF that plays a critical role in response to low oxygen levels (Hoang & Joseph, 2020). In addition, a-KG has been studied for its inhibitory role in TOR pathway which has been linked to lifespan extension (Chin et al., 2014).

Based on the available literature and the preliminary experiments, we designed an experiment in which three TCA cycle metabolites fumarate, malate and a-KG were supplemented in conjunction with *idha-1*^{RNAi} to evaluate reprogramming efficiency. Upon expression of TF CHE-1^{oe} in the metabolite-supplemented *idha-1*^{RNAi} plates, we observed an enhancement in induction of *gcy-5*^{prom}*::GFP* reporter in the germline of the animals, compared to those treated with *idha-1*^{RNAi} alone (Figure 2.5 A). Notably, supplementation of a-KG and fumarate resulted in significant increases in germline reprogramming efficiency. In contrast malate supplementation did not yield statistically significant results, although it showed an upward trend of reprogramming rate comparable to a-KG. This variability in significance may stem from differences in reprogramming efficiency across biological replicates.

The unexpected increase in germline reprogramming upon a-KG supplementation raised questions. While we anticipated that the depletion of *idha-1* would lead to reduction in a-KG levels and subsequently lower the germline reprogramming rate, the results suggested otherwise. Replenishment of a-KG into TCA cycle would counteract the effects of *idha-1*^{RNAi} and eventually eliminate or diminish the reprogramming rate. However, the opposite was observed. Additionally, not only a-KG supplementation, but also fumarate feeding boosted reprogramming efficiency, further implicating a complex interplay between TCA cycle products and germline reprogramming.

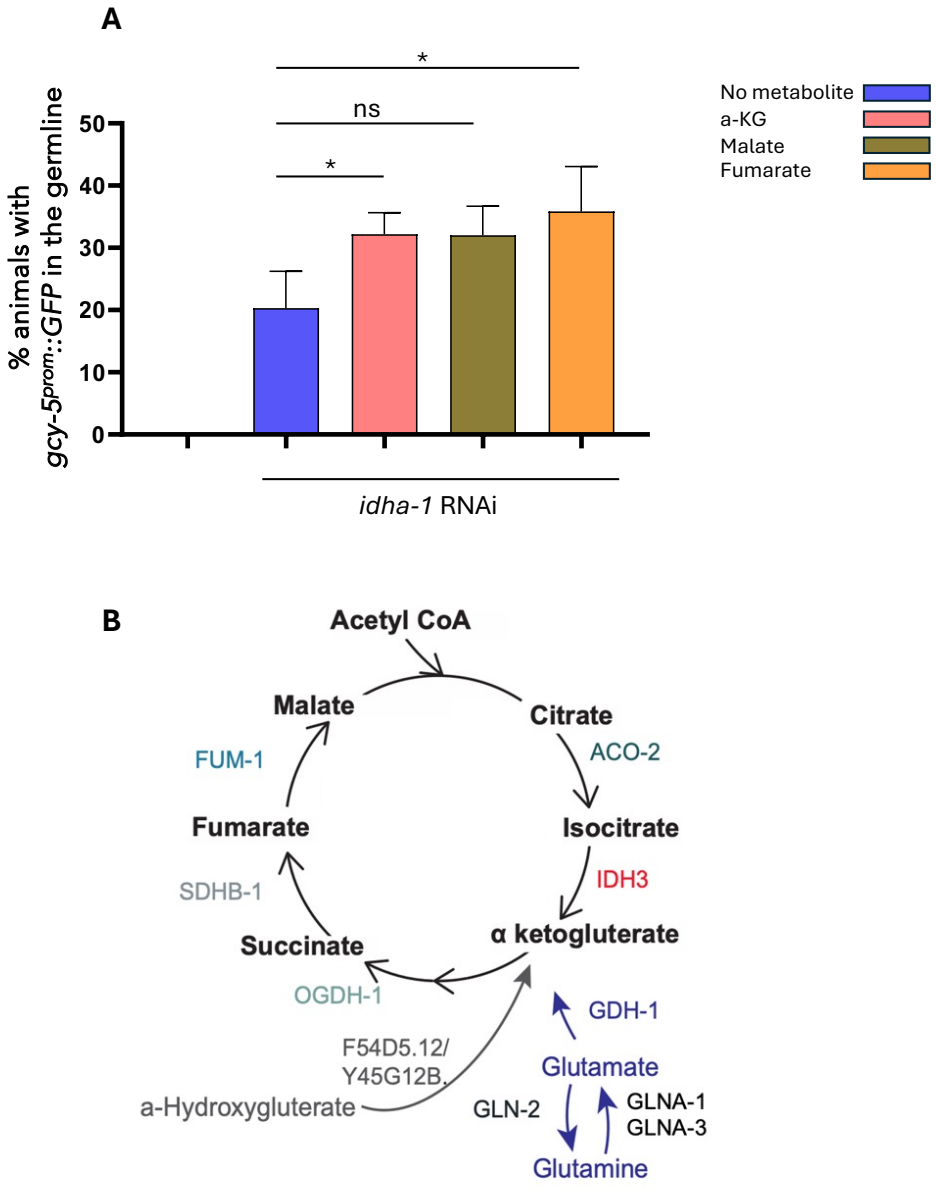

Figure 2.5 Tricarboxylic Acid Cycle metabolites enhance *idha-1*^{RNAi} reprogramming A) Quantification of animals showing ASE neuron fate marker *gcy-5*^{prom}*::GFP* induction in the germline upon CHE-1^{oe} on *idha-1*^{RNAi} *plates. Rluc*^{RNAi} was used as a negative control. Three biological replicates each three technical repeats. n≥450 for each condition. Ordinary one-way ANOVA test was used for statistical comparison, * p<0.05, ns: non-significant. Error bars represent SEM. **B)** Schematic representation of the enzymatic reactions in TCA cycle with their respective products. IDH-3 catalyzes conversion of isocitrate into a-KG. In glutamine anaplerosis pathway enzymatic reactions convert glutamine into glutamate and finally glutamate is converted into a-KG. a-KG can alternatively be produced from 2-Hdroxygluterate by catalytic activity of the enzyme 2-Hydroxygluterate dehydrogenase, D2HD (F54D5.12, Y45G12B.3).

2.6 Glutamine anaplerosis pathway likely contributes to a-ketoglutarate replenishment in idha-1 deficient animals

Previous mass spectrometry analysis of *idha-1* depleted worms revealed that the TCA cycle metabolites remained largely unaltered, with stable a-KG levels despite *idha-1* depletion (Ul Fatima, Unpublished). These findings, combined with results from section 2.5, demonstrating that a-KG supplementation enhances germline reprogramming, suggest the existence of an alternative source or pathway for a-KG production. This implies that a-KG may play a crucial role in *idha-1* depletion-mediated germline reprogramming. One potential source of a-KG supply in the context of a seemingly functional TCA cycle with impaired IDH-3 activity is the glutamine anaplerosis pathway (Xiao et al., 2016). In certain cancer cells it was observed that cells utilize glutamine to produce glutamate, subsequently feeding into a-KG as an alternative way of replenishing the metabolite (Jeong et al., 2016; Yoo et al., 2020; Bott et al., 2019). Additionally, a-KG can also be produced from 2-Hydroxygluterate by enzymatic activity of D2HD dehydrogenase (F54D5.12, Y45G12B.3) (Figure 2.5 B). However, knockdown of D2HD does not affect the germ cell conversion phenotype (Ul Fatima, Unpublished).

To further investigate the role of glutamine anaplerosis in a-KG replenishment, we hypothesized that absence of the key enzymes in glutamine anaplerosis pathway would lead to alterations in reprogramming efficiency. Specifically, GLNA-1, GLNA-3 and GDH-1 are enzymes involved in a-KG replenishment via glutamine anaplerosis pathway, while GLNA-2 can also catalyze the reverse chemical reaction as it converts glutamate back into glutamine (Figure 2.5 B). To test this, we aimed to generate CRISPR/Cas9-edited strains targeting these enzymes. We successfully created and tested a *glna-3* knockout (*glna-3*$^{-/-}$) strain, which was then crossed with CHE-1^{oe} and *gcy-5*^{prom}*::GFP* reporter strain to assess reprogramming efficiency. This experiment

was conducted alongside metabolite supplementation, as we had previously confirmed that feeding a-KG, malate and fumarate had an enhancing effect on the *idha-1* depletion-mediated reprogramming phenotype.

As shown in Figure 2.6.1, a significant decrease in reprogramming efficiency was observed in *glna-3*$^{-/-}$ compared to wildtype animals under conditions of TF CHE-1^{oe} and *idha-1*^{RNAi}. Supplementation with TCA cycle metabolites (a-KG, malate and fumarate) enhances reprogramming rate in both *glna-3*$^{-/-}$ mutants and WT *glna-3* animals. Although the enhancing effect of exogenously provided a-KG was not statistically significant, an upward trend was observed (Figure 2.5 A & Figure 2.6.1). This variability may be attributed to differences in reprogramming efficiency across biological replicates performed on different days. Notably, metabolite supplemented conditions consistently resulted in lower germline reprogramming rate in *glna-3*$^{-/-}$ mutants compared to WT *glna-3* worms, suggesting that glutamine anaplerosis plays a key role in *idha-1* depletion-mediated reprogramming

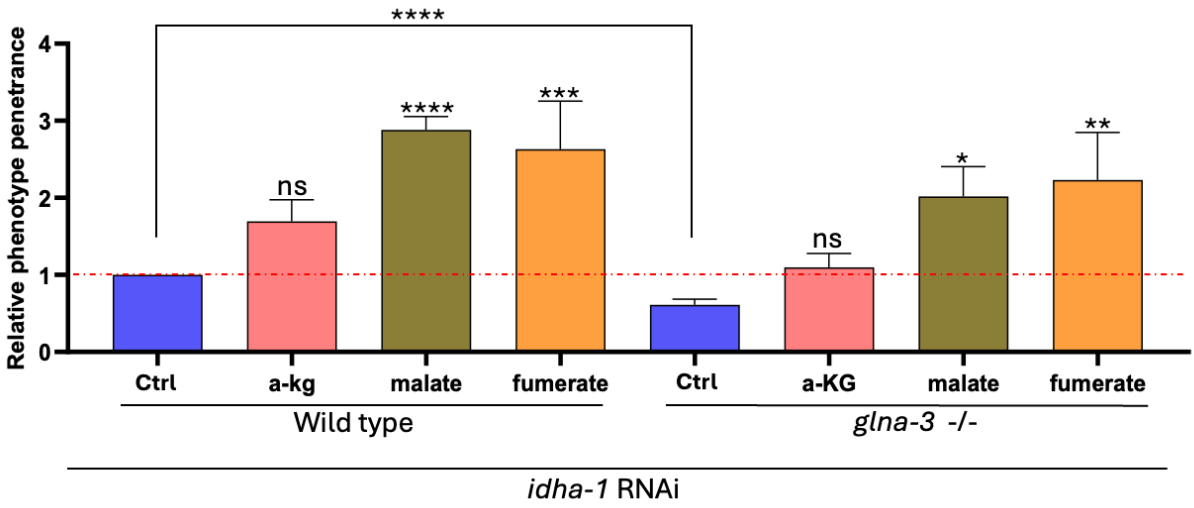

Figure 2.6.1 *glna-3* deficient animals exhibit reduced germline reprogramming rates. Quantification of animals displaying induction of ASE neuron fate marker *gcy-5*^{prom}*::GFP* in the germline under conditions of CHE-1^{oe} in conjunction with *idha-1*^{RNAi}. Control conditions of *idha-1*^{RNAi} were not

supplemented with any metabolites. *Rluc*^{RNAi} was used as a negative control and showed no *gcy-5*^{prom}*::GFP* induction in the germline (data not shown). Overall, *glna-3*$^{-/-}$ mutant animals exhibited a significant decrease in reprogramming rates compared to the WT controls. For statistical comparison of WT versus the *glna-3*$^{-/-}$ mutant control, unpaired student's t-test was used. For comparison of all conditions relative to WT control ordinary one-way ANOVA test was used. Three biological replicates each three technical repeats. n≥450 for each condition, ****p< 0.0001, *** p<0.001, ** p<0.01, * p<0.05, ns: non-significant. Error bars represent SEM.

During glutamine anaplerosis, byproducts such as ammonia and aspartate are formed (Sullivan et al., 2015; Hensley et al., 2013). If the reprogramming observed upon *idha-1* depletion is driven by one of these byproducts, specifically aspartate, then supplementing the system with additional aspartate should enhance germline reprogramming. To test this hypothesis, we supplemented the worms with D-aspartate, one of the most abundant aspartate isoforms, which has been detected in tissues such as the reproductive and neural tissues (D'Aniello et al., 2005; Lamanna et al., 2007; D'Aniello et al., 2007).

We performed *idha-1*^{RNAi} treatment in *CHE-1*^{oe} animals using both WT *glna-3* worms and mutant *glna-3* knockouts. This allowed us to assess the effect of aspartate supplementation in two contexts: first, a presumably functional glutamine anaplerosis pathway (WT *glna-3*) and second, worms lacking *glna-3*, an essential enzyme for glutamine anaplerosis. As shown in Figure 2.6.2 A, the data reaffirm the importance of glutamine anaplerosis for reprogramming efficiency, as the knockout of *glna-3* significantly reduced reprogramming efficiency. However, aspartate supplementation in the *CHE-1oe* background under *idha-1*^{RNAi} did not enhance reprogramming levels, neither in WT *glna-3* worms nor in *glna-3* knockouts (Figure 2.6.2 A).

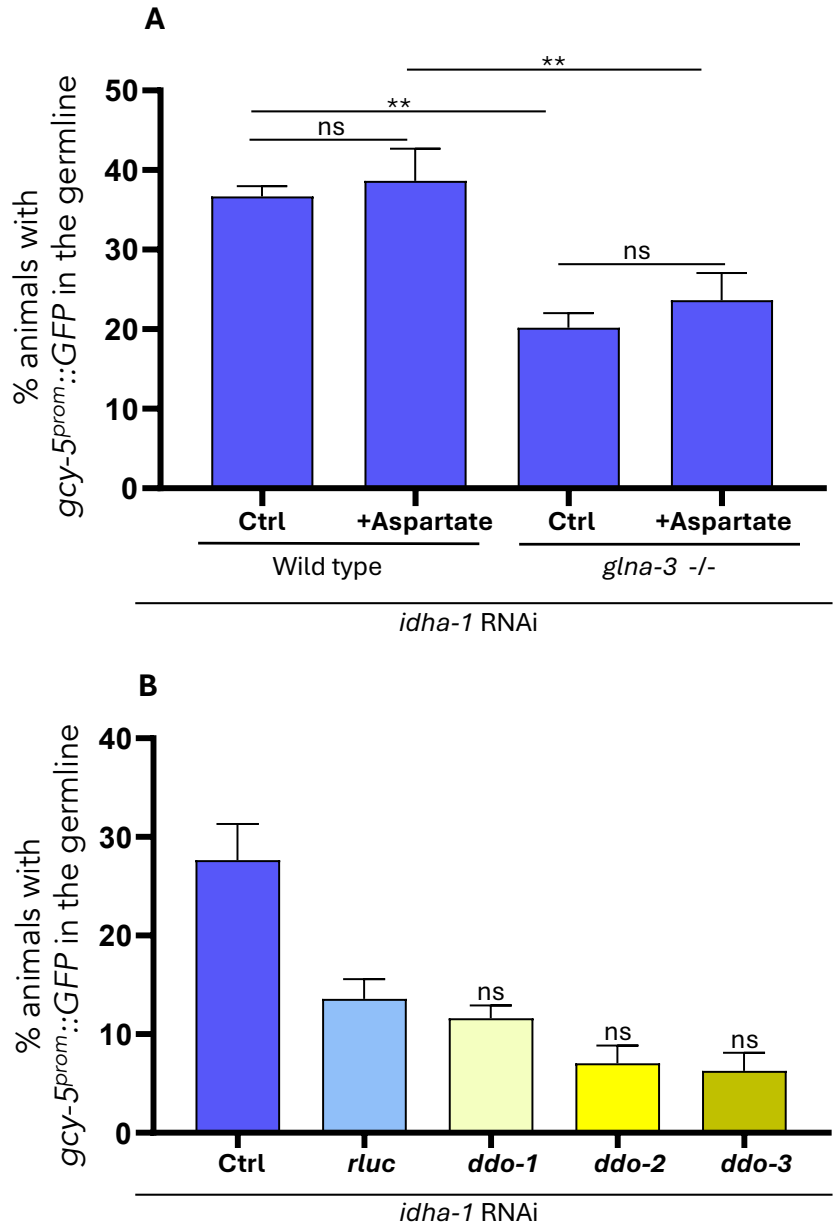

Figure 2.6.2 Aspartate does not affect germline reprogramming. Quantification of animals displaying induction of ASE neuron fate marker *gcy-5^{prom}::GFP* in the germline under conditions of CHE-1^{oe} in conjunction with *idha-1*^{RNAi}. **A)** Comparison of metabolite free control versus aspartate supplemented conditions in WT *and glna-3*$^{-/-}$ *mutant* worms under *idha-1*^{RNAi}. *Rluc*^{RNAi} was used as a negative control (data not shown). **B)** Double RNAi targeting *idha-1* and candidate genes *ddo-1, ddo-2, ddo-3. idha-1* and *Rluc* double RNAi was used as control conditions. Single *idha-1* RNAi was used as a reprogramming efficiency control. *Rluc*^{RNAi} was used as a negative control (data not shown). one-way ANOVA test was used. Three biological replicates each three technical repeats. n≥450 for each condition, ** p<0.01, ns: non-significant. Error bars represent SEM.

Despite the unanticipated negative result from the aspartate supplementation experiment, we proceeded to investigate whether the depletion of aspartate-degrading enzymes would influence germline reprogramming. D-Aspartate oxidases (DDO-1, DDO-2, and DDO-3) are known to degrade aspartate. Notably, DDO-3 has been implicated in extracellular secretions within both hermaphrodite and male germlines, where it plays role in self-fertility, hatching, and lifespan regulation (Saitoh et al., 2019). We hypothesized that knocking down these *ddo* genes in conjunction with *idha-1* depletion in a *CHE-1*^{oe} background would enhance reprogramming if D-aspartate were indeed involved in this process. However, no such effects were observed. Co-depletion of *idha-1* and *ddo* genes did not result in any significant suppressive or enhancing changes in germline reprogramming rates (Figure 2.6.2 B).

2.7 Rapamycin extends the maximal lifespan of *C. elegans* without affecting the germline reprogramming rates upon *idha-1* depletion

As reported by Chin et al. (2014), the metabolite a-KG extends the life span of *C. elegans* by interacting and inhibiting TOR pathway components or through independent or parallel pathways converging on a downstream effector. Since *idha-1* is involved in a-KG production, the interaction between a-KG and TOR pathway became ever more relevant to our research. Considering the current research on interaction of a-KG with TOR pathway, we expect *idha-1* depletion to increase TOR activity due to decreased a-KG levels. Rapamycin, a well-studied longevity inducing drug, rescues traits associated with aging phenotypes and has been studied on both vertebrates and invertebrate models, including *C. elegans* (Harrison et al., 2009; Neff et al., 2013; Blagosklonny, 2013). It has been shown to extend life span of the worms by interacting with TOR pathway, the nematode counterpart of mTOR mammalian target of rapamycin (Chin et al., 2014; Robida-Stubbs et al., 2012).

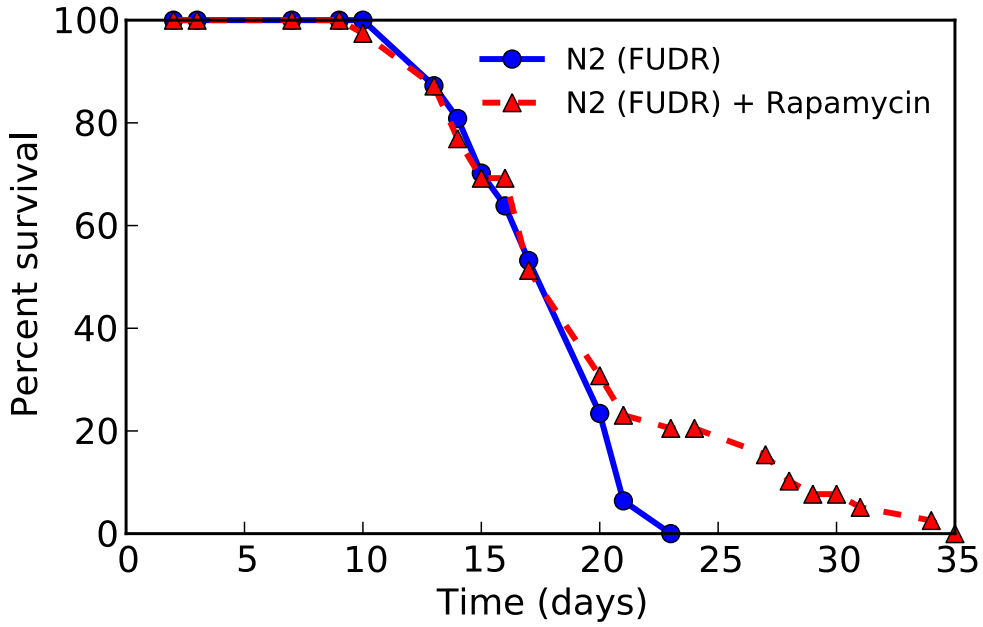

Figure 2.7.1 Rapamycin treatment extends the maximal lifespan of *C. elegans*. Worms were supplemented with 100mM rapamycin added on OP50 agar plates containing FUDR for lifespan assay. For statistical comparison between drug treatment and control group Log-Rank test was used, *p*-value ns: non-significant. Three biological replicates.

.

To investigate the potential interplay between TOR pathway activity and the germline reprogramming we modulated TOR activity using rapamycin treatment. Specifically, we aimed to determine whether reduced TOR activity influences the reprogramming phenotype observed upon *idha-1* depletion. First, we conducted a lifespan assay to observe the lifespan extension reported with rapamycin administration in *C. elegans* (Figure 2.7.1). Although the observed maximum lifespan extension confirmed the rapamycin delivery, the median lifespan remained unchanged.

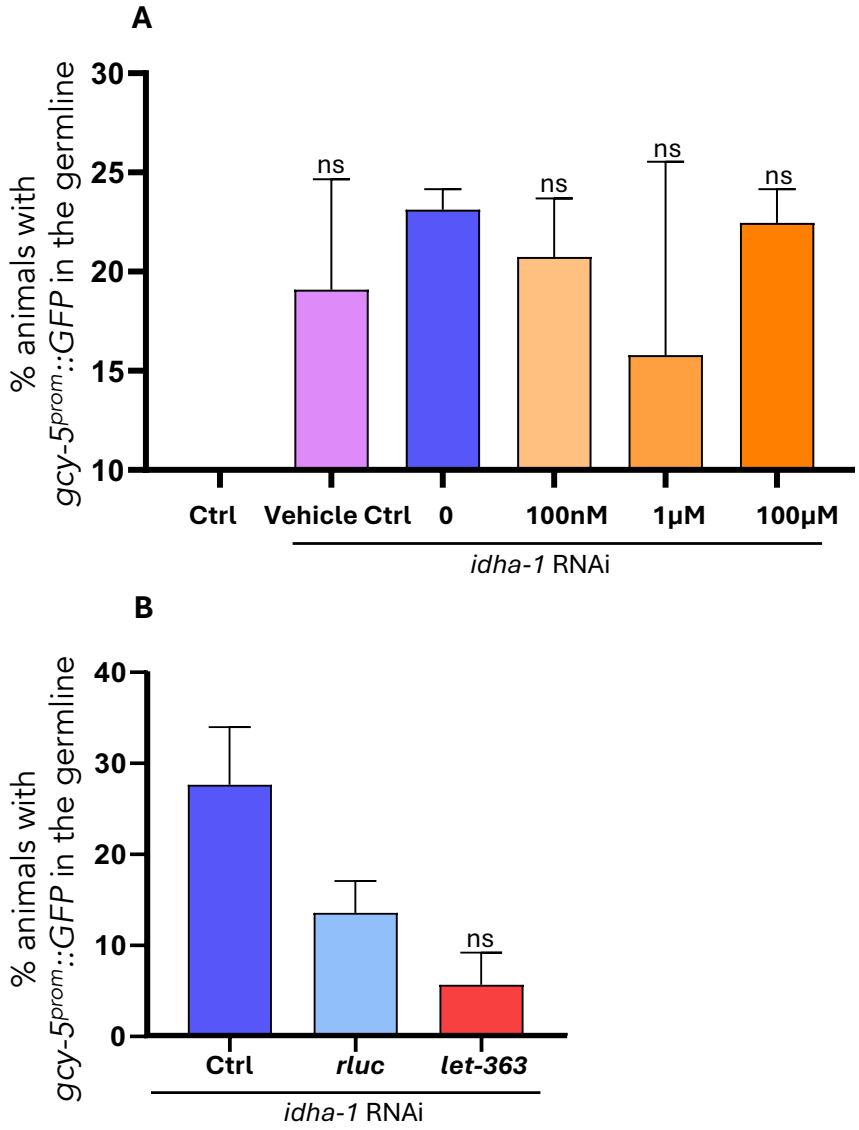

Figure 2.7.2 Modulation of TOR pathway does not affect germline reprogramming. Quantification of animals showing ASE neuron fate marker *gcy-5*^{prom}*::GFP* induction in the germline upon CHE-1^{oe} in conjunction with *idha-1*^{RNAi}. **A)** Rapamycin treatment at varying concentrations did not enhance germline reprogramming. DMSO vehicle control was used. *Rluc*^{RNAi} served as a negative control. **B)** Double RNAi of *idha-1* and *let-363*. *idha-1* and *Rluc* double RNAi was used as control condition. Just *idha-1* single RNAi was used as a reprogramming efficiency control. *Rluc*^{RNAi} was used as a negative control (data not shown). Three biological replicates each three technical repeats. n≥450 for each condition. Ordinary one-way ANOVA test was used for statistical comparison, ns: non-significant. Error bars represent SEM.

Following the lifespan assay, we designed an experiment to evaluate the effects of rapamycin top of *idha-1* depletion-mediated germline reprogramming. Different concentrations of rapamycin were added to *idha-1*^{RNAi} plates, and the induction of the ASE neuron fate marker *gcy-5*^{prom}*::GFP* in the germline was quantified under TF CHE-1^{oe}. The results revealed great variability in reprogramming efficiency across different conditions and statistically significance patterns were not observed (Figure 2.7.2 A). To further investigate the role of TOR pathway, we aimed to deplete *let-363*, the *C. elegans* ortholog of TOR (Long et al., 2002). Double RNAi depletion of *let-363* and *idha-1* did not yield suppressive or enhancing results in germline reprograming rate (Figure 2.7.2 B). These findings suggest that repression of TOR activity does not influence the reprogramming rate mediated by *idha-1* depletion.

2.8 Methionine supplementation suppresses germline reprogramming

Mitochondria, though relatively isolated compared to other organelles in the cell, maintain dynamic interactions with various cellular components. One of such interactions involves the methionine cycle, a cytosolic process during which methionine is converted into s-adenosyl methionine (SAM), the universal methyl donor; SAM is subsequently transported into the mitochondria or the nucleus to modify metabolites and nucleic acids (Monné et al., 2022; Tassinari et al., 2024). Methylation processes play critical roles in biological functions, such as modulating protein activity through protein methylation and regulating gene expression via mitochondrial DNA (mtDNA) methylation (Malecki et al., 2022; Iacobazzi et al., 2013).

The methionine cycle is affected by cobalamin (vitamin B12), a co-factor for the enzyme methionine synthase (MS), which is essential for methionine regeneration (Green et al., 2017). In the literature, vitamin B12 supplementation has been shown to enhance reprogramming efficiency in both *in vitro* and *in vivo* experiments,

including the conversion of fibroblasts into induced pluripotent stem cells (iPSCs) and studies in mice (Kovatcheva et al., 2023). Enhanced vitamin B12 supplementation could lead to a more robust methionine cycle, increasing SAM production. This, in turn, could either enhance methylation reactions that modulate gene activity or, through the catabolism of excess SAM, generate toxic methylation inhibitors that reduce methylation patterns (Chiang et al., 1996; Fukumoto et al., 2022).

Given the effectiveness of metabolite feeding experiments in *C. elegance* for studying reprogramming, we aimed to evaluate the effects of B12 supplementation on the *idha-1*^{RNAi} mediated germline reprogramming in a parallel project. As shown in figure 2.8 A, vitamin B12 supplementation did not have any significant enhancement effects on the rate of *gcy-5*^{prom}*::GFP* reporter induction in the germline. To directly assess the effects of SAM on reprogramming, we bypassed modulation of the methionine cycle via B12 and supplemented SAM directly. However, SAM supplementation also failed to enhance reprogramming (Figure 2.8 B). Due to the high instability of SAM under normal ambient conditions, we could not rule out the possibility of failed SAM delivery to the worms (Giese et al., 2020; Morana et al., 2002).

Since SAM is derived from methionine, we next performed a methionine feeding experiment combined with *idha-1*^{RNAi}. Surprisingly, methionine supplementation resulted in repression of reprogramming rate in the germline (Figure 2.8 C). The occurrence of reprogramming suppression in RNAi experiments may sometimes be attributed to unfavorable RNAi conditions for example decreased ingestion of the RNAi bacteria by the worms or compromised RNAi machinery (Baumanns et al., 2023). To exclude these factors, we designed a control experiment where methionine supplementation was accompanied with *idha-1*^{RNAi} and *lin-53*^{RNAi} (Figure 2.8 D). The

results showed that the efficiency of *lin-53* depletion-mediated reprogramming remained unaffected by methionine feeding and *idha-1*^{RNAi} was again confirmed to be suppressed by exogenous methionine.

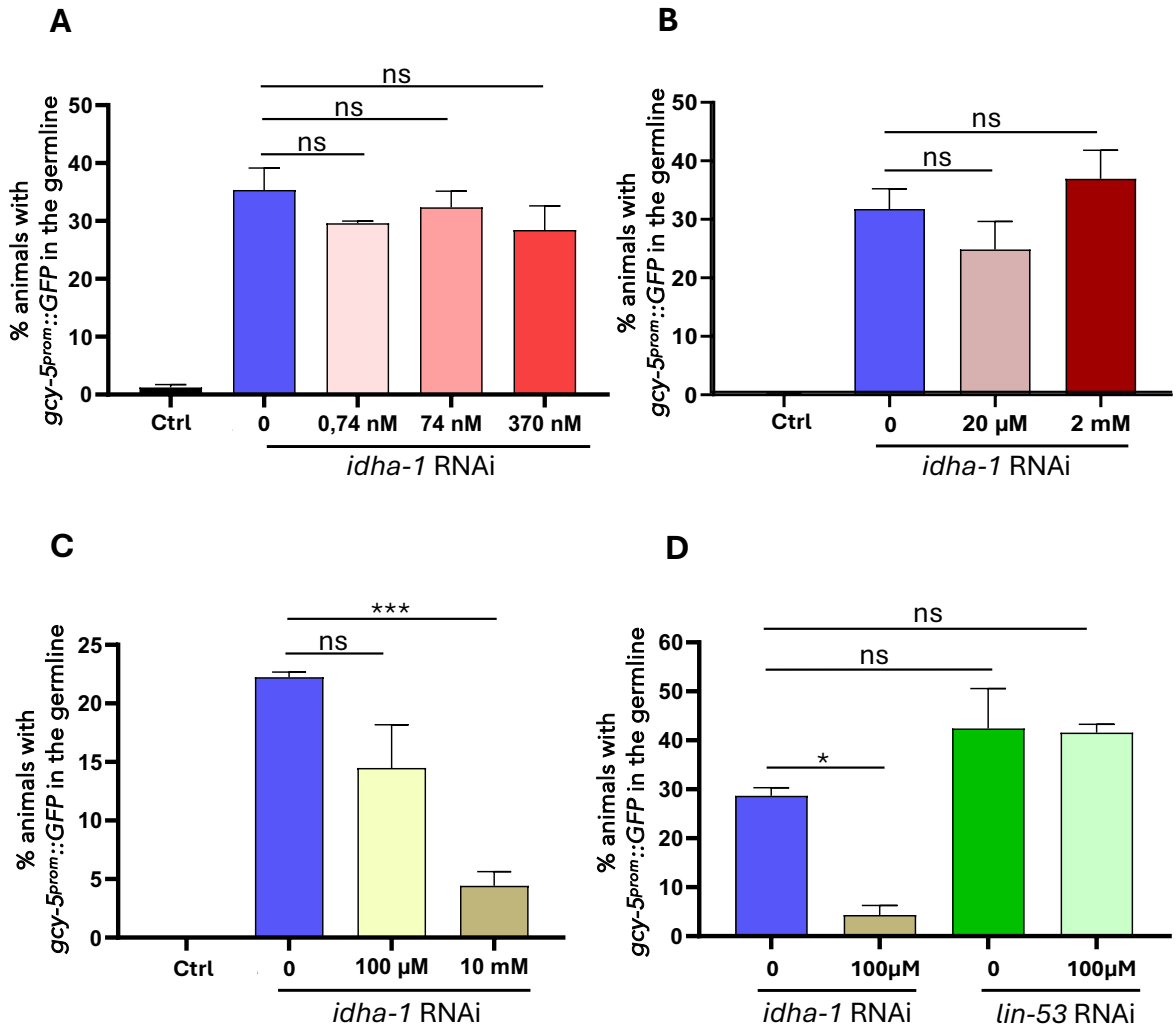

Figure 2.8 Significance of methionine cycle in *idha-1* depletion-mediated germline reprogramming. Quantification of animals displaying ASE neuron fate marker *gcy-5*^{prom}*::GFP* induction in the germline upon TF CHE-1^{oe} in conjunction with either *idha-1*^{RNAi} or *lin-53*^{RNAi} and various supplementations. **A)** Vitamin B12 supplementation at varying concentrations did not affect the germline reprogramming rate. *Rluc*^{RNAi} was used as negative control. **B)** SAM supplementation at varying concentrations did not affect the germline reprogramming rate. *Rluc*^{RNAi} was used as negative control. **C)** Methionine supplementation at 10mM concentration significantly decreased reprogramming efficiency. *Rluc*^{RNAi} was used as negative control. **D)** The suppressive effect of

exogenous methionine is specific to *idha-1*^{RNAi} and does not affect lin-53 depletion-mediated germline reprogramming. Three biological replicates each three technical repeats. n≥450 for each condition. Ordinary one-way ANOVA test was used for statistical comparisons, *** p<0.001, * p<0.5, ns: non-significant. Error bars represent SEM.

2.9 Hermaphrodite-specific spermatogenesis genes are required for *idha-1* depletion-mediated reprogramming

When observing the germline to ASE neuron conversion phenotype visible in *idha-1* depletion-mediated reprogramming, it becomes evident that there is an overlap with the spermatheca region of the *C. elegans* germline. Due to this observation we aimed to assess the reprogramming efficiency based on the male associated components of the germline. However, as previously shown *idha-1* depletion did not lead to reprogramming in CHE-1^{oe} of *him-8 (e1489)* mutant males except in very few animals (Section 2.2). The results suggested the likelihood of hermaphrodite-specific sperm or spermatheca developmental pathways involvement rather than pathways shared between males and hermaphrodites.

The *spe* genes are a class of sex specific genes that are crucial in development and motility of spermatids specifically in hermaphrodites. Mutations in *spe-8*, *spe-12*, *spe-27*, and *spe-29* block the activation of spermatids and cause self-sterile hermaphrodites (L'Hernault et al., 1988; Minniti et al., 1996). We evaluated the enhancing or suppressing effects of *spe-8* and *spe-27* depletion in a double RNAi experiment with *idha-1*^{RNAi}. Two other genes *mog-7* and *gld-2* were also included in this screen due to their roles in the germline biology.

The gene *mog-7* belongs to the mog family of genes (masculinization of germline), which are involved in RNA splicing and regulate the switch from spermatogenesis to oogenesis in hermaphrodites. Mutations in *mog* genes are associated with defects in

spermatogenic germline development (Graham & Kimble, 1993; Graham et al., 1993). Loss-of-function mutations in *mog-7* inhibit germline development and lead to sterility (Cao et al., 2022). Although *mog-7* is not specific to hermaphrodites, studying its depletion could provide insights into the role of male-specific physiology in germline reprogramming.

In contrast, *gld-2* is involved in cell division and meiosis I, primarily active in the distal arms of the germline as germ cells exit the stem cell niche (*WormBook*). This suggests that *gld-2* plays a crucial role in the healthy development and flow of germ cells toward the vulva, where reprogramming is predominantly observed in *idha-1* depletion experiments. Hypothetically, *gld-2* depletion could either reduce reprogramming efficiency due to a decreased abundance of germ cells or have no effect, as it is not directly involved in spermatogenesis or spermatheca function. Another intriguing gene to study in the context of sex determination and its impact on germline reprogramming is *tra-1*. As the master regulator of somatic sexual development, *tra-1* activity determines the hermaphrodite state when active and male development when inactive (Lawson et al., 2020; Hunter & Wood, 1990).

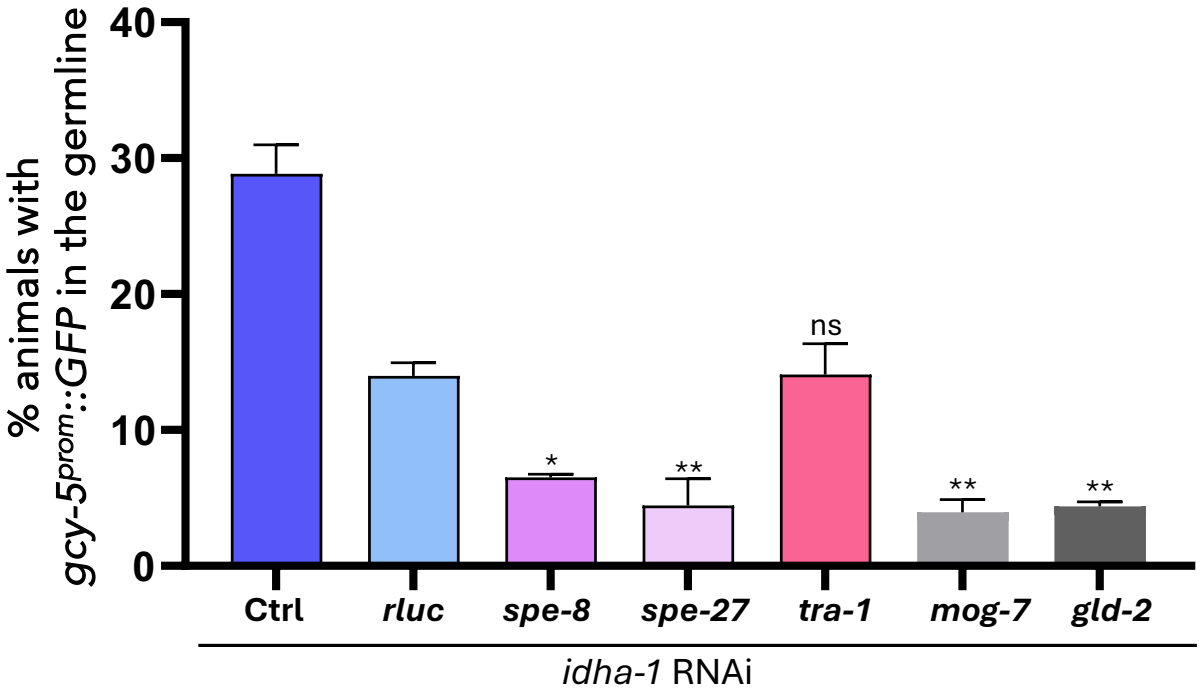

Figure 2.9.1 Hermaphrodite spermatogenesis is required for germ cell reprogramming

Quantification of animals showing ASE neuron fate marker *gcy-5^{prom}::GFP* induction in the germline upon CHE-1^{oe} in combination with double RNAi of *idha-1* and other candidate genes. Mixed *idha-1* and *Rluc* double RNAi was used as a control condition. Single *idha-1^{RNAi}* was used as a reprogramming efficiency control. Depletion of *spe-8*, *spe-27*, *mog-7* and *gld-2* under *idha-1^{RNAi}* significantly decrease reprogramming rate compared to *Rluc* control RNAi. Three biological replicates each three technical repeats. n≥450 for each condition. Ordinary one-way ANOVA test was used for statistical comparison, *p<0.05 ** p<0.01. Error bars represent SEM.

Upon TF CHE-1^{oe} combined with *idha-1* double RNAi targeting the genes, *spe-8*, *spe-27*, *mog-7* and *gld-2* we observed a significant decline in germline reprogramming efficiency. However, *tra-1* depletion in combination with *idha-1*^{RNAi} did not result in any changes in reprogramming rate (Figure 2.9.1).

The gene *fkh-6*, a regulator of sexual dimorphism, promotes male gonadal cell fate and lies downstream of tra-1. Green fluorescent protein (GFP)-tagged FKH-6 (FKH-6::GFP) localizes to the hermaphrodite spermatheca and sheath cells (Chang et al.,

2004; Hope et al., 2003). We utilized this strain to visualize the effects of *idha-1*^{RNAi} treatment under a fluorescent microscope (Figure 2.9.2). Our observations revealed that *idha-1*-depleted animals exhibited reduced GFP signal around the spermatheca compared to control treatments, where the spermatheca displayed a stronger GFP signal, and fluorescence was also visible in the sheath cells.

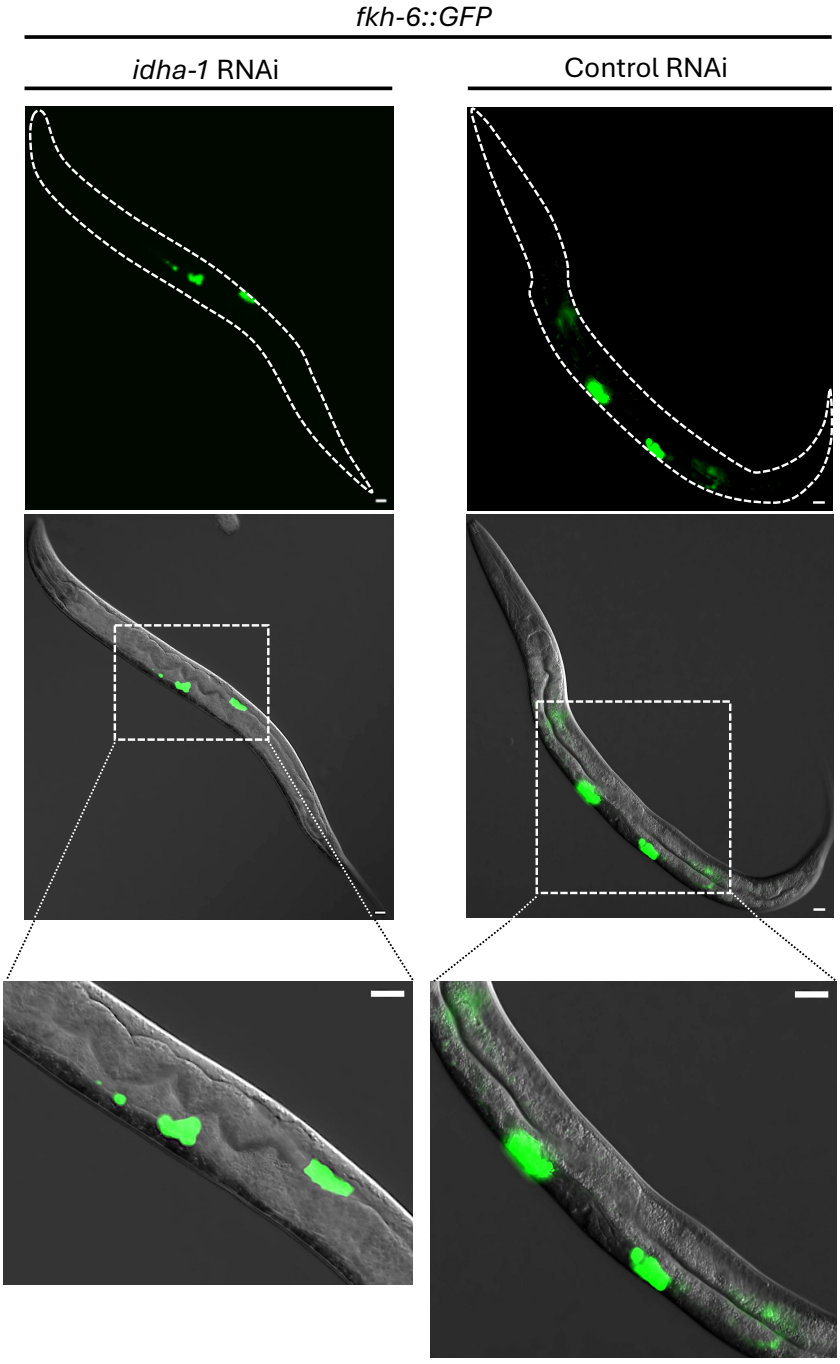

Figure 2.9.2 IDH-3 depletion reduces FKH-6::GFP signal in spermatheca. GFP fused FKH-6 expression in adult hermaphrodite spermatheca is bright and weak staining is also observed in the proximal sheath cells. ezIs2 [fkh-6::GFP + unc-119(+)]. *fkh-6::GFP* expression in the germline under *idha-1*^{RNAi} and *Rluc* as *control*^{RNAi}.

3. DISCUSSION

Previous research carried out by Ul Fatima and colleagues has demonstrated that, upon knockdown of the mitochondrial isocitrate dehydrogenase IDHA-1 combined with CHE-1^{oe}, germ cells start expressing neuronal genes such as expression of the pan neuronal reporter *rab-3::RFP* and synaptic protein UNC-10 (Figure S1 B). Furthermore, the cells acquire axo-dendritic like morphological changes supporting the finding that the germ cells convert into neuron-like cells. In conjunction to these findings, it has been observed that the levels of repressive histone methylation marks such as H3K27me3 and H3K9me3, are reduced in *C. elegans* treated with *idha-1*^{RNAi}. These results support the cell fate safeguarding function of IDHA-1. Upon knockdown of *idha-1*, the TF CHE-1^{oe} can activate *gcy-5*^{prom}*::GFP* reporter, along with the manifestation of other characteristics indicative of neuronal fate induction (Ul Fatima, Unpublished).

In our quest to elucidate the mechanisms by which a mitochondrial protein is leading to changes in the nucleus for direct reprogramming, we had to address multiple aspects of our phenotype in this study. This included investigation of metabolic modulators in the form of membrane transporters, which support metabolic reactions and various metabolites. Additionally, we also focused on the physiology of *C. elegans* concerning germline reprogramming, as working with an animal model offered the opportunity to study a complete living system with diverse tissue types. We leveraged our observations to inform our understanding of the region undergoing reprogramming.

3.1 Membrane transporter FDGT-2 is involved in germline reprogramming and is likely a key element in modulating metabolism

FDGT-2 (*F14E5.1*) is characterized as a putative hexose membrane transporter implicated in monosaccharide transmembrane transportation (Garde et al., 2022; Mueckler & Thorens 2013; Pao et al., 1998). In a suppressor/enhancer screen, it was identified to increase phenotype penetrance when co-depleted with IDHA-1. Given its function as a transmembrane protein and transportation of metabolic substrates, its involvement in IDHA-1 suppression-mediated reprogramming aligns with its potential influence on metabolism. The human ortholog of FDGT-2 is GLUT-1, which has been implicated in having an increased expression level in various human cancers as cancerous cells are known to exploit regular metabolic pathways for their proliferation; including prostate, breast and ovarian cancers (Zambrano et al., 2019; Nishioka et al., 1992; Cantuaria et al., 2001). Metabolism is the important cellular process that connects the energetic state of a cell to development, maintenance and proliferative pathways. Therefore, we propose that the function of FDGT-2 under the experimental conditions with *idha-1*^{RNAi} treatment to serve as a compensatory mechanism that partially mitigates the metabolic changes induced by IDHA-1 depletion. The co-depletion of *fdgt-2*^{RNAi} and *idha-1*^{RNAi} is likely an approach that disrupts this compensatory mechanism. Ultimately, this causes the molecular changes associated with *idha-1*^{RNAi} to persist.

Given that FDGT-2 is a putative glucose transporter, it is reasonable to assume that the transported molecule be of the similar description. However, upon *idha-1*^{RNAi} the nature of the transported molecules may change due to the unconventional shift in metabolic processes. Potentially, neighboring cells can utilize the available communication channels to rescue the adjacent cells undergoing reprogramming. Previous research has indicated that *idha-1* depletion-mediated reprogramming

mainly relies on its depletion in the somatic gonad in order for the germline reprogramming to occur (Ul Fatima, Unpublished). This unexpected finding demonstrated the cell non-autonomous nature of germline reprogramming upon *idha-1*^{RNAi}. For germline reprogramming to function efficiently, *idha-1*^{RNAi} must exert its effect in the somatic gonad, which highlights the need for inter-tissue communication for the germline reprogramming. The pathways involving FDGT-2 are likely operating with analogous communication and signaling mechanisms.

The findings from whole-worm immunostaining of FDGT-2 provide initial insights into its potential functional roles in *C. elegans*, particularly in regions critical for development and reproduction (Figure 2.4.2). The 3xHA-tagged FDGT-2 is observed to be expressed from the anterior to the posterior end, primarily along the gut tissue and across the germline. Similarly, Mitotracker staining of whole worms reveals a dense distribution of mitochondria along the gut lining and reproductive organs, as shown in Figure 2.1.2 A. These observations shed light on the role of the hexose membrane transporter FDGT-2 in facilitating energy exchange from the digestive tract, where energy is sourced, to the energy-demanding germline in close proximity.

3.2 Involvement of glutamine anaplerosis pathway in replenishment of a-KG levels in *idha-1* depleted worms

Metabolites and their intermediates can affect chromatin accessibility, as many key chromatin modifying enzymes, the regulators of epigenetic changes, require the products of the anabolic and catabolic pathways in metabolism (Nieborak & Schneider, 2018). Since alpha-Ketoglutarate (a-KG) is a product of *idha-1* it is natural to presume that its levels must have changed upon *idha-1*^{RNAi}. (Lin et al., 2022; Ugur et al., 2017). The change in a-KG levels were measured by gas chromatography/mass spectrometry metabolomics, which showed decreases in glutamate levels but

surprisingly stable levels of a-KG despite *idha-1*^{RNAi}. The results suggested a new means of replenishment for a-KG levels, which would point to glutamine anaplerosis pathway or glutaminolysis, a metabolic pathway that converts glutamine to a-KG via glutamate (Yoo et al., 2020; Lauzier et al., 2013). This explains the decrease in glutamate level since its used for conversion into a-kg (Figure 2.5 A). During the glutamine metabolism GLNA-1 and GLNA-3 glutaminase enzymes are involved in glutamate biosynthesis from glutamine. The enzyme GLNA-2 is also a glutaminase, but unlike GLNA-1 and GLNA-2 it also catalyzes the reverse reaction. Glutamate is then further catalyzed to a-KG by glutamate dehydrogenase (GDH-1). To confirm the involvement of this pathway, by using CRISPR/Cas9 a knockout mutant strain of *glna-3* was created. The *glna-3*$^{-/-}$ mutants would theoretically exhibit decreased levels of glutamine anaplerosis compared to wild type (WT) animals, as the loss of a major glutaminase would impair the conversion of glutamine to glutamate. Under *idha-1*^{RNAi} conditions, the *glna-3*$^{-/-}$ mutants showed a significantly decreased reprogramming rate compared to WT *glna-3* worms under the same *idha-1*^{RNAi} treatment (Figure 2.6). This finding supports the role of GLNA-3 in production of glutamate and its involvement in the glutamine anaplerosis pathway. Furthermore, the observed decrease in reprogramming efficiency in *glna-3*$^{-/-}$ mutants could not be restored even after supplementation of reprogramming enhancing metabolites such as a-KG and other TCA cycle intermediates.

Glutamine anaplerosis serves as a critical pathway for replenishing a-KG, but this process also leads to accumulation of byproducts such as glutamate, aspartate, carbon dioxide and ammonia, which can affect other cellular reactions. These byproducts may act as signaling molecules in hypoxic environments and play a role autophagy activation (Yoo et al., 2020; Villar et al., 2015; Sullivan et al., 2015). Consequently, making glutamine anaplerosis more relevant to broader cellular

functions. Moreover, glutamine metabolism has been shown to activate mammalian target of rapamycin complex 1 (mTORC1) (Villar et al., 2017). Conversely, mTORC1 can promote glutamine anaplerosis by enhancing the activity of glutamate dehydrogenase (GDH-1) (Csibi et al., 2013). This mutual relationship highlights the intricate regulation of glutamine metabolism in cellular signaling and metabolic pathways. While much of the research on glutamine anaplerosis has been conducted in the context of cancer, the role of this pathway in other biological processes, such as germline reprogramming remains to be characterized in more depth.

The expected increase in aspartate levels upon *idha-1* depletion became increasingly relevant to our research, as aspartate has been implicated in various cellular functions. For instance, D-aspartate plays a role in the glutamatergic neuron system and the reproductive system, particularly in spermatogenesis and sperm motility (Errico et al., 2013; Cristino et al., 2015; Santillo et al., 2016; Di Fiore et al., 2018). However, aspartate supplementation did not significantly alter reprogramming efficiency (Figure 2.6.2 A). Enzymes that degrade D-aspartate, such as D-aspartate oxidases (DDOs), have been linked to egg-laying events, self-fertily, extracellular secretions and development (Saitoh et al., 2012; Saitoh et al., 2019). To further investigate, we increased endogenous aspartate levels by depleting DDO-1, DDO-2, and DDO-3 in conjunction with IDHA-1 depletion. However, this approach did not result in any observable changes in the reprogramming phenotype. So far, we have not been able to establish a clear relationship between aspartate levels and the germline reprogramming phenotype. It is possible that a ceiling effect for aspartate concentration had already been reached, or that the L-aspartate isoform may be more relevant to the observed phenotype.

3.3 Alpha ketoglutarate is more than just a metabolite in the TCA cycle

Supplementation of a-KG in *C. elegans* can influence pathways beyond the tricarboxylic acid (TCA) cycle, as increasing evidence highlights the role of metabolites in aging and their function as cofactors for various enzymes (Gut & Verdin, 2013; van der Knaap & Verrijzer;2016). For instance, a-KG has been shown to modulate the TOR pathway by decreasing the activity of Complex V of the electron transport chain in the mitochondria, also known as the ATP synthase (Chin et al., 2014). This inhibition reduces ATP production, decrease in oxygen consumption and downregulates TOR pathway activity which is known to a play role in longevity. Elevated a-KG levels have also been observed in fasting, post-exercise conditions and the livers of under fed animals, further implicating a-KG in nutrient sensing and insulin secretions. (Hoang & Joseph, 2020).

Although metabolomics analysis revealed relatively stable a-KG levels following *idha-1*^{RNAi}, these levels were still altered compared to those in WT systems. It is possible that these changes in metabolite levels could impact ATP synthesis and subsequently affect TOR pathway activity. To investigate this, we designed an experiment (Section 2.7) to mimic reduced TOR activity by supplementing rapamycin to *C. elegans* and maintained them on *idha-1*^{RNAi}. The goal was to replicate the reduction in TOR pathway activity induced by elevated a-KG levels, which decrease ATP synthesis. If IDHA-1 depletion-mediated reprogramming were linked to increased TOR activity due to reduce a-KG availability, we would expect to observe a decrease in reprogramming rate following rapamycin-induced TOR inhibition. However, no significant enhancement or suppression of the reprogramming phenotype was observed neither with rapamycin supplementation nor with *let-363* double RNAi. This suggests that the reprogramming phenotype induced *idha-1*^{RNAi} may not be influenced by the TOR pathway, or that the downstream effectors of TOR pathway

may have already reached their maximum threshold of activity, rendering rapamycin ineffective due to a ceiling effect.

3.4 Relationship between methionine cycle and IDH-3

The methionine cycle is a critical component of the cellular metabolism, playing a key role in S-adenosylmethionine (SAM) production, one carbon metabolism, amino acid metabolism and the folate cycle (Tassinari et al., 2024; JT Brosnan & ME Brosnan 2006). Initially, we aimed to investigate the effect of vitamin B12 supplementation on germline reprogramming, which later expanded to include other molecules within the methionine cycle (Section 2.8). However, neither vitamin B12 nor SAM supplementation yielded conclusive results regarding enhancement or suppression of reprogramming. Notably, SAM is reported to be highly unstable in both solid and liquid forms, making it prone to degradation (Morana et al., 2002). In contrast, methionine supplementation was found to suppress germline reprogramming under *idha-1*^{RNAi} conditions. This effect was specific to *idha-1* depletion-mediated reprogramming, as it was not observed with *lin-53*^{RNAi}. In studies on primed human pluripotent stem cells, increased intracellular a-KG levels have been shown to induced DNA demethylation (TeSlaa et al., 2016; Dai et al., 2018). If methionine supplementation were to increase SAM availability and its activity as a methyl donor, this mechanism, combined with reduced a-KG levels resulting from *idha-1*^{RNAi}, could shift chromatin accessibility to a more permissive state. Direct cellular programming requires expression of fate-related genes and an accessible chromatin state to facilitate TF binding (Tursun et al., 2011; Kolundzic et al., 2018). To better understand the relationship between methionine and *idha-1,* further investigation of individual components within the methionine cycle is necessary in the context of germline reprogramming.

3.5 Hermaphrodite germline reprogramming may be assigned to gender specific cells

Experiments with *lin-53*^{RNAi} revealed the induction of reprogramming in various parts of the *C. elegans* germline. However, *idha-1* depletion-mediated reprograming was predominantly observed around the vulval region of the nematode, in proximity of spermatheca, suggesting that male-specific cells were being reprogrammed (Section 2.2 and Figure 2.3.3). Germline imaging of the *him-8(e1489)* mutant strain, which more frequently generates males, did not narrow down the reprogramming to sperm or spermatheca as previously speculated, at least not in majority of the male-gendered worms. In some rare cases, reprogramming was observed in the male germline, with the reprogrammed regions overlapping with either the testis or vas deferens tissues (Figure 1.10 and Figure 2.2.2).

Reprogramming of sperm/spermatheca in fully feminized hermaphrodites would not be achievable if the reprogramming is indeed associated with the male germline components. The absence of reprogramming in feminized *fem-2(b245)* mutant worms initially appeared to support the idea of male gonadal reprogramming (Figure 2.3.2) (Ahringer & Kimble, 1991). However, upon closer examination, it suggested otherwise. As the feminized hermaphrodites lack male gonadal structures, the reduced prevalence of reprogramming could be attributed to this deficiency, thereby supporting the hypothesis that the male-specific germ cells are reprogramming.

Further examination of the germline in heat shocked TF CHE-1^{oe} *fem-2(b245)* mutant worms treated with *idha-1*^{RNAi} revealed a less robust germline tissue. Transferring L2 worms to 25°C for feminization caused germline deterioration due to the presence of the heat shock promoter which is activated at temperatures above 15°C. Premature activation of the heat shock promoter likely resulted in compromised development,

manifesting as reduced body size and diminished brood size. The absence of a healthy germline also precluded the possibility of reprogramming due to insufficient germ cell quantity. The reprogramming mechanism's dependence on ectopic expression of heat shock CHE-1 during the L4 stage in F1 progeny underscores its critical role in the experiment. Therefore, the animals must be maintained at 15°C prior to this stage.

To exclude the possibility of reprogramming suppressive effects associated with *fem-2* mutation and in order to draw the most accurate conclusions from this experiment, the CHE-1^{oe} method must avoid temperatures above 15°C before the L4 stage as higher temperatures might compromise the experimental results. The exact prevalence of damage caused by high heat in the *CHE-1oe* background requires more detailed investigation using strains with reporter fused germline proteins to assess the abundance of germline cells (Figure 2.3.3) (Rog & Dernburg, 2015; Wirshing & Cram, 2017). Crossing the CHE-^{1oe} and *gcy-5^{prom}::GFP* ASE neuron reporter strain with the strain carrying SUN-1::mRuby germline nuclei reporter should enable more precise conclusions about the impact of heat stress and RNAi on germ cell population.

Additionally, an improved experimental approach could utilize conditional depletion of FEM-2 by using AID (auxin-inducible degron) system. This system provides targeted degradation of an AID-tagged protein under auxin supplementation. The AID tag is introduced into the *fem-2* gene by using CRISPR/Cas9 gene editing tool. The co-expression of TIR1 machinery in the same system is required to target the AID tagged protein for proteasomal degradation. This method allows temporal control over protein depletion at precise life stages and also tissue specific degradation of

the protein of interest through expression of TIR1 under tissue-specific promoters (Nishimura et al., 2009; Holland et al., 2012; Yesbolatova et al., 2020).

Both mutant *fem-2(b245)* and WT *fem-2* animals were maintained at 25°C before heat shock. However, the wildtype animals exhibited less autofluorescence in the germline, an indicator of tissue damage that can interfere with GFP reporter signal scoring. In contrast, *fem-2(b245)* mutants displayed more prevalence of autofluorescence (Figure 2.3.2).

Another conclusion drawn from the presence of germline reprogramming in hermaphrodites in contrast to its absence in male worms could be due to differences in genetic make-up of germline development in different sexes. If reprogramming to ASE neuron can be attributed to the spermatocytes or spermatheca due to overlap of the region in germline with the prevalence of reprogrammed sites, then it becomes crucial to understand the reasons behind exclusive occurrence of successful reprogramming in hermaphrodites.

Spermatogenesis in hermaphrodites differs from that of males, particularly in genes such as *gld-1*, *fog-2*, *tra-1* and the *spe* family of genes. Hermaphrodites require specific molecular mechanisms to switch from spermatogenesis to oogenesis during late larval stages. To assess whether spermatogenesis-related genes suppress or enhance germline reprogramming specifically in hermaphrodites, we conducted a double RNAi experiment (Section 2.9).

A suppression of germline reprogramming was observed upon co-depletion of *idha-1* with *spe-8*, *spe-27*, *mog-7*, and *gld-2* (Figure 2.9). The reduced reprogramming efficiency in *mog-7*^{RNAi} is likely due to disruptions in gametogenesis and germline

defects, given *mog-7*'s role in the removal of introns in over 5,000 genes (Cao et al., 2022). Similarly, the reduced reprogramming efficiency observed with *gld-2* and *idha-1* co-depletion may result from defective meiosis I, which decreases germ cell proliferation. Although *gld-2* is not directly involved in spermatogenesis, its role in meiosis positions it as an upstream regulator of germ cell formation, explaining the sharp decline in reprogramming efficiency.

Interestingly, no significant changes in reprogramming rates were observed upon *tra-1* depletion. As the master regulator of sex determination, *tra-1* is essential for sexual development, driving dimorphic changes between sexes and even determining the fate of some gender-specific neurons (Ellis et al., 2020; Ryan et al., 2014; Oren-Suissa et al., 2016). The lack of effect from *tra-1* depletion in *idha-1*-depeltion mediated germline reprogramming highlights that earlier sex determination pathways are not directly related to this process, while other genes, such as *spe-8* and *spe-27*, play a more significant role. The activation of hermaphrodite self-sperms relies on *spe-8* pathway and the deletion of any of the *spe-8* pathway members *spe-8*, *spe-12*, *spe-19*, *spe-27*, and *spe-29* result in hermaphrodite's failure to produce self-progeny (Geldziler et al., 2005; Muhlrad et al., 2014; Nance at al., 2000). The suppressive effects of $spe\text{-}8^{RNAi}$ and $spe\text{-}27^{RNAi}$ confirmed the predictions about the type of the cells undergoing reprogramming, as these genes are associated with male-specific germline regions of the hermaphrodite. Overall, the results suggests that the reprogramming phenotype may be generally attributed to hermaphrodite germline components and not males.

3.6 Conclusion and future directions

The role of IDH-3 in the TCA cycle, as well as the significance of a functional TCA cycle, has been a focal point of interest in metabolism research and various human diseases (Cavalcanti et al., 2014; Ugur et al., 2017; Liu et al., 2020; Jimenez-Uribe et al., 2021). However, our research shines light on an additional aspect of IDH-3. We have identified *idha-1* as a crucial factor in maintaining cell fate in *C. elegans*. The exact relationship between IDH-3 and the prevention of germline conversion into ASE neuron requires to be studied in further detail. Metabolism is well-known to have a direct effect on chromatin regulation and several of the underlying mechanisms in this process have been identified (Berger, 2007; Cheng, 2014; Shiraki et al., 2014; Li et al., 2018) Some of these events involve membrane transporters, some involve metabolites, some function through enzymes and some through tissue specific pathways.

Currently, we are dissecting the molecular steps involved in germline reprogramming that occur following adoption of alternative a-KG supply source in the context of *idha-1* depletion, which is glutamine anaplerosis pathway. It is likely that multiple other additional intermediates contribute to the observed phenotype, potentially including coenzymes such as NADH or compounds like ammonia and aspartate, the byproducts of glutamine anaplerosis.

We also had the objective to identify the cell types undergoing reprogramming in the *idha-1*^{RNAi} treated germline. Our findings suggested the cells converting to ASE neuron fate in the germline, originate in the region surrounding the vulva and we linked this to male-specific components of the hermaphrodite germline. However more research is necessary to clarify the relationship between sperm/spermatheca reprogramming and IDH-3 depletion.

In a novel approach to reprogramming, we intend to utilize the previously identified enhancers in combination to evaluate their cumulative reprogramming potential in the context of TF CHE-1^{oe}, without the *idha-1* depletion. The various features of the reprogramming observed points to cascades of events that take place under *idha-1*^{RNAi}. Given these complexities, it becomes essential to question whether the safeguarding role of a reprogramming barrier might be compromised by simultaneously targeting multiple of its molecular pathways.

We believe our research will enhance the understanding the role of metabolism and its intermediates in the field of direct cellular reprogramming. The occurrence of evolutionarily conserved pathways between the biology of humans and *C. elegans* cellular mechanisms paves the way for the translation of our findings for application in treatment of human diseases and cellular replacement therapies.

4 MATERIALS

4.1 Antibiotics

Table 4.1 List of antibiotics

Name	Stock concentration	Company
Carbenicillin	50 mg/ml	Carl Roth GmbH + Co. KG
Tetracycline	12,5 mg/ml	Carl Roth GmbH + Co. KG

4.2 Antibodies

Table 4.2 List of Antibodies

Name	Target	Species	Company
PA5	Anti-HA	Mouse	Roche
PA23	Anti-HA-HRP	Rat	Roche
PA49	Anti-Histone H3 acetyl K14	Rabbit	Abcam
PA72	5-6-s - myosin heavy chain A	Mouse	Hybridoma Bank
PA179	Anti-HA High Affinity	Rat	Roche
PA185	Anti-V5	Mouse	Invitrogen by Thermo Fisher
SA4	Anti-rabbit IgG-HRP	Rabbit	Santa Cruz
SA1	Anti-rat IgI-HRP	Rat	Santa Cruz
SA2	Anti-mouse IghG-HRP	Mouse	Santa Cruz
SA10	AlexaFluor568	Goat Anti-Mouse	Invitrogen by Thermo Fisher
SA20	Alexa Fluor 488	goat anti-rat IgG (H+L)	Invitrogen by Thermo Fisher

4.3 *C. elegans* strains

Table 4.3 List of *C. elegans* strains

Strain name	Description
N2	*C. elegans* wildtype variant Bristol
BAT28	*otIs305 [hsp::che-1::3xHA] ntIs1 [gcy-5^{prom}::GFP] V*
BAT420	*[snb-1::NLS::RFP + pBX] line 17; pha-1(e2123) III; him-8(e1489) IV; ntIs1 [gcy-5^{prom}::GFP + lin-15(+)] V. otIs305 [hsp-16.2p::che-1::3xHA::BLRP + rol-6(su1006)]*
BAT1971	*idha-1(barSi25[idha-1::3xHA]) I*
BAT1994	*ieSi57 [eft-3p::TIR1::mRuby::unc-54 3'UTR + Cbr-unc-119(+)] II; otIs305 (hsp::che-1::3xHA) V; ntIs1 (gcy-5 ^{prom}::GFP) V; barSi30 (idha-1::AID degron::3xHA I)*
BAT2122	*barSi41[lim-7 prom::TIR-1:mRuby:unc-54 3'UTR, unc-18(+)] II rol-6, otIs305(hsp-prom-che-1::FLAG); ntIS1 (gcy-5 ^{prom}::gfp), barSi30 (idha- 1::AID degron::3xHA I)*
BAT2151	*F14E5.1.1::aptamer(K5) ; otIs305 (hsp::che-1::3xHA) V; ntIs1 (gcy-5::GFP) V*
BAT2193	*F14E5.1.1::AID::3xHA*
BAT2214	*F14E5.1 mutant (CRISPR KO); otIs305 [hsp::che-1::3xHA]; ntIs1 [gcy-5^{prom}::GFP] V*
BAT2215	*glna-3 mutant CRISPR KO; otIs305 [hsp::che-1::3xHA]; ntIs1 [gcy-5^{prom}::GFP] V*
BAT2231	*fem-2(b245) III; otIs305 (hsp::che-1::3xHA) V; ntIs1 (gcy-5 ^{prom}::GFP) V*

4.4 CRISPR generated worm strains

Table 4.4 List of CRISPR generated worm strains

Strain name	Genotype	Purpose
BAT2208	*F14E5.1 mutant CRISPR KO*	Deletion of *F14E5.1*
BAT2210	*glna-3 mutant CRISPR KO*	Deletion of *glna-3*

4.5 Bacteria and plasmid strains

Table 4.5 List of bacteria and plasmid strains

Strain	Genotype	Purpose
Escherichia Coli: OP50	uracil auxotroph E. coli bacteria Food source for *C.elegans*	uracil auxotroph E. coli bacteria Food source for *C.elegans*

4.6 Solutions, media and buffers

Table 4.6 List of solutions, media and buffers

Name	Composition
HEPES Based lysis Buffer	10 mM HEPES, ddH2O, 0.25 mM Levamisol, 0.1%, Tween20
LB-carb medium	20g LB broth, ddH2O, (50 µg/ml final concentration)
M9 (1 L)	6 g Na2HPO4, 3 g KH2PO4, 5 g NaCl, 50 mg Gelatine, ddH2O; before usage: add 1 ml 1M MgSO4
NGM+RNAi	3 g NaCl, 20 g Agar, 2,5 g Bacto Peptone, ddH2O after autoclaving add: 1 ml Cholesterol (5 mg/ml in 95% EtOH stock), 1 ml 1 M MgSO4, 1 ml 1 M CaCl2, 25 ml 1 M K2PO4, 1 ml fungizone (Amphotericin B 2,5 mg/ml stock), 1 ml 1 M IPTG, 500 µl Carbenicil- lin (50 mg/ml stock)
SDS	10% w/v SDS, 10 mM dithiothreitol (DTT), 20% v/v glycerol, 0.2 M Tris-HCl pH 6.8, 0.05% w/v bromophenolblue
1x SDS Running buffer	24,8 mM Tris-HCl, 192 mM Glycin, 0,01 % SDS (w/v)
TAE buffer (1 l), pH 8,5 50x	242 g Tris base, 57,1 ml glacial acetic acid, 18,6 g EDTA, ddH2O 25 mM Tris, 192 mM glycine (pH 8,3), 20% MeOH, 0,025-0,1% SDS (optional), ddH2O
Tankblot transfer buffer	25 mM Tris, 192 mM glycine pH 8.3, 20% MeOH
TBST 1x	1x TBS, 0,1% Tween20
TBST 3% BSA	1x TBS, 0,1% Tween20

Tetracycline solution	10ml ddH2O, 80 µl tetracycline
2xYT medium (1L), pH 7,5	16 g tryptone, 10 g yeast extract, 5 g NaCl, ddH2O
Nematode freezing solution	100 mM NaCl; 20 mM KH_2PO_4 (pH 6); 4 % glycerol (v/v) and 300 mM $MgSO_4$

4.7 Kits

Table 4.7 Kits used in the study

Name	Company
Expand Long Template PCR system	Roche
GeneJET PCR Purification Kit	GeneJET PCR Purification Kit
Zymo DNA Clean & ConcentratorTM-5	Zymo

4.8 Oligonucleotides used for genotyping

Table 4.8 List of genotyping oligonucleotides

Name	Application	Sequence
F14E5.1_AID_set1_F	genotyping F14E5.1 knockincrispr product AID 3XHA	GGAGTTGGTCCAATTTCGTGG
F14E5.1_AID_set1_R	genotyping F14E5.1 knockin crispr product AID 3XHA	AGTTCCGCCAGGTCAAACAA
F14E5.1_AID_set2_F	genotyping F14E5.1 knockin crispr product AID 3XHA	TGGAGTTGGTCCAATTTCGTG
idha-1_KI_F	To genotype *idha-1* CRISPR insertion	AACACGCTGCTCGTATCGAA
idha-1_KI_R	To genotype *idha-1* CRISPR insertion	CAAAGTGTTTTAGTGTCTAA CAGCC

idhg-1_KI_F	To genotype *idha-1* CRISPR insertion	ATCGGAACTCGTTCAATCAG TA
idhg-1_KI_R	To genotype *idha-1* CRISPR insertion	TCAGTCAACGGGGTCAAACA
glna-3-KO-F	To genotype *glna-3* knockout CRISPR mutant	CAACTCGCACAAATCATTCGGA
glna-3-KO-R	To genotype *glna-3* knockout CRISPR mutant	TTCTAGGCTTCTCCGACGGT

4.9 sgRNAs

Table 4.9 List of sgRNAs use in the study

Target gene	sgRNA name	Sequence
F14E5.1	sgRNA_1 F14E5.1 (AID)	ttgaaaacgttcatacggcc
F14E5.1	sgRNA_2 F14E5.1 (AID)	aacctttgaaaacgttcata
F14E5.1	sgRNA_1 F14E5.1	aaattttacttgatcgagcc
glna-3	glna-3 KO sgRNA1 (reverse)	aagaaactcatcgaatgcat
glna-3	*glna-3 KO sgRNA2*	GCTGCTAGAAGAGGCAATTA
glna-3	*glna-3 KO sgRNA3 (reverse)*	agtaggcggagacaagacgg
glna-3	*glna-3 KO sgRNA4*	AGATCGAACAGTTTTACACG

4.10 Chemicals and reagents

Table 4.10 List of Chemicals and reagents

Name	Company
2-Propanol	Sigma Aldrich
Acetic acid	Carl Roth GmbH + Co. KG
Acetone	Sigma Aldrich
Agar-Agar, Kobe I Kobe I	Carl Roth GmbH + Co. KG
Agarose NEEO Ultra-Quality Roti®garose	R Carl Roth GmbH + Co. KG

Alpha ketogluterate	Sigma
Amphotericin B (Fungizone)	USBiological
Bacto Peptone, BD Difco	A. Hartenstein GmbH
Boric acid ≥99,8 %, p.a., ACS, ISO	Carl Roth GmbH + Co. KG
Bovine Serum Albumin	Sigma Aldrich
Calcium chloride, Dihydrate	Carl Roth GmbH + Co. KG
Chloroform	Carl Roth GmbH + Co. KG
Cholesterol	Carl Roth GmbH + Co. KG
Citrate	Sigma Aldrich
Dipotassium phosphate	Carl Roth GmbH + Co. KG
DMSO	Carl Roth GmbH + Co. KG
EDTA (Ethylenediaminetetraacetic acid)	Carl Roth GmbH + Co. KG
EGTA (ethylene glycol-bis(**β**-aminoethyl ether)- N,N,N′,N′-tetraacetic acid	Carl Roth GmbH + Co. KG
Ethanol unvergällt 99%	MDC, Hamburg University
Ethanol vergällt 99%	MDC, Hamburg University
Ethidium bromide (EtBr)	Carl Roth GmbH + Co. KG
Floxuridine (5-fluorodeoxyuridine)	Abcam
Formaldehyde 37 % p.A.	Sigma Aldrich
Fumaric acid	Sigma Aldrich
Gelatin	Carl Roth GmbH + Co. KG
Gelatine 2% solution from bovine skin cell	Sigma Aldrich
Glucose	Carl Roth GmbH + Co. KG
Glycerol 98%	Carl Roth GmbH + Co. KG
Glycin PUFFERAN®	Carl Roth GmbH + Co. KG
HEPES Buffer	Applichem
Hydrochloric acid 37 %	Carl Roth GmbH + Co. KG
Hydrogen Peroxide 30 % p.A.	Carl Roth GmbH + Co. KG
Hydroxyurea 98 %	Sigma Aldrich
Indole-3-acetic acid, 98+% (Auxin) IPTG	
IPTG	Carl Roth GmbH + Co. KG
IS Mounting medium	Dianova
IS Mounting medium (DAPI)	Dianova
L- Malic acid	J & K Scientific
L-Glutamine	Fischer Scientific
LB-Agar (Luria/Miller)	Carl Roth GmbH + Co. KG
LB-Medium (Luria/Miller)	Carl Roth GmbH + Co. KG

Magnesium chloride hexahydrate	Carl Roth GmbH + Co. KG
Magnesium sulphate	Carl Roth GmbH + Co. KG
Methanol	Carl Roth GmbH + Co. KG
Polyvinylpyrrolindone	Sigma Aldrich
Potassium chloride	Carl Roth GmbH + Co. KG
RNase A	Invitrogen
RNase away	M&P Molecular Bio Products
Rotiphorese Gel 30 (37,5:1)	Carl Roth GmbH + Co. KG
Sodium acetate	Carl Roth GmbH + Co. KG
Sodium azide	Fluka-Sigma
Sodium chloride	Carl Roth GmbH + Co. KG
Sodium deoxycholate	Applichem
Sodium dodecyl sulfate	Carl Roth GmbH + Co. KG
Sodium hydroxide solution 4 N	Carl Roth GmbH + Co. KG
Sodium hypochlorite solution	Carl Roth GmbH + Co. KG
Spermidine	Sigma Aldrich
Succinic acid	Sigma Aldrich
TEMED 99%	Carl Roth GmbH + Co. KG
TRIS PUFFERAN®	Carl Roth GmbH + Co. KG
Triton® X-100	Sigma Aldrich
Trizol® Reagent	life technologies
Tween20	Sigma Aldrich

4.11 Facilities and outsourced services

Oligonucleotide synthesis and Sanger sequencing were performed by Eurofins Genomics. Repair templates and sgRNA for CRISPR were synthesized by Integrated DNA Technologies (IDT). The aforementioned experimental methods were conducted using laboratory equipment purchased from Thermo Fischer Scientific, Eppendorf, BIO-RAD, Nikon and Jena Analytik.

5 METHODS

5.1 Nematode Specific methods

5.1.1 C. elegance maintenance and care

The animals were maintained on plates with Nematode Growth Medium (NGM) agar (3 g NaCl, 20 g Agar, 2,5 g Peptone for 1L ddH_2O, supplemented with 5µg/mL Cholesterol, 1 mM $MgSO_4$, 1 mM $CaCl_2$, 25 mM K_2PO_4, 2.5 µg/mL Amphotericin B) and OP50 bacteria as food source at 15°C (Brenner, 1974). All temperature sensitive strains and non-temperature sensitive strains were maintained at 15°C, unless mentioned otherwise for specific experimental protocols. The worms were transferred onto fresh plates every one to two weeks depending on bacterial food supply. During general maintenance and experiments a Nikon C-DS dissecting microscope was used. The male population of *C. elegance* is naturally very low (0.1 – 0.2). In order to increase male prevalence in the population, males were crossed with hermaphrodites of the same genotype every two weeks. The *C. elegans* strains used and generated in this study are listed in table 4.1.3 and 4.1.4.

5.1.2 Bleaching for animal synchronization

Experimental protocols requiring homogenous larval or adult stage animals were performed after animal synchronization. Fully grown non-starved animals were collected from the plates by washing with M9 buffer (22 mM KH2PO4, 42 mM Na2HPO4, 86 mM NaCl, 1 mM MgSO4 in ddH2O) into a 1.5 ml eppendorf tube. The animals were exposed to 1 ml bleaching solution (4% NaClO, 2 M NaOH in ddH2O) for 3 minutes and 30 seconds accompanied by consistent shaken. The worms burst open and release eggs by the bleaching process. However, the eggshell provides protection to the larvae. The egg pellet is then collected by centrifugation and then

washed three times with 1 ml of M9 buffer. At the final stage the eggs are transferred to fresh NGM plates seeded with OP50 bacteria for hatching.

5.1.3 Whole worm lysis

For lysing worms, 1 to 10 worms are placed in PCR tubes with 20 µl of lysis buffer (50 mM KCl, 10 mM Tris pH 8.3, 2,5 mM $MgCl_2$, 0,45% Tween20 (v/v), 0,01% Gelatin (v/v) in ddH_2O) supplemented with 1 mg/ml of proteinase K. Worms are then freeze cracked at -80°C for minimum 30 minutes. Then the sample tubes are placed in a thermocycler for 1 hour at 65°C followed by another 30 minutes incubation at 95°C for inactivation of proteinase K. The lysates are then stored at -20°C or used for genotyping at volumes equivalent to 1-2 µl.

5.1.4 Transgenic crossing

Working with *C. elegans* provides the opportunity to cross different strains, creating new strains with desired genetic compositions. For mating, one hermaphrodite at the L4 to early young adult stage is placed on an NGM plate alongside 11 males. The plate contains a single drop-sized OP50 bacterial lawn at its center, creating a restricted, food-rich environment that increases the likelihood of successful mating. After an overnight incubation, single hermaphrodites are transferred to fresh NGM plates to lay progeny. Following a successful cross, approximately 50% of the F1 progeny are males, significantly higher than the natural frequency of 0.1 – 0.2%. The F1 progeny are then singled out, and the F1 mothers are lysed after laying F2 progeny on fresh plates. The lysed hermaphrodites are genotyped to determine the status of the allele of interest. If all F1 progeny are heterozygous, additional hermaphrodites are singled out and lysed after laying eggs. Genotyping continues until a homozygous hermaphrodite with the desired genetic alleles is identified. Crosses exhibiting a roller

phenotype with over 80% penetrance, meaning a significant majority of the population displays the phenotype, are considered homozygous for the trait. In addition to phenotype expression, F2 progeny are also identified through reporter gene expression or genotyping (Fay, 2013).

5.1.5 Plate preparation

Petri dishes, each measuring 6 cm in diameter, were used for all plate preparations. Each plate was filled with 8 mL of Nematode Growth Media (NGM), prepared by combining 3 g NaCl, 20 g agar, and 2.5 g peptone in 1 L of double-distilled water (ddH2O). The medium was supplemented with 5 µg/mL cholesterol, 1 mM MgSO4, 1 mM CaCl2, 25 mM K2PO4, and 2.5 µg/mL amphotericin B. After pouring, the plates were allowed to dry for 2–3 days. Once dried, the plates were seeded with OP50, a strain of *E. coli* bacteria used as a food source for *C. elegans*. The bacterial lawn typically formed within 2–4 days. The plates were either used immediately or stored at 4°C for long-term use.

5.1.6 Genotyping and DNA amplification

The worms were genotype to identify mutations or transgenic sequences following crossing, CRISPR injections or transgenesis. A volume of 1-2 µl from each worm lysate sample (see lysis protocol) were used as the template in the PCR reactions using Mango Taq (Bioline) (Table 5.1 and Table 5.2) Deletions and insertions were detected by the difference in size of the PCR product bands. Subsequently, sanger sequencing was utilized for confirming insertions and point mutations. N2 worms were used as wild-type control. Repair templates for CRIPSR/Cas9 injections were produced by Integrated DNA Technologies (IDT) and amplified by using high fidelity Q5 DNA.

Table 5.1 Mango Taq genotyping reaction mix

Reagent	Volume (µl)
5x Mango Taq Buffer	5
MgCl2	2
10 mM dNTPs	1
10 mM F Primer	1
10 mM R Primer	1
Template	3
Mango Taq	0,25
MQW (up to 25 µl)	11,75

Table 5.2 Thermocycler settings for PCR

		Mango Taq polymerase		Q5 DNA	
	Step	Temp. (°C)	Duration	Temp. (°C)	Duration
	Pre-heat	95		98	
	Initial denaturation	94	3 minutes	98	30 seconds
35 cycles	denaturation	94	20 seconds	98	10 seconds
	annealing	--*	40 seconds	--*	20 seconds
	Elongation	72	35 seconds	72	20 seconds
	Final Extension	72	5 minutes	72	2 minutes
	Hold	4	Infinite	4	Infinite

*Optimized for each primer set

Table 5.3 Q5 DNA polymerase reaction mix

Reagents	Volume (µl)
5xQ5 Reaction buffer	10
10 mM dNTPs	1
10 mM Primer F	2,5
10 mM Primer R	2,5
Template	1
Q5 polymerase	0,5
MQW (up to 50 µl)	32,5

5.1.7 RNAi treatment

To investigate the loss-of-function phenotypes of specific genes in *C. elegans*, RNA interference (RNAi) by feeding was employed (Timmons et al., 2001; Conte Jr et al., 2015). Bacteria expressing RNAi plasmids were spread onto plates containing Isopropyl **β**-D-1-thiogalactopyranoside (IPTG) to induce RNAi activity. Nematode Growth Medium (NGM) was heated to 60°C, after which 1 mM IPTG and 50 µg/mL carbenicillin were added. The plates were allowed to cool and solidify at room temperature and, after two days, were seeded with 150 µL of a 5X concentrated RNAi bacterial culture. The bacterial cultures were grown overnight (12–16 hours) at 37°C from the Ahringer RNAi library (Source Bioscience) (Kamath et al., 2003). As a negative control, RNAi targeting *Renilla luciferase (rluc)* was used. The seeded plates were incubated at room temperature for three days, protected from sunlight, and were either used immediately or stored at 4°C for up to three months.

To synchronize the developmental stage of the worms, a bleaching protocol was used to isolate eggs. For P0 experiments, the bleached eggs were directly transferred onto RNAi plates and maintained at 15°C until they reached the L4 larval stage. At this stage, the worms were heat-shocked at 37°C for 30 minutes, followed by overnight incubation at 25°C (Seelk et al., 2016). To prevent overheating, the upper and lower plates of the triplicate stacks were shielded with empty stacks of 6 cm plates. The following day, the plates were screened for germline expression of GFP.

For F1 RNAi treatment, the bleached eggs were first hatched and grown on OP50-seeded NGM plates at 15°C before being transferred to experimental RNAi plates. The P0 generation was transferred to RNAi plates at the L4 stage and maintained until most of the F1 progeny reached the L4 stage at 15°C. At this point, the plates were heat-shocked at 37°C for 30 minutes, followed by overnight incubation at 25°C, as

described earlier. The following day, the plates were screened for ectopic GFP expression in the germline. Unless otherwise stated, all reprogramming experiments were conducted using F1 RNAi.

For experiments requiring double RNAi targeting two genes, bacterial cultures were measured for optical density at 600 nm (OD600) using a DeNovix DS-11 Series spectrophotometer. The cultures were diluted accordingly and mixed in a 1:1 ratio. The double RNAi cultures, including the *Rluc* control mixed with the gene of interest, were then seeded onto RNAi plates and grown under the same conditions as described above.

5.1.8 Plate preparation for metabolite feeding and general drug treatments

For the feeding experiments, RNAi plates were prepared using the standard NGM plate media supplemented with 1 mM IPTG and 50 µg/mL carbenicillin. Stock solutions of the metabolites **α**-ketoglutarate (a-KG), fumarate, and malate were prepared at a concentration of 50 mM and subsequently diluted to a final concentration of 10 mM for the experimental plates. The pH of the RNAi media was adjusted to 6.0, as described by Chin et al. (2014) and Edwards et al. (2015). For auxin feeding experiments, a stock solution of 400 mM was prepared and diluted according to the specific experimental requirements. Once the plates solidified, they were seeded with RNAi bacteria cultured overnight in LB-Carb medium. The worms were then subjected to F1 RNAi treatment following the protocol described earlier. This approach ensured consistent and controlled conditions for studying the effects of metabolite supplementation and auxin treatment in conjunction with RNAi-mediated gene knockdown.

5.1.9 Freezing for long term storage

C. elegans can be preserved for long-term storage at -80°C, as described by Brenner et al. (1974). For this purpose, NGM plates seeded with OP50 and containing a predominantly L1-stage worm population were collected and washed three times with M9 buffer to remove residual bacteria. The worms were then suspended in a 1:1 mixture of M9 buffer and freezing solution (100 mM NaCl, 20 mM KH2PO4 [pH 6.0], 4% glycerol [v/v], and 300 mM MgSO4) (Brenner, 1974). A 500 µL aliquot of the worm suspension was transferred into CryoTubes, which were initially placed in styrofoam boxes and stored at -80°C to ensure gradual freezing. After two weeks, one test vial from each frozen batch was thawed and examined to assess the survival rate of the animals. This method ensures the viability of the worms for future use.

5.1.10 Generation of CRISPR/Cas9 edited strains

Some of the strains used in this study were generated using CRISPR-Cas9 genetic editing, a widely adopted method for creating transgenic animals (Dickinson, 2016). Twenty *C. elegans* hermaphrodites were microinjected with a mixture containing the single guide RNA (sgRNA), Cas9 protein, a DNA repair template with homology arms in case of target insertion site, and a plasmid encoding a fluorescent marker (*myo-2:RFP*) (Dokshin et al., 2018). The sgRNA protospacer adjacent motif (PAM) site, repair templates, and oligonucleotides were designed using the computer software tool A plasmid Editor (ApE © 2003-2022). Following injection, the F1 progeny were screened for RFP expression in the pharynx, and positive animals were isolated onto individual plates. These selected animals were then genotyped to confirm the presence of the desired mutation, as previously described (Arribere et al., 2014). To establish homozygous lines, animals were singled out and allowed to self-propagate. The homozygous state of the edited sequence was subsequently confirmed by

Sanger sequencing. This approach ensured the generation of stable, genetically edited strains for further analysis.

5.1.11 Lifespan assay

The lifespan assay was conducted on NGM plates containing 45 µM FUDR to inhibit egg laying and prevent progeny production. Synchronized L4-stage worms were maintained on FUDR plates at 20°C. Using a dissection microscope, the worms were gently tapped daily and assessed for movement and pharyngeal pumping in the head region. Worms displaying signs of life, such as movement or pharyngeal pumping, were recorded as alive, while those showing no movement were considered dead and removed from the plate. The plates were replaced 2–3 times per week to ensure an adequate bacterial food supply. This process of monitoring and recording the survival status of the worms was repeated until all worms had died, as described by Sutphin & Kaeberlein (2009). The collected survival data were analyzed using the online application OASIS 2 (Yang et al., 2011), which facilitated the calculation of lifespan statistics and generation of survival curves.

5.2 Biochemical methods

5.2.1 Worm protein lysis

Protein lysis was performed to extract proteins from whole-animal samples for subsequent western blot analysis. F1 generation worms treated with RNAi were collected at the L4 stage and washed three times with M9 buffer to remove residual bacteria. To denature the proteins, disrupt protein-protein interactions, and maintain a negative charge, 5X SDS sample buffer (10% w/v SDS, 10 mM dithiothreitol [DTT], 20% v/v glycerol, 0.2 M Tris-HCl [pH 6.8], and 0.05% w/v bromophenol blue) was

added directly to the worm pellet. The samples were then incubated at 96°C for 10 minutes and stored at -20°C until further use.

5.2.2 SDS polyacrylamide gel electrophoresis

For the separation of protein lysate samples, SDS polyacrylamide gel electrophoresis (SDS-PAGE) was performed. Protein samples were loaded onto 4–20% Mini-PROTEAN Precast Protein Gels (BioRad) and run in a vertical Mini-PROTEAN Tetra Electrophoresis system (BioRad) using 1X SDS running buffer (24.8 mM Tris-HCl, 192 mM glycine, 0.01% SDS [w/v]). Electrophoresis was initially conducted at 10 mA per gel until the samples migrated from the stacking gel into the separating gel. The current was then increased to 20 mA per gel and maintained for approximately 2 hours. A PageRuler Plus Prestained Protein Ladder (Thermo Scientific) was used as a molecular weight marker.

5.2.3 Westen Blot

Proteins separated on Mini-PROTEAN Precast Protein Gels were transferred onto nitrocellulose membranes for immunological detection using specific antibodies. Wet blotting chambers containing Tankblot transfer buffer (25 mM Tris, 192 mM glycine [pH 8.3], 20% methanol) were used for the transfer, which was performed at a constant voltage of 100 V for 60 minutes. Following transfer, the nitrocellulose membrane was blocked with 3% bovine serum albumin (BSA) in 1X TBST (25 mM Tris [pH 7.5], 150 mM NaCl, 0.1% v/v Tween 20) at room temperature for 1 hour with gentle shaking. After blocking, the membrane was incubated with the primary antibody overnight at 4°C or for 4 hours at room temperature. The membrane was then washed three times with 1X TBST for 15 minutes each. Subsequently, the membrane was incubated with an HRP-linked secondary antibody for 1 hour at room temperature. Detection of the

antibody-antigen complex was achieved using Lumi-Light Western Blotting Substrate (Roche Applied Sciences) according to the manufacturer's instructions. The chemiluminescent signal was visualized using a Luminescent Image Analyzer (GE Healthcare) and analyzed with ImageQuant LAS4000 software.The antibodies used in this study are listed in Table 4.1.2.

5.2.4 Antibody staining

For the detection of 3xHA-tagged FDGT-2 in whole worms, animals were fixed and permeabilized following the method described by Duerr (Duerr, 2006; Jones et al., 1996). Briefly, worms were washed off plates using M9 buffer. Glass Superfrost slides were placed on a metal tray on dry ice, and a drop of worms suspended in M9 buffer was pipetted onto the slide. Another slide was placed on top, and the two slides were split apart. The samples were then fixed in methanol for 10 minutes, followed by acetone for another 10 minutes. After fixation, the samples were washed with 1X PBS. Next, the samples were blocked in blocking buffer (1 mL 10X PBS, 0.1 mL 25% Triton X-100, 1 mL 2% gelatin, 40 µL 10% NaN3, and ddH2O to a total volume of 10 mL) for 30 minutes. The samples were then incubated with primary antibody (diluted in PBS containing 0.25% Triton X-100 and 0.2% gelatin) overnight at 4°C with gentle shaking. Following this, the samples were washed five times with PBS containing 0.25% Triton X-100. Secondary antibodies (Alexa Fluor dyes at 1:1000 dilution) in PBS with 0.25% Triton X-100 and 0.2% gelatin were added, and the samples were incubated overnight at 4°C with gentle shaking. After five additional washes with PBS containing 0.25% Triton X-100, the samples were mounted on glass slides using DAPI-containing mounting medium (ThermoFisher, #P36966). The slides were visualized under fluorescent microscope after 4 hours of DAPI incubation. The antibodies used in this study are listed in Table 4.1.2.

5.2.5 Microscopy

Worms were imaged with using Zeiss Axio Imager 2 fluorescent microscope connected to a digital camera (Sensicam, PCO), Nikon Eclipse Ni-E fluorescent microscope connected to a back illuminated sCMOS camera (edge, PCO) and Fluorescent Microscope DM6B (Leica). Animals were mounted on 2 % agarose pads on glass slides in M9 and 20 mM tetramisole droplet for anesthesia.

5.3 Computational analysis

Students t-test and one-way ANOVA were used for data analysis unless indicated otherwise.

REFERENCES

1. Ahringer, J., & Kimble, J. (1991). Control of the sperm–oocyte switch in Caenorhabditis elegans hermaphrodites by the fem-3 3′ untranslated region. Nature, 349(6307), 346-348.
2. Albert Hubbard, E. J., & Schedl, T. (2019). Biology of the Caenorhabditis elegans germline stem cell system. Genetics, 213(4), 1145-1188.
3. Alberts, B., Bray, D., Lewis, J., Raff, M., Roberts, K., & Watson, J. D. (1994). Molecular biology of the cell (Vol. 3). Garland New York.
4. Allis, C. D., & Jenuwein, T. (2016). The molecular hallmarks of epigenetic control. Nature Reviews Genetics, 17(8), 487-500.
5. Alvarado, A. S., & Yamanaka, S. (2014). Rethinking differentiation: stem cells, regeneration, and plasticity. Cell, 157(1), 110-119.
6. Ansari, H. R., & Raghava, G. P. (2010). Identification of NAD interacting residues in proteins. BMC bioinformatics, 11, 1-8.
7. Arnold, P. K., & Finley, L. W. (2023). Regulation and function of the mammalian tricarboxylic acid cycle. Journal of Biological Chemistry, 299(2).
8. Ashley, G. E., Duong, T., Levenson, M. T., Martinez, M. A., Johnson, L. C., Hibshman, J. D., Saeger, H. N., Palmisano, N. J., Doonan, R., & Martinez-Mendez, R. (2021). An expanded auxin-inducible degron toolkit for Caenorhabditis elegans. Genetics, 217(3), iyab006.
9. Bannister, A. J., & Kouzarides, T. (2011). Regulation of chromatin by histone modifications. Cell research, 21(3), 381-395.
10. Barbato, V., Talevi, R., Braun, S., Merolla, A., Sudhakaran, S., Longobardi, S., & Gualtieri, R. (2017). Supplementation of sperm media with zinc, D-aspartate and co-enzyme Q10 protects bull sperm against exogenous oxidative stress and improves their ability to support embryo development. Zygote, 25(2), 168-175.
11. Barski, A., Cuddapah, S., Cui, K., Roh, T.-Y., Schones, D. E., Wang, Z., Wei, G., Chepelev, I., & Zhao, K. (2007). High-resolution profiling of histone methylations in the human genome. Cell, 129(4), 823-837.
12. Baumanns, S., Beis, D. M., & Wenzel, U. (2023). RNA-interference in the nematode Caenorhabditis elegans is effective using paraformaldehyde-inactivated E. coli HT115 bacteria as a food source. Biochimica et Biophysica Acta (BBA)-Molecular Cell Research, 1870(1), 119375.

13. Berger, S. L. (2007). The complex language of chromatin regulation during transcription. Nature, 447(7143), 407-412.
14. Bird, A. (2002). DNA methylation patterns and epigenetic memory. Genes & development, 16(1), 6-21.
15. Blackwell, T. K., Sewell, A. K., Wu, Z., & Han, M. (2019). TOR signaling in Caenorhabditis elegans development, metabolism, and aging. Genetics, 213(2), 329-360.
16. Blagosklonny, M. V. (2013). Rapamycin extends life-and health span because it slows aging. Aging (Albany NY), 5(8), 592.
17. Blau, H. M., & Baltimore, D. (1991). Differentiation requires continuous regulation. The Journal of cell biology, 112(5), 781-783.
18. Boiani, M., & Schöler, H. R. (2005). Regulatory networks in embryo-derived pluripotent stem cells. Nature Reviews Molecular Cell Biology, 6(11), 872-881.
19. Borkent, M., Bennett, B. D., Lackford, B., Bar-Nur, O., Brumbaugh, J., Wang, L., Du, Y., Fargo, D. C., Apostolou, E., & Cheloufi, S. (2016). A serial shRNA screen for roadblocks to reprogramming identifies the protein modifier SUMO2. Stem cell reports, 6(5), 704-716.
20. Borkum, J. M. (2023). The tricarboxylic acid cycle as a central regulator of the rate of aging: implications for metabolic interventions. Advanced Biology, 7(7), 2300095.
21. Bott, A. J., Shen, J., Tonelli, C., Zhan, L., Sivaram, N., Jiang, Y.-P., Yu, X., Bhatt, V., Chiles, E., & Zhong, H. (2019). Glutamine anabolism plays a critical role in pancreatic cancer by coupling carbon and nitrogen metabolism. Cell reports, 29(5), 1287-1298. e1286.
22. Brosnan, J. T., & Brosnan, M. E. (2006). The sulfur-containing amino acids: an overview. The Journal of nutrition, 136(6), 1636S-1640S.
23. Byrd, D. T., Knobel, K., Affeldt, K., Crittenden, S. L., & Kimble, J. (2014). A DTC niche plexus surrounds the germline stem cell pool in Caenorhabditis elegans. PLoS One, 9(2), e88372.
24. Cantó, C., Houtkooper, R. H., Pirinen, E., Youn, D. Y., Oosterveer, M. H., Cen, Y., Fernandez-Marcos, P. J., Yamamoto, H., Andreux, P. A., & Cettour-Rose, P. (2012). The NAD+ precursor nicotinamide riboside enhances oxidative metabolism and protects against high-fat diet-induced obesity. Cell Metabolism, 15(6), 838-847.

25. Cantó, C., Menzies, K. J., & Auwerx, J. (2015). NAD+ metabolism and the control of energy homeostasis: a balancing act between mitochondria and the nucleus. Cell Metabolism, 22(1), 31-53.
26. Cantuaria, G., Fagotti, A., Ferrandina, G., Magalhaes, A., Nadji, M., Angioli, R., Penalver, M., Mancuso, S., & Scambia, G. (2001). GLUT-1 expression in ovarian carcinoma: association with survival and response to chemotherapy. Cancer: Interdisciplinary International Journal of the American Cancer Society, 92(5), 1144-1150.
27. Cao, W., Tran, C., Archer, S. K., Gopal, S., & Pocock, R. (2022). Functional recovery of the germ line following splicing collapse. Cell Death & Differentiation, 29(4), 772-787.
28. Cavalcanti, J. H. F., Esteves-Ferreira, A. A., Quinhones, C. G., Pereira-Lima, I. A., Nunes-Nesi, A., Fernie, A. R., & Araujo, W. L. (2014). Evolution and functional implications of the tricarboxylic acid cycle as revealed by phylogenetic analysis. Genome biology and evolution, 6(10), 2830-2848.
29. Chandel, N. S. (2014). Mitochondria as signaling organelles. BMC biology, 12, 1-7.
30. Chang, W., Tilmann, C., Thoemke, K., Markussen, F.-H., Mathies, L. D., Kimble, J., & Zarkower, D. (2004). A forkhead protein controls sexual identity of the C. elegans male somatic gonad.
31. Cheloufi, S., Elling, U., Hopfgartner, B., Jung, Y. L., Murn, J., Ninova, M., Hubmann, M., Badeaux, A. I., Euong Ang, C., & Tenen, D. (2015). The histone chaperone CAF-1 safeguards somatic cell identity. Nature, 528(7581), 218-224.
32. Cheng, X. (2014). Structural and functional coordination of DNA and histone methylation. Cold Spring Harbor perspectives in biology, 6(8), a018747.
33. Chiang, P. K., Gordon, R. K., Tal, J., Zeng, G., Doctor, B., Pardhasaradhi, K., & McCann, P. P. (1996). S-Adenosylmetliionine and methylation. The FASEB journal, 10(4), 471-480.
34. Chin, R. M., Fu, X., Pai, M. Y., Vergnes, L., Hwang, H., Deng, G., Diep, S., Lomenick, B., Meli, V. S., & Monsalve, G. C. (2014). The metabolite **α**-ketoglutarate extends lifespan by inhibiting ATP synthase and TOR. Nature, 510(7505), 397-401.
35. Choi, Y. J., Lin, C.-P., Ho, J. J., He, X., Okada, N., Bu, P., Zhong, Y., Kim, S. Y., Bennett, M. J., & Chen, C. (2011). miR-34 miRNAs provide a barrier for somatic cell reprogramming. Nature cell biology, 13(11), 1353-1360.

36. Conlon, N. J. (2022). The role of NAD+ in regenerative medicine. Plastic and reconstructive surgery, 150, 41S-48S.
37. Conte Jr, D., MacNeil, L. T., Walhout, A. J., & Mello, C. C. (2015). RNA Interference in Caenorhabditis elegans. Current protocols in molecular biology, 109(1), 26.23. 21-26.23. 30.
38. Corsi, A. K., Wightman, B., & Chalfie, M. (2015). A transparent window into biology: a primer on Caenorhabditis elegans. Genetics, 200(2), 387-407.
39. Cristino, L., Luongo, L., Squillace, M., Paolone, G., Mango, D., Piccinin, S., Zianni, E., Imperatore, R., Iannotta, M., & Longo, F. (2015). d-Aspartate oxidase influences glutamatergic system homeostasis in mammalian brain. Neurobiology of aging, 36(5), 1890-1902.
40. Csibi, A., Fendt, S.-M., Li, C., Poulogiannis, G., Choo, A. Y., Chapski, D. J., Jeong, S. M., Dempsey, J. M., Parkhitko, A., & Morrison, T. (2013). The mTORC1 pathway stimulates glutamine metabolism and cell proliferation by repressing SIRT4. Cell, 153(4), 840-854.
41. D'Aniello, G., Grieco, N., Di Filippo, M., Cappiello, F., Topo, E., D'Aniello, E., & Ronsini, S. (2007). Reproductive implication of D-aspartic acid in human pre-ovulatory follicular fluid. Human Reproduction, 22(12), 3178-3183.
42. D'Aniello, G., Ronsini, S., Guida, F., Spinelli, P., & D'Aniello, A. (2005). Occurrence of D-aspartic acid in human seminal plasma and spermatozoa: possible role in reproduction. Fertility and sterility, 84(5), 1444-1449.
43. Dai, Z., Mentch, S. J., Gao, X., Nichenametla, S. N., & Locasale, J. W. (2018). Methionine metabolism influences genomic architecture and gene expression through H3K4me3 peak width. Nature communications, 9(1), 1955.
44. Dang, L., Yen, K., & Attar, E. (2016). IDH mutations in cancer and progress toward development of targeted therapeutics. Annals of Oncology, 27(4), 599-608.
45. DeBerardinis, R. J., Mancuso, A., Daikhin, E., Nissim, I., Yudkoff, M., Wehrli, S., & Thompson, C. B. (2007). Beyond aerobic glycolysis: transformed cells can engage in glutamine metabolism that exceeds the requirement for protein and nucleotide synthesis. Proceedings of the National Academy of Sciences, 104(49), 19345-19350.
46. Di Fiore, M. M., Santillo, A., Falvo, S., Baccari, G. C., Venditti, M., Russo, F. D. G., Lispi, M., & D'Aniello, A. (2018). Sex hormone levels in the brain of d-aspartate-treated rats. Comptes Rendus Biologies, 341(1), 9-15.

47. Duerr, J. S. (2006). Immunohistochemistry. WormBook: The Online Review of C. elegans Biology [Internet].
48. Ellis, R., & Schedl, T. (2007). Sex determination in the germ line. WormBook: The Online Review of C. elegans Biology [Internet].
49. Ellis, R. E. (2020). Sex determination: TRA-1 Is a non-binary regulator of sexual identity. Current Biology, 30(18), R1036-R1038.
50. Errico, F., Napolitano, F., Squillace, M., Vitucci, D., Blasi, G., de Bartolomeis, A., Bertolino, A., D'Aniello, A., & Usiello, A. (2013). Decreased levels of D-aspartate and NMDA in the prefrontal cortex and striatum of patients with schizophrenia. Journal of psychiatric research, 47(10), 1432-1437.
51. Folmes, C. D., & Terzic, A. (2015). Metabolic determinants of embryonic development and stem cell fate. Reproduction, Fertility and Development, 27(1), 82-88.
52. Fukumoto, K., Ito, K., Saer, B., Taylor, G., Ye, S., Yamano, M., Toriba, Y., Hayes, A., Okamura, H., & Fustin, J.-M. (2022). Excess S-adenosylmethionine inhibits methylation via catabolism to adenine. Communications Biology, 5(1), 313.
53. Fukushige, T., Hawkins, M. G., & McGhee, J. D. (1998). The GATA-factor elt-2 is essential for formation of the Caenorhabditis elegans intestine. Developmental biology, 198(2), 286-302.
54. Fukushige, T., & Krause, M. (2005). The myogenic potency of HLH-1 reveals wide-spread developmental plasticity in early C. elegans embryos.
55. Garde, A., Kenny, I. W., Kelley, L. C., Chi, Q., Mutlu, A. S., Wang, M. C., & Sherwood, D. R. (2022). Localized glucose import, glycolytic processing, and mitochondria generate a focused ATP burst to power basement-membrane invasion. Developmental Cell, 57(6), 732-749. e737.
56. Geldziler, B., Chatterjee, I., & Singson, A. (2005). The genetic and molecular analysis of spe-19, a gene required for sperm activation in Caenorhabditis elegans. Developmental biology, 283(2), 424-436.
57. Geng, T., Zhang, D., & Jiang, W. (2019). Epigenetic regulation of transition among different pluripotent states: concise review. Stem Cells, 37(11), 1372-1380.
58. Giese, G. E., Walker, M. D., Ponomarova, O., Zhang, H., Li, X., Minevich, G., & Walhout, A. J. (2020). Caenorhabditis elegans methionine/S-adenosylmethionine cycle activity is sensed and adjusted by a nuclear hormone receptor. Elife, 9, e60259.

59. Graf, T. (2011). Historical origins of transdifferentiation and reprogramming. Cell stem cell, 9(6), 504-516.
60. Graham, P. L., & Kimble, J. (1993). The mog-1 gene is required for the switch from spermatogenesis to oogenesis in Caenorhabditis elegans. Genetics, 133(4), 919-931.
61. Graham, P. L., Schedl, T., & Kimble, J. (1993). More mog genes that influence the switch from spermatogenesis to oogenesis in the hermaphrodite germ line of Caenorhabditis elegans. Developmental genetics, 14(6), 471-484.
62. Green, R., Allen, L. H., Bjørke-Monsen, A.-L., Brito, A., Guéant, J.-L., Miller, J. W., Molloy, A. M., Nexo, E., Stabler, S., & Toh, B.-H. (2017). Vitamin B12 deficiency. Nature reviews Disease primers, 3(1), 1-20.
63. Guerra, F., Guaragnella, N., Arbini, A. A., Bucci, C., Giannattasio, S., & Moro, L. (2017). Mitochondrial dysfunction: a novel potential driver of epithelial-to-mesenchymal transition in cancer. Frontiers in oncology, 7, 295.
64. Guo, C., & Morris, S. A. (2017). Engineering cell identity: establishing new gene regulatory and chromatin landscapes. Current opinion in genetics & development, 46, 50-57.
65. Gut, P., & Verdin, E. (2013). The nexus of chromatin regulation and intermediary metabolism. Nature, 502(7472), 489-498.
66. Hall, D. H., Winfrey, V. P., Blaeuer, G., Hoffman, L. H., Furuta, T., Rose, K. L., Hobert, O., & Greenstein, D. (1999). Ultrastructural features of the adult hermaphrodite gonad of Caenorhabditis elegans: relations between the germ line and soma. Developmental biology, 212(1), 101-123.
67. Hansson, J., Rafiee, M. R., Reiland, S., Polo, J. M., Gehring, J., Okawa, S., Huber, W., Hochedlinger, K., & Krijgsveld, J. (2012). Highly coordinated proteome dynamics during reprogramming of somatic cells to pluripotency. Cell reports, 2(6), 1579-1592.
68. Harrison, D. E., Strong, R., Sharp, Z. D., Nelson, J. F., Astle, C. M., Flurkey, K., Nadon, N. L., Wilkinson, J. E., Frenkel, K., & Carter, C. S. (2009). Rapamycin fed late in life extends lifespan in genetically heterogeneous mice. Nature, 460(7253), 392-395.
69. Harvey, A. J., Rathjen, J., & Gardner, D. K. (2016). Metaboloepigenetic regulation of pluripotent stem cells. Stem Cells International, 2016(1), 1816525.

70. Hensley, C. T., Wasti, A. T., & DeBerardinis, R. J. (2013). Glutamine and cancer: cell biology, physiology, and clinical opportunities. The Journal of clinical investigation, 123(9), 3678-3684.
71. Hirsh, D., Oppenheim, D., & Klass, M. (1976). Development of the reproductive system of Caenorhabditis elegans. Developmental biology, 49(1), 200-219.
72. Hoang, M., & Joseph, J. (2020). The role of **α**-ketoglutarate and the hypoxia sensing pathway in the regulation of pancreatic **β**-cell function. Islets, 12(5), 108-119.
73. Hodgkin, J., Horvitz, H. R., & Brenner, S. (1979). Nondisjunction mutants of the nematode Caenorhabditis elegans. Genetics, 91(1), 67-94.
74. Holland, A. J., Fachinetti, D., Han, J. S., & Cleveland, D. W. (2012). Inducible, reversible system for the rapid and complete degradation of proteins in mammalian cells. Proceedings of the National Academy of Sciences, 109(49), E3350-E3357.
75. Hom, J. R., Quintanilla, R. A., Hoffman, D. L., de Mesy Bentley, K. L., Molkentin, J. D., Sheu, S.-S., & Porter, G. A. (2011). The permeability transition pore controls cardiac mitochondrial maturation and myocyte differentiation. Developmental Cell, 21(3), 469-478.
76. Hope, I. A., Mounsey, A., Bauer, P., & Aslam, S. (2003). The forkhead gene family of Caenorhabditis elegans. Gene, 304, 43-55.
77. Horner, M. A., Quintin, S., Domeier, M. E., Kimble, J., Labouesse, M., & Mango, S. E. (1998). pha-4, anHNF-3 homolog, specifies pharyngeal organ identity inCaenorhabditis elegans. Genes & development, 12(13), 1947-1952.
78. Hubbard, E. J., & Greenstein, D. (2005). Introduction to the germ line. WormBook, 1(4).
79. Huh, T.-L., Kim, Y.-O., Oh, I.-U., Song, B. J., & Inazawa, J. (1996). Assignment of the human mitochondrial NAD+-specific isocitrate dehydrogenase alpha subunit (IDH3A) gene to 15q25. 1--> q25. 2by in situ hybridization. Genomics, 32(2), 295-296.
80. Hunter, C. P., & Wood, W. B. (1990). The tra-1 gene determines sexual phenotype cell-autonomously in C. elegans. Cell, 63(6), 1193-1204.
81. Iacobazzi, V., Castegna, A., Infantino, V., & Andria, G. (2013). Mitochondrial DNA methylation as a next-generation biomarker and diagnostic tool. Molecular genetics and metabolism, 110(1-2), 25-34.

82. Ieda, M., Fu, J.-D., Delgado-Olguin, P., Vedantham, V., Hayashi, Y., Bruneau, B. G., & Srivastava, D. (2010). Direct reprogramming of fibroblasts into functional cardiomyocytes by defined factors. Cell, 142(3), 375-386.
83. Imai, S.-I., Armstrong, C. M., Kaeberlein, M., & Guarente, L. (2000). Transcriptional silencing and longevity protein Sir2 is an NAD-dependent histone deacetylase. Nature, 403(6771), 795-800.
84. Imai, S.-i., & Guarente, L. (2014). NAD+ and sirtuins in aging and disease. Trends in cell biology, 24(8), 464-471.
85. Jaenisch, R., & Bird, A. (2003). Epigenetic regulation of gene expression: how the genome integrates intrinsic and environmental signals. Nature Genetics, 33(3), 245-254.
86. Jaenisch, R., & Young, R. (2008). Stem cells, the molecular circuitry of pluripotency and nuclear reprogramming. Cell, 132(4), 567-582.
87. Jeong, S. M., Hwang, S., Park, K., Yang, S., & Seong, R. H. (2016). Enhanced mitochondrial glutamine anaplerosis suppresses pancreatic cancer growth through autophagy inhibition. Scientific reports, 6(1), 30767.
88. Jiménez-Uribe, A. P., Hernández-Cruz, E. Y., Ramírez-Magaña, K. J., & Pedraza-Chaverri, J. (2021). Involvement of tricarboxylic acid cycle metabolites in kidney diseases. Biomolecules, 11(9), 1259.
89. Jin, Y., Hoskins, R., & Horvitz, H. R. (1994). Control of type-D GABAergic neuron differentiation by C. elegans UNC-30 homeodomain protein. Nature, 372(6508), 780-783.
90. Kaelin, W. G., & McKnight, S. L. (2013). Influence of metabolism on epigenetics and disease. Cell, 153(1), 56-69.
91. Kajimura, S., Seale, P., Kubota, K., Lunsford, E., Frangioni, J. V., Gygi, S. P., & Spiegelman, B. M. (2009). Initiation of myoblast to brown fat switch by a PRDM16–C/EBP-**β** transcriptional complex. Nature, 460(7259), 1154-1158.
92. Kamath, R., Martinez-Campos, M., Zipperlen, P., Fraser, A., & Ahringer, J. Effectiveness of specific RNA-mediated interference through ingested double-stranded RNA in C. elegans. Genome Biol, 2.
93. Kang, W., Suzuki, M., Saito, T., & Miyado, K. (2021). Emerging role of TCA cycle-related enzymes in human diseases. International journal of molecular sciences, 22(23), 13057.

94. Kaufmann, S., & Tyers, M. (2005). Cell division, growth and death-Editorial overview: The cellular trinity of division, growth and death. Current Opinion in Cell Biology, 17(6), 565-567.
95. Khacho, M., Clark, A., Svoboda, D. S., Azzi, J., MacLaurin, J. G., Meghaizel, C., Sesaki, H., Lagace, D. C., Germain, M., & Harper, M.-E. (2016). Mitochondrial dynamics impacts stem cell identity and fate decisions by regulating a nuclear transcriptional program. Cell stem cell, 19(2), 232-247.
96. Khacho, M., Harris, R., & Slack, R. S. (2019). Mitochondria as central regulators of neural stem cell fate and cognitive function. Nature Reviews Neuroscience, 20(1), 34-48.
97. Kimble, J., & Crittenden, S. L. (2005). Germline proliferation and its control. WormBook: The Online Review of C. elegans Biology [Internet].
98. Kimble, J., Edgar, L., & Hirsh, D. (1984). Specification of male development in Caenorhabditis elegans: the fem genes. Developmental biology, 105(1), 234-239.
99. Kimble, J., & Hirsh, D. (1979). The postembryonic cell lineages of the hermaphrodite and male gonads in Caenorhabditis elegans. Developmental biology, 70(2), 396-417.
100. Kimble, J., & White, J. (1981). On the control of germ cell development in Caenorhabditis elegans. Developmental biology, 81(2), 208-219.
101. Kolundzic, E., Ofenbauer, A., Bulut, S. I., Uyar, B., Baytek, G., Sommermeier, A., Seelk, S., He, M., Hirsekorn, A., & Vucicevic, D. (2018). FACT sets a barrier for cell fate reprogramming in Caenorhabditis elegans and human cells. Developmental Cell, 46(5), 611-626. e612.
102. Kouzarides, T. (2002). Histone methylation in transcriptional control. Current opinion in genetics & development, 12(2), 198-209.
103. Kovatcheva, M., Melendez, E., Chondronasiou, D., Pietrocola, F., Bernad, R., Caballe, A., Junza, A., Capellades, J., Holguín-Horcajo, A., & Prats, N. (2023). Vitamin B12 is a limiting factor for induced cellular plasticity and tissue repair. Nature Metabolism, 5(11), 1911-1930.
104. Kühlbrandt, W. (2015). Structure and function of mitochondrial membrane protein complexes. BMC biology, 13, 1-11.
105. Kulessa, H., Frampton, J., & Graf, T. (1995). GATA-1 reprograms avian myelomonocytic cell lines into eosinophils, thromboblasts, and erythroblasts. Genes & development, 9(10), 1250-1262.

106. Kuzmichev, A., Nishioka, K., Erdjument-Bromage, H., Tempst, P., & Reinberg, D. (2002). Histone methyltransferase activity associated with a human multiprotein complex containing the Enhancer of Zeste protein. Genes & development, 16(22), 2893-2905.
107. L'Hernault, S. W. (2006). Spermatogenesis. WormBook: The Online Review of C. elegans Biology [Internet].
108. L'Hernault, S. W., Shakes, D. C., & Ward, S. (1988). Developmental genetics of chromosome I spermatogenesis-defective mutants in the nematode Caenorhabditis elegans. Genetics, 120(2), 435-452.
109. Ladewig, J., Mertens, J., Kesavan, J., Doerr, J., Poppe, D., Glaue, F., Herms, S., Wernet, P., Kögler, G., & Müller, F.-J. (2012). Small molecules enable highly efficient neuronal conversion of human fibroblasts. Nature methods, 9(6), 575-578.
110. Lamanna, C., Assisi, L., Botte, V., & Di Fiore, M. M. (2007). Involvement of D-Asp in P450 aromatase activity and estrogen receptors in boar testis. Amino acids, 32, 45-51.
111. Lauzier, B., Vaillant, F., Merlen, C., Gélinas, R., Bouchard, B., Rivard, M.-E., Labarthe, F., Dolinsky, V. W., Dyck, J. R., & Allen, B. G. (2013). Metabolic effects of glutamine on the heart: anaplerosis versus the hexosamine biosynthetic pathway. Journal of molecular and cellular cardiology, 55, 92-100.
112. Lawson, H. N., Wexler, L. R., Wnuk, H. K., & Portman, D. S. (2020). Dynamic, non-binary specification of sexual state in the C. elegans nervous system. Current Biology, 30(18), 3617-3623. e3613.
113. Lee, H., Lee, Y. J., Choi, H., Ko, E. H., & Kim, J.-w. (2009). Reactive oxygen species facilitate adipocyte differentiation by accelerating mitotic clonal expansion. Journal of Biological Chemistry, 284(16), 10601-10609.
114. Lee, J. (2024). The emerging era of multidisciplinary metabolism research. Molecules and Cells, 47(2).
115. Li, P., Burke, S., Wang, J., Chen, X., Ortiz, M., Lee, S.-C., Lu, D., Campos, L., Goulding, D., & Ng, B. L. (2010). Reprogramming of T cells to natural killer–like cells upon Bcl11b deletion. Science, 329(5987), 85-89.
116. Li, X., Egervari, G., Wang, Y., Berger, S. L., & Lu, Z. (2018). Regulation of chromatin and gene expression by metabolic enzymes and metabolites. Nature Reviews Molecular Cell Biology, 19(9), 563-578.

117. Lin, Z.-H., Chang, S.-Y., Shen, W.-C., Lin, Y.-H., Shen, C.-L., Liao, S.-B., Liu, Y.-C., Chen, C.-S., Ching, T.-T., & Wang, H.-D. (2022). Isocitrate Dehydrogenase Alpha-1 Modulates Lifespan and Oxidative Stress Tolerance in Caenorhabditis elegans. International journal of molecular sciences, 24(1), 612.
118. Liu, X., Qiao, Y., Ting, X., & Si, W. (2020). Isocitrate dehydrogenase 3A, a rate-limiting enzyme of the TCA cycle, promotes hepatocellular carcinoma migration and invasion through regulation of MTA1, a core component of the NuRD complex. American journal of cancer research, 10(10), 3212.
119. Long, X., Spycher, C., Han, Z. S., Rose, A. M., Müller, F., & Avruch, J. (2002). TOR deficiency in C. elegans causes developmental arrest and intestinal atrophy by inhibition of mRNA translation. Current Biology, 12(17), 1448-1461.
120. Małecki, J. M., Davydova, E., & Falnes, P. Ø. (2022). Protein methylation in mitochondria. Journal of Biological Chemistry, 298(4).
121. Mango, S. E., Lambie, E. J., & Kimble, J. (1994). The pha-4 gene is required to generate the pharyngeal primordium of Caenorhabditis elegans. Development, 120(10), 3019-3031.
122. Marchal, I., & Tursun, B. (2021). Induced neurons from germ cells in Caenorhabditis elegans. Frontiers in Neuroscience, 15, 771687.
123. Marlow, F. (2015). Primordial germ cell specification and migration. F1000Research, 4.
124. Martínez-Reyes, I., & Chandel, N. S. (2020). Mitochondrial TCA cycle metabolites control physiology and disease. Nature communications, 11(1), 102.
125. Matoba, S., & Zhang, Y. (2018). Somatic cell nuclear transfer reprogramming: mechanisms and applications. Cell stem cell, 23(4), 471-485.
126. Mattick, J. S., & Rinn, J. L. (2015). Discovery and annotation of long noncoding RNAs. Nature structural & molecular biology, 22(1), 5-7.
127. McCarter, J., Bartlett, B., Dang, T., & Schedl, T. (1997). Soma–Germ Cell Interactions inCaenorhabditis elegans: Multiple Events of Hermaphrodite Germline Development Require the Somatic Sheath and Spermathecal Lineages. Developmental biology, 181(2), 121-143.
128. Melton, C., Judson, R. L., & Blelloch, R. (2010). Opposing microRNA families regulate self-renewal in mouse embryonic stem cells. Nature, 463(7281), 621-626.

129. Miles, D. C., de Vries, N. A., Gisler, S., Lieftink, C., Akhtar, W., Gogola, E., Pawlitzky, I., Hulsman, D., Tanger, E., & Koppens, M. (2017). TRIM28 is an epigenetic barrier to induced pluripotent stem cell reprogramming. Stem Cells, 35(1), 147-157.
130. Miller, M. A., Nguyen, V. Q., Lee, M.-H., Kosinski, M., Schedl, T., Caprioli, R. M., & Greenstein, D. (2001). A sperm cytoskeletal protein that signals oocyte meiotic maturation and ovulation. Science, 291(5511), 2144-2147.
131. Milne, T. A., Briggs, S. D., Brock, H. W., Martin, M. E., Gibbs, D., Allis, C. D., & Hess, J. L. (2002). MLL targets SET domain methyltransferase activity to Hox gene promoters. Molecular cell, 10(5), 1107-1117.
132. Min, H., Lee, M., Kang, S., & Shim, Y.-H. (2023). Vitamin B12 Supplementation Improves Oocyte Development by Modulating Mitochondria and Yolk Protein in a Caffeine-Ingested Caenorhabditis elegans Model. Antioxidants, 13(1), 53.
133. Min, K., Kang, J., & Lee, J. (2010). A modified feeding RNAi method for simultaneous knock-down of more than one gene in Caenorhabditis elegans. Biotechniques, 48(3), 229-232.
134. Minniti, A. N., Sadler, C., & Ward, S. (1996). Genetic and molecular analysis of spe-27, a gene required for spermiogenesis in Caenorhabditis elegans hermaphrodites. Genetics, 143(1), 213-223.
135. Monné, M., Marobbio, C. M., Agrimi, G., Palmieri, L., & Palmieri, F. (2022). Mitochondrial transport and metabolism of the major methyl donor and versatile cofactor S-adenosylmethionine, and related diseases: A review. IUBMB life, 74(7), 573-591.
136. Morana, A., Stiuso, P., Colonna, G., Lamberti, M., Carteni, M., & De Rosa, M. (2002). Stabilization of S-adenosyl-L-methionine promoted by trehalose. Biochimica et Biophysica Acta (BBA)-General Subjects, 1573(2), 105-108.
137. Mueckler, M., & Thorens, B. (2013). The SLC2 (GLUT) family of membrane transporters. Molecular aspects of medicine, 34(2-3), 121-138.
138. Muhlrad, P. J., Clark, J. N., Nasri, U., Sullivan, N. G., & LaMunyon, C. W. (2014). SPE-8, a protein-tyrosine kinase, localizes to the spermatid cell membrane through interaction with other members of the SPE-8 group spermatid activation signaling pathway in C. elegans. BMC genetics, 15, 1-11.
139. Müller, J., Hart, C. M., Francis, N. J., Vargas, M. L., Sengupta, A., Wild, B., Miller, E. L., O'Connor, M. B., Kingston, R. E., & Simon, J. A. (2002). Histone

methyltransferase activity of a Drosophila Polycomb group repressor complex. Cell, 111(2), 197-208.

140. Nagy, N., & Goldstein, A. M. (2006). Endothelin-3 regulates neural crest cell proliferation and differentiation in the hindgut enteric nervous system. Developmental biology, 293(1), 203-217.
141. Nakamura, T., Mori, T., Tada, S., Krajewski, W., Rozovskaia, T., Wassell, R., Dubois, G., Mazo, A., Croce, C. M., & Canaani, E. (2002). ALL-1 is a histone methyltransferase that assembles a supercomplex of proteins involved in transcriptional regulation. Molecular cell, 10(5), 1119-1128.
142. Nance, J., Davis, E. B., & Ward, S. (2000). spe-29 encodes a small predicted membrane protein required for the initiation of sperm activation in Caenorhabditis elegans. Genetics, 156(4), 1623-1633.
143. Neff, F., Flores-Dominguez, D., Ryan, D. P., Horsch, M., Schröder, S., Adler, T., Afonso, L. C., Aguilar-Pimentel, J. A., Becker, L., & Garrett, L. (2013). Rapamycin extends murine lifespan but has limited effects on aging. The Journal of clinical investigation, 123(8), 3272-3291.
144. Nieborak, A., & Schneider, R. (2018). Metabolic intermediates–cellular messengers talking to chromatin modifiers. Molecular metabolism, 14, 39-52.
145. Nishimura, K., Fukagawa, T., Takisawa, H., Kakimoto, T., & Kanemaki, M. (2009). An auxin-based degron system for the rapid depletion of proteins in nonplant cells. Nature methods, 6(12), 917-922.
146. Nishioka, T., Oda, Y., Seino, Y., Yamamoto, T., Inagaki, N., Yano, H., Imura, H., Shigemoto, R., & Kikuchi, H. (1992). Distribution of the glucose transporters in human brain tumors. Cancer research, 52(14), 3972-3979.
147. Ogonuki, N., Inoue, K., Yamamoto, Y., Noguchi, Y., Tanemura, K., Suzuki, O., Nakayama, H., Ohtomo, Y., Satoh, M., & Nishida, A. (2002). Early death of mice cloned from somatic cells. Nature Genetics, 30(3), 253-254.
148. Onder, T. T., Kara, N., Cherry, A., Sinha, A. U., Zhu, N., Bernt, K. M., Cahan, P., Mancarci, B. O., Unternaehrer, J., & Gupta, P. B. (2012). Chromatin-modifying enzymes as modulators of reprogramming. Nature, 483(7391), 598-602.
149. Oren-Suissa, M., Bayer, E. A., & Hobert, O. (2016). Sex-specific pruning of neuronal synapses in Caenorhabditis elegans. Nature, 533(7602), 206-211.
150. Orlando, V. (2003). Polycomb, epigenomes, and control of cell identity. Cell, 112(5), 599-606.

151. Pao, S. S., Paulsen, I. T., & Saier Jr, M. H. (1998). Major facilitator superfamily. Microbiology and molecular biology reviews, 62(1), 1-34.
152. Parthun, M. R., Widom, J., & Gottschling, D. E. (1996). The major cytoplasmic histone acetyltransferase in yeast: links to chromatin replication and histone metabolism. Cell, 87(1), 85-94.
153. Patel, T., Tursun, B., Rahe, D. P., & Hobert, O. (2012). Removal of Polycomb repressive complex 2 makes C. elegans germ cells susceptible to direct conversion into specific somatic cell types. Cell reports, 2(5), 1178-1186.
154. Phillips, C. M., Wong, C., Bhalla, N., Carlton, P. M., Weiser, P., Meneely, P. M., & Dernburg, A. F. (2005). HIM-8 binds to the X chromosome pairing center and mediates chromosome-specific meiotic synapsis. Cell, 123(6), 1051-1063.
155. Picard, M., & Shirihai, O. S. (2022). Mitochondrial signal transduction. Cell Metabolism, 34(11), 1620-1653.
156. Polo, J. M., Liu, S., Figueroa, M. E., Kulalert, W., Eminli, S., Tan, K. Y., Apostolou, E., Stadtfeld, M., Li, Y., & Shioda, T. (2010). Cell type of origin influences the molecular and functional properties of mouse induced pluripotent stem cells. Nature biotechnology, 28(8), 848-855.
157. Priess, J. R., Schnabel, H., & Schnabel, R. (1987). The glp-1 locus and cellular interactions in early C. elegans embryos. Cell, 51(4), 601-611.
158. Qin, H., Diaz, A., Blouin, L., Lebbink, R. J., Patena, W., Tanbun, P., LeProust, E. M., McManus, M. T., Song, J. S., & Ramalho-Santos, M. (2014). Systematic identification of barriers to human iPSC generation. Cell, 158(2), 449-461.
159. Raimundo, N., Baysal, B. E., & Shadel, G. S. (2011). Revisiting the TCA cycle: signaling to tumor formation. Trends in molecular medicine, 17(11), 641-649.
160. Reiten, O. K., Wilvang, M. A., Mitchell, S. J., Hu, Z., & Fang, E. F. (2021). Preclinical and clinical evidence of NAD+ precursors in health, disease, and ageing. Mechanisms of Ageing and Development, 199, 111567.
161. Rieckher, M., & Tavernarakis, N. (2017). Generation of Caenorhabditis elegans transgenic animals by DNA microinjection. Bio-protocol, 7(19), e2565-e2565.
162. Robida-Stubbs, S., Glover-Cutter, K., Lamming, D. W., Mizunuma, M., Narasimhan, S. D., Neumann-Haefelin, E., Sabatini, D. M., & Blackwell, T. K. (2012). TOR signaling and rapamycin influence longevity by regulating SKN-1/Nrf and DAF-16/FoxO. Cell Metabolism, 15(5), 713-724.
163. Rog, O., & Dernburg, A. F. (2015). Direct visualization reveals kinetics of meiotic chromosome synapsis. Cell reports, 10(10), 1639-1645.

164. Rohrschneider, M. R., & Nance, J. (2013). The union of somatic gonad precursors and primordial germ cells during Caenorhabditis elegans embryogenesis. Developmental biology, 379(2), 139-151.
165. Rokavec, M., Li, H., Jiang, L., & Hermeking, H. (2014). The p53/miR-34 axis in development and disease. Journal of molecular cell biology, 6(3), 214-230.
166. Ryall, J. G., Dell'Orso, S., Derfoul, A., Juan, A., Zare, H., Feng, X., Clermont, D., Koulnis, M., Gutierrez-Cruz, G., & Fulco, M. (2015). The NAD+-dependent SIRT1 deacetylase translates a metabolic switch into regulatory epigenetics in skeletal muscle stem cells. Cell stem cell, 16(2), 171-183.
167. Ryan, D. A., Miller, R. M., Lee, K., Neal, S. J., Fagan, K. A., Sengupta, P., & Portman, D. S. (2014). Sex, age, and hunger regulate behavioral prioritization through dynamic modulation of chemoreceptor expression. Current Biology, 24(21), 2509-2517.
168. Saitoh, Y., Katane, M., Kawata, T., Maeda, K., Sekine, M., Furuchi, T., Kobuna, H., Sakamoto, T., Inoue, T., & Arai, H. (2012). Spatiotemporal localization of D-amino acid oxidase and D-aspartate oxidases during development in Caenorhabditis elegans. Molecular and cellular biology.
169. Saitoh, Y., Katane, M., Miyamoto, T., Sekine, M., Sakamoto, T., Imai, H., & Homma, H. (2019). Secreted d-aspartate oxidase functions in C. elegans reproduction and development. The FEBS Journal, 286(1), 124-138.
170. Santillo, A., Falvo, S., Chieffi, P., Di Fiore, M. M., Senese, R., & Chieffi Baccari, G. (2016). D-Aspartate induces proliferative pathways in spermatogonial GC-1 cells. Journal of cellular physiology, 231(2), 490-495.
171. Schedl, T. (1997). Developmental genetics of the germ line. C. elegans II.
172. Seelk, S., Adrian-Kalchhauser, I., Hargitai, B., Hajduskova, M., Gutnik, S., Tursun, B., & Ciosk, R. (2016). Increasing Notch signaling antagonizes PRC2-mediated silencing to promote reprograming of germ cells into neurons. Elife, 5, e15477.
173. Sepulveda-Rincon, L. P., Wang, Y.-F., Whilding, C., Moyon, B., Ojarikre, O. A., Maciulyte, V., Hamazaki, N., Hayashi, K., Turner, J. M., & Leitch, H. G. (2024). Determining the potency of primordial germ cells by injection into early mouse embryos. Developmental Cell, 59(6), 695-704. e695.
174. Shi, Y., Lan, F., Matson, C., Mulligan, P., Whetstine, J. R., Cole, P. A., Casero, R. A., & Shi, Y. (2004). Histone demethylation mediated by the nuclear amine oxidase homolog LSD1. Cell, 119(7), 941-953.

175. Shiraki, N., Shiraki, Y., Tsuyama, T., Obata, F., Miura, M., Nagae, G., Aburatani, H., Kume, K., Endo, F., & Kume, S. (2014). Methionine metabolism regulates maintenance and differentiation of human pluripotent stem cells. Cell Metabolism, 19(5), 780-794.
176. Shyh-Chang, N., Daley, G. Q., & Cantley, L. C. (2013). Stem cell metabolism in tissue development and aging. Development, 140(12), 2535-2547.
177. Simon, J. A., & Kingston, R. E. (2013). Occupying chromatin: Polycomb mechanisms for getting to genomic targets, stopping transcriptional traffic, and staying put. Molecular cell, 49(5), 808-824.
178. Smith, L. C., Bordignon, V., Babkine, M., Fecteau, G., & Keefer, C. (2000). Benefits and problems with cloning animals. The Canadian Veterinary Journal, 41(12), 919.
179. Solnica-Krezel, L., & Sepich, D. S. (2012). Gastrulation: making and shaping germ layers. Annual review of cell and developmental biology, 28(1), 687-717.
180. Spitz, F., & Furlong, E. E. (2012). Transcription factors: from enhancer binding to developmental control. Nature Reviews Genetics, 13(9), 613-626.
181. Sullivan, L. B., Gui, D. Y., Hosios, A. M., Bush, L. N., Freinkman, E., & Vander Heiden, M. G. (2015). Supporting aspartate biosynthesis is an essential function of respiration in proliferating cells. Cell, 162(3), 552-563.
182. Sulston, J. E., & Horvitz, H. R. (1977). Post-embryonic cell lineages of the nematode, Caenorhabditis elegans. Developmental biology, 56(1), 110-156.
183. Sulston, J. E., Schierenberg, E., White, J. G., & Thomson, J. N. (1983). The embryonic cell lineage of the nematode Caenorhabditis elegans. Developmental biology, 100(1), 64-119.
184. Sutphin, G. L., & Kaeberlein, M. (2009). Measuring Caenorhabditis elegans life span on solid media. Journal of visualized experiments: JoVE(27), 1152.
185. Sybirna, A., Wong, F. C., & Surani, M. A. (2019). Genetic basis for primordial germ cells specification in mouse and human: Conserved and divergent roles of PRDM and SOX transcription factors. Current topics in developmental biology, 135, 35-89.
186. Tassinari, V., Jia, W., Chen, W.-L., Candi, E., & Melino, G. (2024). The methionine cycle and its cancer implications. Oncogene, 43(48), 3483-3488.
187. Tatapudy, S., Aloisio, F., Barber, D., & Nystul, T. (2017). Cell fate decisions: emerging roles for metabolic signals and cell morphology. EMBO reports, 18(12), 2105-2118.

188. Timmons, L., Court, D. L., & Fire, A. (2001). Ingestion of bacterially expressed dsRNAs can produce specific and potent genetic interference in Caenorhabditis elegans. Gene, 263(1-2), 103-112.
189. Tormos, K. V., Anso, E., Hamanaka, R. B., Eisenbart, J., Joseph, J., Kalyanaraman, B., & Chandel, N. S. (2011). Mitochondrial complex III ROS regulate adipocyte differentiation. Cell Metabolism, 14(4), 537-544.
190. Tsukada, Y.-i., Fang, J., Erdjument-Bromage, H., Warren, M. E., Borchers, C. H., Tempst, P., & Zhang, Y. (2006). Histone demethylation by a family of JmjC domain-containing proteins. Nature, 439(7078), 811-816.
191. Ugur, B., Bao, H., Stawarski, M., Duraine, L. R., Zuo, Z., Lin, Y. Q., Neely, G. G., Macleod, G. T., Chapman, E. R., & Bellen, H. J. (2017). The Krebs cycle enzyme isocitrate dehydrogenase 3A couples mitochondrial metabolism to synaptic transmission. Cell reports, 21(13), 3794-3806.
192. van der Knaap, J. A., & Verrijzer, C. P. (2016). Undercover: gene control by metabolites and metabolic enzymes. Genes & development, 30(21), 2345-2369.
193. Vander Heiden, M. G., Cantley, L. C., & Thompson, C. B. (2009). Understanding the Warburg effect: the metabolic requirements of cell proliferation. Science, 324(5930), 1029-1033.
194. Vierbuchen, T., Ostermeier, A., Pang, Z. P., Kokubu, Y., Südhof, T. C., & Wernig, M. (2010). Direct conversion of fibroblasts to functional neurons by defined factors. Nature, 463(7284), 1035-1041.
195. Villar, V. H., Merhi, F., Djavaheri-Mergny, M., & Durán, R. V. (2015). Glutaminolysis and autophagy in cancer. Autophagy, 11(8), 1198-1208.
196. Villar, V. H., Nguyen, T. L., Delcroix, V., Terés, S., Bouchecareilh, M., Salin, B., Bodineau, C., Vacher, P., Priault, M., & Soubeyran, P. (2017). mTORC1 inhibition in cancer cells protects from glutaminolysis-mediated apoptosis during nutrient limitation. Nature communications, 8(1), 14124.
197. Waddington, C. H. (2014). The strategy of the genes. Routledge.
198. Wai, T., & Langer, T. (2016). Mitochondrial dynamics and metabolic regulation. Trends in Endocrinology & Metabolism, 27(2), 105-117.
199. Wang, H., Yang, Y., Liu, J., & Qian, L. (2021). Direct cell reprogramming: approaches, mechanisms and progress. Nature Reviews Molecular Cell Biology, 22(6), 410-424.

200. Wani, N. A., Vettical, B. S., & Hong, S. B. (2017). First cloned Bactrian camel (Camelus bactrianus) calf produced by interspecies somatic cell nuclear transfer: A step towards preserving the critically endangered wild Bactrian camels. PLoS One, 12(5), e0177800.
201. Whitsett, J. A., & Alenghat, T. (2015). Respiratory epithelial cells orchestrate pulmonary innate immunity. Nature immunology, 16(1), 27-35.
202. Wirshing, A. C., & Cram, E. J. (2017). Myosin activity drives actomyosin bundle formation and organization in contractile cells of the Caenorhabditis elegans spermatheca. Molecular biology of the cell, 28(14), 1937-1949.
203. Worringer, K. A., Rand, T. A., Hayashi, Y., Sami, S., Takahashi, K., Tanabe, K., Narita, M., Srivastava, D., & Yamanaka, S. (2014). The let-7/LIN-41 pathway regulates reprogramming to human induced pluripotent stem cells by controlling expression of prodifferentiation genes. Cell stem cell, 14(1), 40-52.
204. Wrana, J. L., & Attisano, L. (2000). The smad pathway. Cytokine & growth factor reviews, 11(1-2), 5-13.
205. Xiao, D., Zeng, L., Yao, K., Kong, X., Wu, G., & Yin, Y. (2016). The glutamine-alpha-ketoglutarate (AKG) metabolism and its nutritional implications. Amino acids, 48, 2067-2080.
206. Xiao, M., Yang, H., Xu, W., Ma, S., Lin, H., Zhu, H., Liu, L., Liu, Y., Yang, C., & Xu, Y. (2012). Inhibition of **α**-KG-dependent histone and DNA demethylases by fumarate and succinate that are accumulated in mutations of FH and SDH tumor suppressors. Genes & development, 26(12), 1326-1338.
207. Xie, H., Ye, M., Feng, R., & Graf, T. (2004). Stepwise reprogramming of B cells into macrophages. Cell, 117(5), 663-676.
208. Yamanaka, S., & Blau, H. M. (2010). Nuclear reprogramming to a pluripotent state by three approaches. Nature, 465(7299), 704-712.
209. Yang, J.-S., Nam, H.-J., Seo, M., Han, S. K., Choi, Y., Nam, H. G., Lee, S.-J., & Kim, S. (2011). OASIS: online application for the survival analysis of lifespan assays performed in aging research. PLoS One, 6(8), e23525.
210. Yesbolatova, A., Saito, Y., Kitamoto, N., Makino-Itou, H., Ajima, R., Nakano, R., Nakaoka, H., Fukui, K., Gamo, K., & Tominari, Y. (2020). The auxin-inducible degron 2 technology provides sharp degradation control in yeast, mammalian cells, and mice. Nature communications, 11(1), 5701.

211. Ying, W. (2008). NAD+/NADH and NADP+/NADPH in cellular functions and cell death: regulation and biological consequences. Antioxidants & redox signaling, 10(2), 179-206.
212. Yoo, H. C., Yu, Y. C., Sung, Y., & Han, J. M. (2020). Glutamine reliance in cell metabolism. Experimental & molecular medicine, 52(9), 1496-1516.
213. Zambrano, A., Molt, M., Uribe, E., & Salas, M. (2019). Glut 1 in cancer cells and the inhibitory action of resveratrol as a potential therapeutic strategy. International journal of molecular sciences, 20(13), 3374.
214. Zhang, D., Wang, Y., Shi, Z., Liu, J., Sun, P., Hou, X., Zhang, J., Zhao, S., Zhou, B. P., & Mi, J. (2015). Metabolic reprogramming of cancer-associated fibroblasts by IDH3**α** downregulation. Cell reports, 10(8), 1335-1348.
215. Zhang, L., Ward, J. D., Cheng, Z., & Dernburg, A. F. (2015). The auxin-inducible degradation (AID) system enables versatile conditional protein depletion in C. elegans. Development, 142(24), 4374-4384.
216. Zhang, Y., & Reinberg, D. (2001). Transcription regulation by histone methylation: interplay between different covalent modifications of the core histone tails. Genes & development, 15(18), 2343-2360.
217. Zhou, G., Meng, S., Li, Y., Ghebre, Y. T., & Cooke, J. P. (2016). Optimal ROS signaling is critical for nuclear reprogramming. Cell reports, 15(5), 919-925.
218. Zhou, Q., Brown, J., Kanarek, A., Rajagopal, J., & Melton, D. A. (2008). In vivo reprogramming of adult pancreatic exocrine cells to **β**-cells. Nature, 455(7213), 627-632.
219. Zhu, J., Fukushige, T., McGhee, J. D., & Rothman, J. H. (1998). Reprogramming of early embryonic blastomeres into endodermal progenitors by a Caenorhabditis elegans GATA factor. Genes & development, 12(24), 3809-3814.

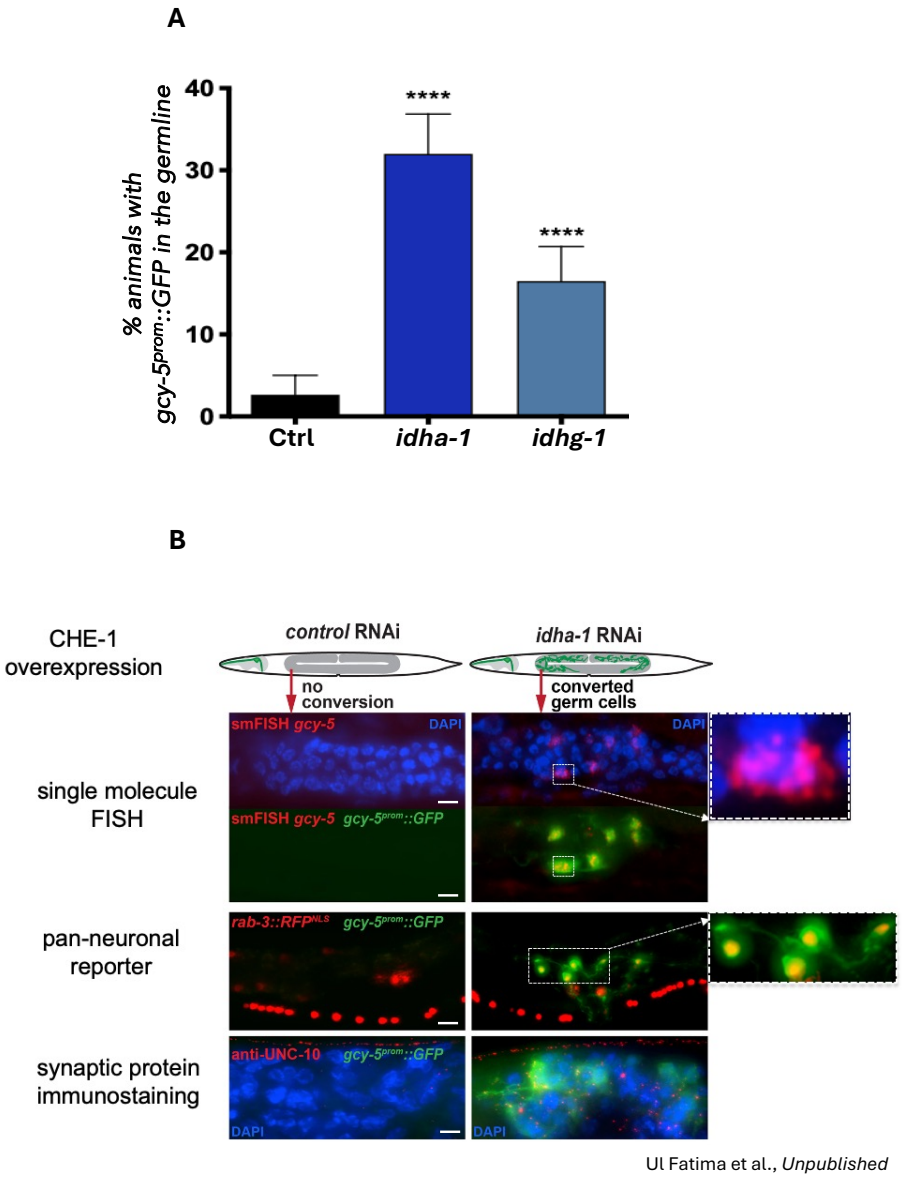

Figure S1 Depletion of IDH-3 allows TF induced neuronal fate expression in germ cells. **A)** Quantification of animals exhibiting ASE neuron fate marker *gcy-5* ^{prom}*::GFP* induction in the germline upon *CHE-1*^{oe} in conjunction with *idha-1*^{RNAi} and *idhg-1*^{RNAi}. *Rluc*^{RNAi} was used as a negative control. Data represent three biological replicates, each with three technical repeats (n ≥ 450 for each condition). Statistical analysis was performed using an ordinary one-way ANOVA test; **** $p < 0.0001$. Error bars represent the standard error of the mean (SEM). **B)** smFISH-based visualization of transcripts derived from endogenous neuronal genes (*gcy-5*, *rab-3*, *unc-119*, and *unc-10*) in germ cells of *idha-1*^{RNAi} *CHE-1*^{oe} animals. Controls were treated with mock hybridizations. Scale bar: 50 µm

LIST OF FIGURES

LIST OF TABLES

LIST OF ABBREVIATIONS

°C	Degree **C**elsius
aa	**a**mino **a**cid
AMP	**Amp**icillin
a-KG	Alpha-ketoglutarate
ASE	**A**mphid neurons (**s**ingle ciliated **e**ndings)
ATAC-seq	**A**ssay for **t**ransposase **a**ccessible **c**hromatin **seq**uencing
ATP	**A**denosine **t**ri**p**hosphate
bp	**b**ase **p**airs
BSA	**B**ovine **S**erum **A**lbumin
C. elegans	***C**aenorhabditis **elegans***
CoA	Acetyl **co**enzyme **A**
CRISPR	**C**lustered **R**egularly **I**nterspaced **S**hort **P**alindromic **R**epeats
DIC	**D**ifferential **I**nterference **C**ontrast
DNA	**D**eoxyribo**n**uncle**a**se

DNTPs	deoxyribonucleotide triphosphate
Dox	Doxycycline
dsRNA	Double stranded RNA
DTC	Distal tip cell
DTT	Dithiothreitol
e.g.	for example
ECM	Extra cellular matrix
EDTA	Ethylenediaminetetraacetic acid
EM	Electron Microscope
endo-siRNA	endogenous small interfering RNAs
ESC	Embryonic stem cell
GABA	glutamate and γ -aminobutyric acid
GC-MS	Gas chromatography mass spectrometry
GeCo	Germline conversion
GFP	Green Fluorescent Protein
HSCs	Hematopoietic stem cells
H3K27me3	histone 3 lysine (K) 27 trimethylation
H3K4me3	Histone 3 Lysine (K) 4 trimethylation
H3K9me3	histone 3 lysine 9 (K) trimethylation
iNs	induced Neurons
iPSCs	induced pluripotent stem cells
IPTG	Isopropyl β-D-1-thiogalactopyranoside
KD	Knockdown
KLF4	Krüppel-like factor 4
KO	Knockout
L1-L4	Larval stage 1-4
MEF	Mouse Embryonic Fibroblast
mL	mili-Liters
mM	mili Molar
mRNA	messenger RNA
MSCs	Mesenchymal stem cells
ng	nanograms
NGM	Nematode Growth Medium
NLS	Nuclear Localization Signal
nM	nano Molar
NSCs	neural stem cells
OCT4	octamer-binding TF 4
OXPHOS	Oxidative phosphorylation

PBS	Phosphate Buffered Saline
PcG	Polycomb Group
PCR	Polymerase Chain Reaction
PFA	Paraformaldehyde
PRC2	Polycomb repressive complex 2
q-PCR	quantitative polymerase chain reaction
RFP	Red Fluorescent Protein
Rluc	Renialla luciferase
RNAi	RNA interreference
RT	Room Temperature
ROS	Reactive oxygen species
SAM	S-adenosyl methionine
SCNT	Somatic Cell Nuclear Transfer
SEM	Standard error of the mean
shRNAs	short hairpin RNAs
siRNAs	small interfering RNAs
smFISH	single molecule Fluorescent in situ Hybridization
SOX2	SRY-box 2
SD	Standard deviation
TCA	Tricarboxylic acid
Tet	Tetracycline
TF	Transcription Factor
trxG	trithorax Group
vs.	versus
WT	wild type
YA	Young Adult
µg	microgram
µM	micro-Molar
µm	micrometer

ACKNOWLEDGEMENTS

First, I want to express my gratitude to Baris for giving me the opportunity to work at his laboratory and being understanding with difficulties faced in life.

I am profoundly thankful to Nida for being such a great mentor and a teacher. I would like to thank Ismail for his continuous support. I would also like to thank Marcel with his help in the project and to all my past and present colleagues at AG Tursun, especially Qinming, Marcel, Gizem, Selman and Tajna for their support.

I would like to thank my dear friends especially Ipek, Alba, Afrah, Annie and Ahmad for sharing their experiences with me in this journey and always being there.

I would like to mention how grateful I am for the support I received from my grandmother and grandfather. It saddens me deeply that I could not see them during the course of this project and that I could not bid them a final farewell before they left this world. I will always carry their love in my heart.

Lastly, but most importantly, I would like to express my deepest gratitude to my family for their unwavering love and support. To my lovely aunts, to my father, my uncles, my one and only sister and specially to my extraordinary mother, in supporting me and standing by me in the most beautiful way possible.
☺